

***MODELING OF SEDIMENT TRANSPORT
IN IRRIGATION CANALS OF PAKISTAN:
EXAMPLES OF APPLICATION***

**Definition of a Simple Simulation Tool
and Test on Two Actual Canals of Pakistan:
Application to Management Strategies**

GILLES BELAUD

**(M.Sc Student, Ecole Nationale du Genie Rural, des Eaux et Forets)
ENGREF, France**

In Collaboration With

**International Sedimentation Research Institute, Pakistan (ISRIP)
Agricultural and Environmental Engineering Research Institute (CEMAGREF)
International Irrigation Management Institute (IIMI)**

OCTOBER 1996

FOREWORD

This report is the thesis or final report for the Master of Science program of Mr. Gilles Belaud. He completed **the** requirements for an **M.S.** degree in Genie Rural (Agricultural Engineering) from the Ecole Nationale du Genie Rural, des **Eaux et Forets** (ENGREF) in Montpellier, France during September 1996. He spent **three** months in Pakistan during 1996 to complete **all** of **the** necessary field work and **analysis**. This reproduction is identical to the document accepted **by** ENGREF.

We have a number of national and international **students** participating in the **research** program of the *Pakistani National Program* of the international Irrigation Management Institute. Their theses and dissertations are retained in our library for ready reference. Only **a** few of **these** documents are selected for publication in our research report series. The principal criteria for publishing is good quality research and a topic that would *be* of interest to many of our national partners.

This report is an output of a collaborative research program with the International Sedimentation Research **Institute**, Pakistan (ISRIP) and CEMAGREF, the French national research organization for agriculture, water and forests. This research program on sediment transport **was** formulated in December 1994 and initiated during 1995. This is one of our first reports on sediment transport.

This **study** investigated the **use** of a simple sediment transport model that could interface with the unsteady hydraulic model **SIC** (Simulation of Irrigation Canals). The calibration and validation was done using **data** collected by ISRIP on Chashma Right Bank Canal and the Chashma-Jhelum Link Canal in Pakistan.

Mr. Gilles Belaud will begin a Ph.D program in December 1996 that is being *funded* **by** CEMAGREF. He will continue **this** research in order to develop **a** general sediment transport model that can **be** linked with SIC.

Gaytord V. Skogerboe, Director
Pakistan National Program
International Irrigation Management Institute

Table of contents

ABSTRACT	IV
ACKNOWLEDGEMENTS	IV
LIST OF ABBREVIATIONS	V
NOTATIONS	VI
<u>1. INTRODUCTION</u>	<u>1</u>
1.1 GENERAL	2
1.2 SOLUTIONS?	2
1.3 A JOINT RESEARCH PROGRAM	2
1.4 PROBLEM STATEMENT	2
1.4.1 BACKGROUND	2
1.4.2 OBJECTIVES OF THIS WORK	3
1.4.3 METHODOLOGY	3
<u>2. ANALYSIS OF ACTUAL SYSTEMS</u>	<u>4</u>
2.1 PRESENTATION OF THE CANALS	4
2.1.1 CHASHMA RIGHT BANK CANAL	4
2.1.2 CHASHMA JHELUM LINK CANAL	5
2.2 MEASUREMENT METHODS	6
2.2.1 CONCENTRATIONS	6
2.2.2 TOPOGRAPHY	6
2.2.3 ACCURACY	7
2.3 INTERPRETATION OF TOPOGRAPHIC DATA	7
2.3.1 PROBLEM STATEMENT	7
2.3.2 DEFINITION OF THE PROCEDURE	8
2.4 SEDIMENTOLOGIC CHARACTERIZATION	9
2.4.1 CHASHMA RIGHT BANK CANAL	9
2.4.2 CHASHMA JHELUM LINK CANAL	11
2.5 SUMMARY	13
<u>3. PRESENTATION OF THE SIMULATION TOOL</u>	<u>14</u>
3.1. COMBINATION OF THE HYDRAULIC AND SEDIMENTOLOGIC MODELS	14
3.1.1. REQUIRED OUTPUTS OF THE MODEL	14
3.1.2. GENERAL ALGORITHM	14
3.2. PRESENTATION OF THE HYDRAULIC MODEL SIC	15
3.2.1. THEORETICAL EQUATIONS	15
3.2.2. NUMERICAL RESOLUTION	16
3.3. MODELING OF SEDIMENT TRANSPORT	16
3.3.1. PHYSICAL APPROACH	16

3.3.2. MODELING OF THE CONCENTRATION EVOLUTION	17
3.4. BED EVOLUTION	20
3.4.1. LONGITUDINAL EVOLUTION	20
3.4.2. DISTRIBUTION OF SCOURING OR SILTATION IN THE CROSS SECTION	21
3.5. DEFINITION OF THE BED MATERIAL LOAD CONCENTRATION	23
3.5.1. GENERAL	23
3.5.2. CHOICE OF THE DISTRIBUTION FUNCTIONS	24
3.5.3. USING ACTUAL DATA (EXAMPLES)	25
3.6. SENSITIVITY ANALYSIS	26
3.6.1. OBJECTIVES AND METHOD	26
3.6.2. ANALYSIS OF THE RESPONSE	37
<u>4. CALIBRATION AND VALIDATION</u>	<u>30</u>
4.1 INTEGRATIVE OR INSTANTANEOUS CALIBRATION?	30
4.1.1 INSTANTANEOUS CALIBRATION	30
4.1.2 INTEGRATIVE CALIBRATION	30
4.1.3 CHOICE OF A METHOD	30
4.2 PROCEDURE OF INTEGRATIVE CALIBRATION	31
4.2.1 PRINCIPLE	31
4.2.2 DEFINITION OF THE CALIBRATION FUNCTIONS	32
4.2.3 ILLUSTRATION OF THE PROCEDURE	32
4.3 CALIBRATION ON CHASMA RIGHT BANK CANAL	35
4.3.1 INPUT DATA	35
4.3.2 RESULTS OF CALIBRATION	36
4.3.3 COMMENTS	37
4.4 CALIBRATION ON CHASMA JHELUM LINK CANAL	38
4.4.1 INPUT DATA	38
4.4.2 RESULTS OF CALIBRATION	38
4.4.3 COMMENTS	39
4.4.4 CONFRONTATION MEASURED/SIMULATED CONCENTRATIONS	40
4.5 EXAMPLE OF APPLICATION: VALIDATION AND PREDICTION STRATEGIES	40
4.5.1 PREDICTION STRATEGIES	40
4.5.2 QUANTIFICATION OF THE ERROR ON PREDICTION	41
4.5.3 APPLICATION TO CRBC	41
4.5.4 APPLICATION TO CJ LINK CANAL	44
4.6 CONCLUSION	45
<u>5. EXAMPLE OF APPLICATION: STRATEGIES FOR WATER MANAGEMENT</u>	<u>46</u>
5.1. INTRODUCTION	46
5.2. DEFINITIONS	46
5.2.1. DEFINITION OF RELEVANT STRATEGIES	46
5.2.2. SIMULATION CANAL	47
5.3. STRATEGY 1: MAXIMUM DISCHARGE	48
5.3.1. FEASIBILITY	48
5.3.2. COMPARISON BETWEEN THREE OPERATING STRATEGIES AT THE REGULATOR	48

5.3.3. GLOBAL COMPARISON	49
5.4. STRATEGY 2: VARIABLE DISCHARGE	50
5.5. EXAMPLE OF APPLICATION	52
5.5.1. SUMMARY	52
5.5.2. EXAMPLE OF INTERPRETATION	52
5.6. SUMMARY	54
5. CONCLUSION	55
5.1 SUMMARY	55
5.2 VIEW ON THE FOLLOWING	55
5.2.1 MODELING	55
5.2.2 APPLICATIONS	56
5.2.3 DATA COLLECTION	56
REFERENCES	57

APPENDICES

Abstract

In 1995, a program of collaboration started between IIMI, ISRIP and CEMAGREF in order to minimize the effects of sedimentation in the irrigation canals. For this purpose, it has been chosen to combine a model of sediment transport to the hydraulic software SIC used for water management in the irrigation canals.

During this Master of Science, strategies for modeling the evolution of the concentrations along the canals have been proposed. Then a simulation tool, deliberately simple, was developed, associating a sediment transport model to the existing hydraulic model. Two laws, an equilibrium law and a loading law, are necessary and three parameters have to be calibrated.

The tool has been tested in calibration and validation on two canals thanks to data collected by ISRIP: Chashma Right Bank Canal and Chashma Jhelum Link Canal.

A calibration procedure is defined and tested on each canal for six equilibrium laws. All these laws give similar results, and although many problems remain in the calibration, the general trends can be reproduced.

In prediction, we compared the errors between measured and calculated volume variations. These errors vary from 30% to 70% in average, except for very short terms where they were much higher. Such errors are expected in sediment transport problems (measurement inaccuracies, approximations in the model...) and the quality of a prediction must not only be assessed through the error on the deposited volumes.

The model will have to be developed and tested on many other systems, at different scales and for longer series.

As an example of application, we also show how it is possible to use the simulation tool to observe the effect of different water management strategies on sedimentation.

Acknowledgements

Three persons accepted to supervise this work and they are acknowledged: Professor Skogerboe, director of IIMI Pakistan. Docteur Siddique, director of ISRIP, Lahore, and Docteur Pascal Kosuth, head of the Irrigation Division of Cemagref Montpellier, France.

The Hydraulics Division of Cemgref Lyon (France) and Dr B. Le Guennec (IMF Toulouse, France) is also specially acknowledged for their theoretical support, their experience and above all their availability. I also remain grateful to Pierre-Olivier Malaterre and Jean-Pierre Baume without whom my numerous technical problems might have remained unsolved.

List of abbreviations

ACOP: Alluvial Channel Observation Project, later

ISRIP: International Sediment Research Institute in Pakistan:

ACOP was created in 1973 as research formation of WAPDA*, from an agreement between the Government of Pakistan and the US National Science Foundation. This organism was felt necessary at the beginning of the Indus Basin Project which consisted of the construction of huge link canals. It participated in important research projects in alluvial mechanics and constituted a large database of sediment characterization in irrigations, rivers and reservoirs. It was remodeled in 1987 into ISRIP*. ISRIP is using advanced technologies for field and laboratory measurements, data processing and mathematical modelling.

CEMAGREF: Agricultural and Environmental Engineering Research Institute (France)

The main missions of Cemagref are to give answers to the major environmental and agricultural problems the society is faced with. Applied research is conducted in economics, social sciences, hydraulics, hydrology, water management, agronomy... in a all kinds of natural mediums.

IIMI: International Irrigation Management Institue:

Extract from a research paper: "IIMI is an autonomous, nonprofit international research and training institute supported by the Consultative Group on International Agricultural Research (CGIAR). The CGIAR is sponsored by the Food and Agriculture Organization (FAO) of the United Nations, the International Bank for Reconstruction and Development (World Bank), and the United Nations Development Programme (UNDP) and comprises more than 45 donor countries, international and regional organizations, and private foundations.

IIMI's mission is to strengthen national efforts to improve and sustain the performance of irrigation systems in developing countries. With its headquarters at Colombo, Sri Lanka, IIMI conducts a worldwide program to develop and disseminate improved approaches towards irrigation management."

WAPDA: Water and Power Development Authority

WAPDA is a powerful organism in Pakistan. Among its missions, it is responsible for the construction and the supply of most of the main irrigation canals.

Notations

General variables

g : acceleration due to gravity
 t : time
 T : duration of a period of steady flow
 x : longitudinal abscissa
 Z : water elevation
 h : water depth
 H : hydraulic charge
 Q : liquid discharge
 q : liquid discharge per unit width
 S : wetted area
 J : slope of energy line (hydraulic gradient)
 K : Strickler coefficient
 P : wetted perimeter
 $R_h = S/P$: hydraulic radius
 $U = Q/S$: average velocity
 ρ : specific weight of water
 ν : kinematic viscosity of water

Variables and parameters relative to sediment transport

Q_s : solid discharge
 q_s : solid discharge per unit width
 d : diameter of a grain
 d_x : superior diameter of the $x\%$ finer particles of a mixing.
 ρ_s : specific weight of the grains
 p : porosity of the grains
 ΔV : variation of volume during a period in a reach
 ΔS : variation of area for a cross section
 C : sediment concentration
 C^* : equilibrium concentration
 w : terminal velocity
 Φ : deposited quantity per unit width, length and time.
 u, v : local velocities in x, y directions
 τ : total shear stress
 τ_0 : total shear stress at the bed surface $\tau_0 = \gamma h J$
 $u_* = \sqrt{\tau_0 / \rho}$: shear velocity. It is a characteristic velocity at the grain level and in the vicinity of the bed.
 cr : critical stage.
 $f(d)$: distribution function (percentage of particles finer than the diameter d)
 β : multiplicative coefficient for the equilibrium law
 α_d, α_e : constants of deposition and erosion
 $J(\cdot, \cdot)$: quadratic error function.

Dimensionless variables

$Y = \frac{\tau_0}{(\gamma_s - \gamma) d}$: Shields dimensionless shear stress, or mobility number.

$Re^* = \frac{u_* \cdot d}{\nu}$: Reynolds number at grain scale.

$\Phi = q_s \cdot \sqrt{\frac{\rho}{g \cdot (\rho_s - \rho) d^3}}$: dimensionless solid discharge per unit width.

1. Introduction

7.7 General

The agricultural performances in Pakistan depend to a large extent on the efficiency of the irrigation systems, which cover some 16 million hectares (third largest in the world).

This system was initiated under the British Government in the middle of the 19th century. At the beginning, only the available water from rivers were derived but very soon cross devices were constructed to supply more water for longer periods. Then the British engineers started to think of improving the efficiency of the canals. They were rapidly faced with the problems of sediment transport. They observed that if the flow velocity was too high, scouring could appear and affect the stability of the earthen channels. On the other hand, the canals had a tendency to siltation when they received a high amount of sediments (coming from upstream) and when the flow velocity was too low.

After flume experiments, the engineers started to define empirical rules for channel design (see literature review), giving an equilibrium profile for given discharges (solid and liquid) and slope (which is imposed by the natural slope of the ground). These rules assume that the average concentration at the head of the channel is limited (500 mg/l in Lacey's approach).

But there are some cases where the sediment loads cannot be controlled easily. For example, the Himalayan areas suffer from an important surface erosion, inducing high material loads in the rivers. In 1981, Ning Chien and Tai Ting Chung published a survey giving average concentrations in the biggest Himalayan rivers: 4 g/l in Ganges river, 2.5 g/l in Indus river... the record being 38 g/l in the Yellow river where a maximum of 666 g/l has already been measured.

These sediments are very fine and can be transported for long distances. The major induced problem is siltation in the storage basins where the sediments settle because of the low flow velocities. But high concentrations are also released when the water level in the reservoir is low and the needs for irrigation are high (typically just before the monsoon, in June). That is why irrigation canals also suffer from high solid discharge. Although the head regulators of the canals can be closed in case of exceptional concentrations, and despite desilting devices, the average concentrations are still high and sedimentation ineluctably occurs when the flow velocity decreases downstream from the offtakes.

The hydraulic consequences of siltation are well identified now: limitation of the conveyance capacity and increase of delivery heterogeneity. The raising of the bed level also raises the water level (for a same discharge but the capacity of hydraulic transport of a channel is limited by its banks and the acceptable discharge is decreased). If too high a discharge passes through the silted canal, overtopping and breaches can occur. But in some distributaries (secondary canals), the farmers at head benefit from the decreasing of the transport capacity of the tail: even if the total discharge is decreased, the water level raises at head and the feeding of the outlets is favored; the farmers at head receive more water at the expense of the farmers downstream. To preserve the interests of the tail farmers, maintenance has to be done, by the farmers themselves under the control of the Irrigation Department or by the Irrigation Department themselves when the problems are too sharp.

In the province of Sindh (south of Pakistan), Jamrao Canal silted up from 7 to 9 feet (2 to 3 meters) since its construction in 1974. To preserve the transport capacity of the canal, the Irrigation Department has been obliged to make daily mechanical dredging, which is very costly. In Punjab, silt clearance usually accounts for half of the operation and maintenance costs (ref. [7]).

1.2 Solutions?

The phenomenon of siltation in the irrigation systems is not controlled but the managers know that the present strategies of water distribution are not optimal from a sedimentologic point of view. Still they have constraints

(water levels, available resources, equity in distribution...) so that it is not always possible to just increase the discharges or decrease the levels at the control regulators.

Nevertheless, it may be possible to improve the present strategies of maintenance, operations and even design of the channels so as to reduce the negative **impacts** of siltation, **but** still *satisfying* the other constraints: the problems of siltation **should be** taken as a constraint, and a better equilibrium between the different constraints might **be** possible.

For that, a better understanding of the sediment transport in the irrigation canals **is necessary**. We should **be** able to predict the behavior of a canal under given hydraulic and sediment inflow conditions: what will be the bed evolution, the deposited volume of sediments, the outflow of sediments... in order to be able to compare different strategies of water management, channel design **or** maintenance.

7.3 Ajoint research program

Three organisms are associated in this research program:

IIMI¹ has a strong experience in the irrigation systems of Pakistan and has been collaborating for more than ten years with the Irrigation and Power Department in improving the efficiency of the irrigated agriculture in Pakistan.

ISRIP², formerly ACOP³, has a long experience (since 1973) in sediment transport characterization in Pakistan (rivers, irrigation canals and reservoirs). They analyzed many systems and constituted a huge database.

Cemagref⁴ developed a software for hydraulic simulation of irrigation canals (SIC model), utilized by IIMI for water management. The Hydraulics Division in Lyon developed models of sediment transport (rivers and waste water collectors).

1.4 Problem statement

1.4.1 Background

The collaboration between IIMI, ISRIP and Cemagref started in 1995 with a preliminary work (Vabre 1995, ref. [21]). This first study consisted of:

- a data analysis on Chashma Right Bank Canal;
- a combination of a sediment transport module to the hydraulic model SIC;
- an analysis of two methods of calibration of the sediment laws parameters.

The objectives for 1996 are to improve the efficiency of the model (work on algorithms), to include more options in the modeling (**developing** the physics of the phenomenon) and to test it on **actual** systems. In parallel, methodologies for maintenance, **operation** and **design** strategies **will** be developed, using the sediment transport model (Alexandre Vabre's Master of Science).

Many sophisticated models of sediment transport have **already** been developed and adapted to rivers and reservoirs. Rather than using these models and adapt them to irrigation canals, it has been chosen to develop a simple tool which can be combined to the operational hydraulic **model** SIC.

¹ International Irrigation Management Institute

² International Sediment Research Institute

³ Alluvial Channel **Observation** Project

⁴ Agricultural and Environmental Engineering **Research** Center

1.4.2 Objectives of this work

This Master of Science study is the **second** step **of** the joint research program. It **is** more a feasibility study than the **research** of an operational and reliable tool.

Its objectives are to propose a simple tool able to **simulate the** deposition process **in the** irrigation canals and to test it on actual **systems** analyzed **by** ISRIP.

1.4.3 Methodology

* analysis of the previous works..

- characterization of *the sedimentologic* problematic;
- analysis of the encountered problems;
- determination of the relevant input **data**;
- **definition** of the expected outputs.

* literature review

* definition of

- the algorithms
- the **laws** to **represent** the **sediment** transport.

* computation of the model.

* sensitivity analysis.

* tests on simple cases (flumes)

* definition of procedures of calibration and validation.

* calibration/validation on actual systems.

* discussion of the results.

* example of application: influence of two operation strategies.

The computation of the model was made in the Irrigation Division of Cemagref (Montpellier) who developed the hydraulic model SIC.

The theoretical support was mainly given **by** the Hydraulics Division **of** Cemagref (Lyon, France) (literature review. definition of modeling strategies).

ISRIP **provided all the** informations on **the** studied systems **and all the** data used in this study.

IIMI highlighted **the** specificity **of the** problems **of** siltation in the **irrigation** canals (field visits in Punjab and Sindh).

2. Analysis of actual systems

This part aims at characterizing the sedimentologic problem on actual canals so as to define appropriate methods of modeling.

The present study was made with the support of two canals of Pakistan, both located partly in Punjab, partly in the North-West Frontier Province: Chashma Right Bank Canal (CRBC) and Chashma Jhelum Link Canal (CJ Link Canal). A location map is presented in appendix 1. They are introduced in the first paragraph. The second paragraph will focus on measurement methods (for sediment characterization) used for the campaigns on these canals. The next one provides some general information on both systems and at last sediment characteristics are extracted in order to orient the computation of the simulation tool.

2.1 Presentation of the canals

Situation maps are given in appendix. Both canals are fed by Chashma Barrage which diverts water from Indus River at about 56 km downstream from Jinnah Barrage. The total storage capacity of Chashma Reservoir is 925 million cubic meters.

2.1.1 Chashma Right Bank Canal

CRBC is a major irrigation project designed to irrigate some 230,000 hectares (570,000 acres). The first stage of the canal was opened in April 1987 but the whole system should not be completed before 1997. The total conveyance capacity of the canal is $135 \text{ m}^3/\text{s}$ (4769 cusecs) and this capacity will be utilized after completion of the whole system. CRBC is a pilot project for strategies of water distribution: the water supply must be driven by the crop requirements (and not the contrary as for most of the irrigation projects in Pakistan). Several cross regulators can control the water levels.

ISRIP was asked to follow the behavior of the first stage of the canal from 1957 to 1994

The present study will deal with the earthen portion of the first stage (completed in 1987), from RD 1+000 to RD 98+000. This portion ends with a combined structure (regulator) which controls the water surface level:

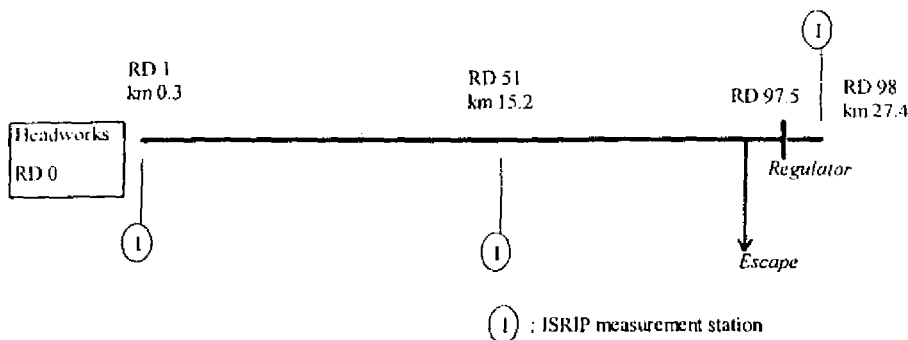


Figure 2.1-1: schematic view of the first reach of CRBC

The lined portion starts at RD120 where the canal narrows. Between RD98 and RD120, two distributaries are fed by the main canal. The discharges at these distributaries were not well enough identified and this study will be limited to the reach upstream from the regulator.

Chashma Right Bank Canal is not a common canal. It has been constructed on the natural ground on which banks have been erected (compacted earth). The design bed level is higher than this natural ground (for the studied portion) and siltation is expected in order to reduce seepage losses. The design data, calculated according to Lacey's theory, are the following:

Characteristic	Imperial units	IS units
design discharge	4769 cfs	135 m ³ /s
Velocity	3.21 ft/s	0.97 m/s
Bed width	174 ft	53 m
Slope of the banks	1.5:1	1.5:1
Water depth	8.35 ft	2.55 m
Water surface slope	1:8093	1:8093

Table 1: design data for *Chashma Right Bank Canal*

A typical cross section is presented on the following schematic plan:

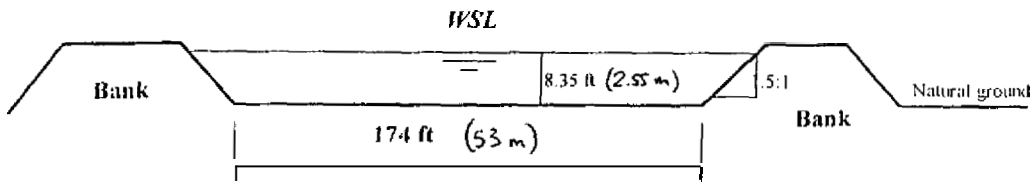


Figure 2.1-2: typical cross section of Chashma Right Bank Canal

2.1.2 Chashma Jhelum Link Canal

This canal was completed in May 1971 to carry water from Indus River (left bank) at Chashma Barrage to Jhelum River (see map). It crosses irrigated areas in its upper part and the Thal Desert in its lower portion. Its design characteristics, calculated from WAPDA and Lacey's theories, are the following:

Characteristic	Imperial units	IS units
Length	67 miles	107 km
Discharge	21700 cusec	615 m ³ /s
Velocity	3.73 ft/s	1.1 m/s
Area	5810 sqft	540 m ²
Bed width	380 ft	116 m
Water depth	14 ft	4.3m
Slope	1/10000	1/10000
Manning coefficient	0.022	0.022
D50 for bed material	0.190 mm	0.190 mm

Table 2: design data of Chashma Jhelum Link Canal

* longitudinal profile.

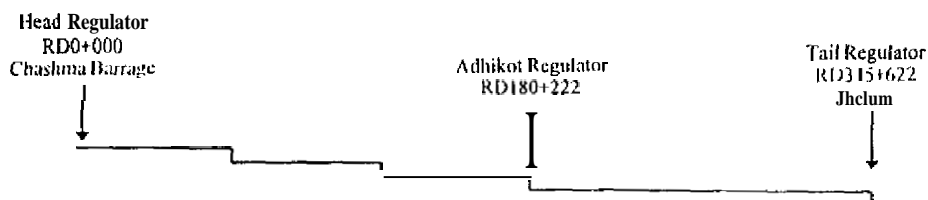


Figure 2.1-3: schematic plan of Chashma Jhelum Link Canal

Two regulators (at head and tail) and three control structures are controlling the water level along the canal. A particular attention will be paid to the last reach, from RDI 80+222 to RDJ 315+622 (41 km).

* design cross sections:

A typical cross section is presented on the following schematic plan:

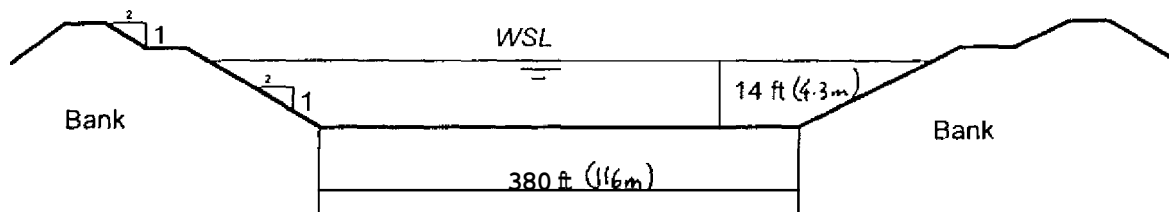


Figure 2.1-4: typical cross section of Chashma Right Bank Canal

* Measurement campaigns:

To address the problem of waterlogging in the 3rd and 4th reaches (RD105 to RD315), it was decided to lower the crest of the tail regulator by 6 feet (1.8 m). The first stage of this lowering (by 3 feet) was completed in August 1981, and ACOP was asked to evaluate the behavioral response for three years.

Two other measurement campaigns were undertaken in 1972-1974 and 1975-1978 but the only one which concerned both cross sections and complete sediment data was achieved between August 1981 and June 1984.

2.2 Measurement methods

2.2.1 Concentrations

Two methods are generally utilized by ISRIP and WAPDA.

The first one consists in collecting *boil samples* in turbulent water, generally at the regulators. Several samples are taken over the cross section so as to obtain the mean concentration for this cross section. The grain size distribution of the samples are then analyzed in a laboratory where concentrations for different classes of particles are determined. This method is used by WAPDA at the headworks for daily measurements.

ISRIP is provided with *depth integrating samplers* (model USD49): "A depth integrating sampler is designed to accumulate a water sediment sample from a stream vertical at such a rate that the velocity in the nozzle at point of intake is always as nearly as possible identical to the immediate stream velocity, while running the vertical at a uniform speed." (definition from the Federal Inter-Agency Sediment Project, 1952). Samples are collected at ten verticals per cross section, giving the mean concentration in the section.

These samplers do not collect sediments in the vicinity of the bed (0.3 feet, 10 cm) and thus only the suspended sediment concentrations are measured.

ISRIP also uses bed material samplers (model BM54) which take a small quantity of bed material 5 centimeters deep from the bed level.

2.2.2 Topography

The recent measurement campaigns utilize sonic sounders which print the water depth on a paper ribbon

The longitudinal profile of the bed is measured in the middle of the channel. The water surface elevation is regularly collected so as to calculate the absolute elevation of the bed.

Cross sections are sometimes measured by this method also. A line is drawn from one bank to the other and the bed level is measured with respect to the water elevation.

	Wetted area	Wetted perimeter	Hydraulic radius
section 1	51 m ²	51.4 m	0.99 m
section 2	51.75 m ²	51.65 m	1.00 m
		0.5 %	

Problems due to discretization may appear when the transversal length step for cross sections is higher, like for Chashma Jhelum Link Canal which was not measured by sonic sounding.

2.3 Interpretation of topographic data

2.3.1 problem statement

To compare two different geometries of a given channel, we can think of analyzing different variables:

- the volumetric differences;
- the bed elevation variations;

Both variables are relevant as far as the managers of the systems are concerned. Analyzing cross sections of CRBC or CJ Link, we are faced with the question: how to define a bed elevation value for a given cross section?

The elevation of the lowest point of the section is an unbiased quantity (it is clearly defined) but it is not a relevant variable from a physical and operational point of view:

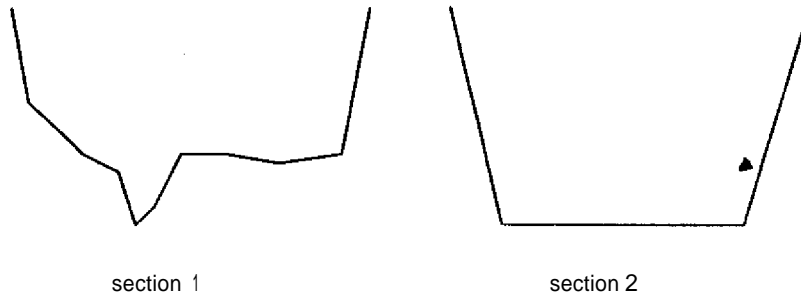


Figure 2.3-1; comparison of cross sections

Section 1 could result from siltation in section 2. They have the same lowest elevation but are quite different!

Thus we propose to **redefine** a section 1', called "equivalent" to section 1, for which the bed level could be easy to compare to the one of section 2. Two methods are proposed:

(1) the total volume of the section is preserved but we remodel the cross section into a trapeze:

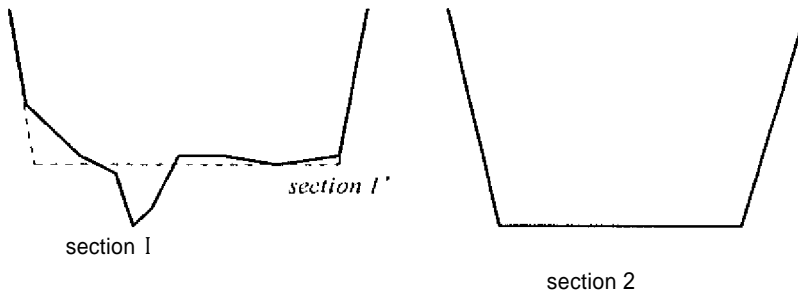


Figure 2.3-2: modified cross section (method 1)

Sections 1' (dotted line) and 2 can easily be compared, and we can say that their bed level elevations are the elevations of their bottom.

Practical problems on actual systems consists of the definition of the side slopes and of the sensitivity of the procedure to the geometric data collection on the sides.

The procedure we selected is presented below.

2.3.2 definition of the procedure

It rests on **empirical** considerations and may be easily criticized for that:

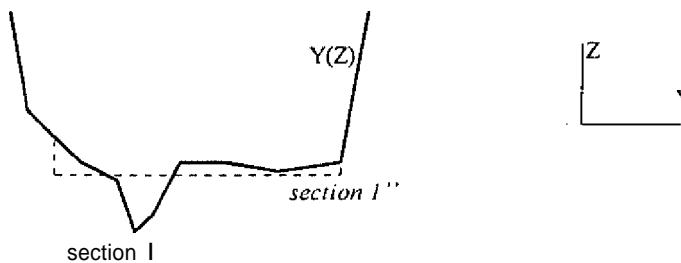


Figure 2.3-3: modified cross section (method 2)

The section is supposed to be defined by the width/elevation relation $Y(Z)$ as it is in SIC model

We also know the relation $S(Z)$, area of the section below the elevation Z .

(1) we define a "bed width" on which the medium bed level will be calculated. Let Y_b be this quantity.

(2) Let $Z_b = Z(Y_b)$ the elevation where the canal width equals Y_b .

(3) we calculate the height of the rectangle which has the area $S(Z_b)$ and the width Y_b : $\Delta Z = S(Z_b)/Y_b$.

(4) the portion of the bed below the elevation Z_b is assumed to be equivalent to a rectangle of same area. The bottom of this rectangle is assumed to represent the medium bed level. Its elevation is given by

$$Z' = Z_b - S(Z_b)/Y_b$$

In the following, we will call "medium bed level" the elevation Z' calculated according to this procedure.

The main advantage of this procedure is that the medium bed level is calculated on the lowest part of the bed, which is the active portion of the bed in the sedimentologic process (the banks are not supposed to be evolve significantly; if they do, we are not able to model it right now).

It main drawback is its dependency on the width of the bed (user-defined) which is defined empirically.

For CRBC, the bed width was fixed to 66,67% of the total width of the cross section, namely around 160 feet (49 meters). For CJ Link canal, the bed width was fixed to 80% of the cross section, namely about 365 feet (110 meters). These widths have been chosen so as to take into account the whole bed bottom but not the sides.

2.4 Sedimentologic characterization

2.4.1 Chashma Right Bank Canal

2.4.1.1 Collected data

* geometric data: They are provided by ISRIP who measure the cross sections every 5000 feet (1524 m) by sonic sounding. The measurements campaigns started in 1987 (opening of the canal) and stopped in 1994.

For our work we used the data for the first reach (earthen portion), 98000 feet long (31 km), controlled by a regulator at RD97+500. The geometries were measured in:

- April 1987;
- January 1988;
- July 1990
- January 1991;
- January 1992;
- February 1993.

* hydraulic data:

They are provided by ISRIP (monthly data) and WAPDA (Water And Power Development Authority) for the operations at the regulators (head and tail, daily measurements). The discharge at head is presented in appendix 3. WAPDA also record the operations at the control regulator (RD97+500): upstream and downstream water levels, gate opening, discharge.

At each measurement campaign, ISRIP records all the hydraulic at different abscissas (RD1+000, RD51+000 and RD98+000). These data are necessary for the calibration of the hydraulic model.

* sedimentologic data: Daily concentrations are available at head (see appendix 3) for five classes of particles: $>177\mu\text{m}$, $125-177\mu\text{m}$, $62-177\mu\text{m}$, $50-62\mu\text{m}$, $5-50\mu\text{m}$ and $<5\mu\text{m}$.

ISRIP also measured monthly concentrations ($>62\mu\text{m}$, $2-62\mu\text{m}$, and $<2\mu\text{m}$).

The bed composition is also measured by ISRIP but only for particles coarser than 62 μ m. The following table gives the medium diameters and the percentages of particles finer than this limit at different abscissas in October 1987 and June 1989:

Abscissa	October 1987 % finer than 62 μ m	October 1987 Medium diameter	June 1989 % finer than 62 μ m	June 1989 Medium diameter
RD 1+000	0.2	238 μ m	0.8	229 μ m
RD10+000	0.4	171 μ m	0.3	268 μ m
RD 20+000	0.7	150 μ m	66.1	53 μ m
RD30+000	70.8	24 μ m	87.7	27 μ m
RD40+000	98.1	22 μ m	96.7	28 μ m
RD60+000	94.9	11 μ m	99.8	23 μ m
RD80+000	98.1	14 μ m	99.9	27 μ m
RD97+000	85.9	21 μ m	81.5	10 μ m

Table 3: bed samples in the earthen portion of CRBC

Obviously, the sand deposits first, then the silt and the clay.

2.4.1.2 General behavior

The following figures present the bed variations between 1987 and 1993:

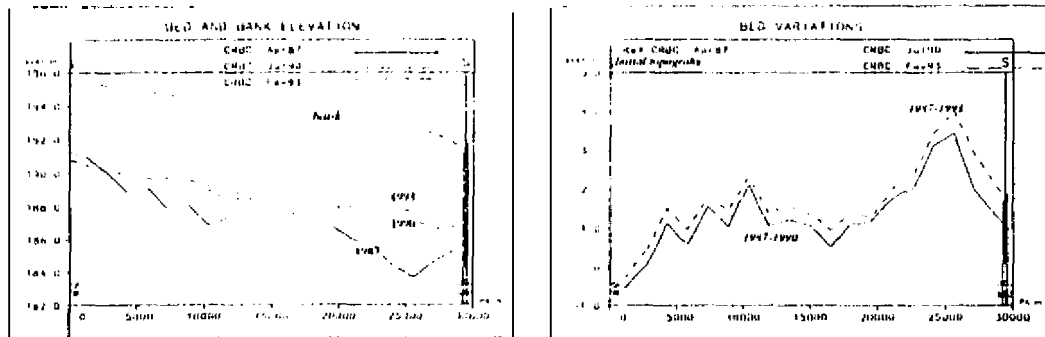


Figure 2.4-1: bed evolutions for CRBC (April 87, July 1990, February 1993)

The other bed topographies are presented in appendix 4.

For the whole period of study, the canal had a tendency to siltation (up to 4 meters of deposition between 1987 and 1993 downstream from the reach).

date	RD1-RD51	RD51-RD98
April 1987	19	32
March 1989	43	50
February 1991	47	44
June 1992	43	46

* general variables: the following table gives some values of hydraulic and sedimentologic parameters, measured at RD51 for 1991. These variables should help to characterize the type of sediment transport (refer to literature review).

Discharge Q (m ³ /s)	Area A (m ²)	Hyd. rad. R _h (m)	Width/ depth	1000.J	Shields Y	u*/w
50	116	2.14	24	0.08	0.66 (d=150 μ)	2.0 (d=150 μ)
					1.99 (d=50 μ)	18 (d=50 μ)
65	122	2.26	22	0.09	0.82 (d=150 μ)	2.2 (d=150 μ)
					2.47 (d=50 μ)	20 (d=50 μ)
80	127	2.33	22	0.10	0.94 (d=150 μ)	2.4 (d=150 μ)
					2.83 (d=50 μ)	21 (d=50 μ)

Table 5: typical hydraulic variables for CRBC

According to Ramette criterion, we should always remain superior to the threshold of motion and suspension should be dominant. Dunes and ripples might also appear.

2.4.2 Chashma Jhelum Link Canal

2.4.2.1 Collected data

The cross sections were measured with a maximum spacing of 5000 ft (1524 m) in August 1981, January 1982, January 1983 and May-June 1984. In the same time, three bed samples were taken at each cross section (left bank, middle and right bank).

The sedimentologic and hydraulic variables were measured at RD1Y0 and RD315 (suspended sediment concentration [boiled samples] and water level) and RD289 (water level, suspended sediment concentrations [with a depth integrative sampler], bed material composition).

* Type of data:

- cross sections (see example in appendix 5)
- bed material sampling: the grain size distribution is given for particles coarser than 62 μ m
- suspended sediments: several classes of particles are distinguished: clays (0-2 μ m), fine silts (2-31 μ m), coarse silts (31-62 μ m), and sands (62-88 μ m, 88-125 μ m, 125-175 μ m, 175-250 μ m).

These campaigns were made for each period of quasi steady flow.

- hydraulic variables: discharge at head regulator, rating curves at RD180 and RD315, water surface levels from RD289 to RD300.

2.4.2.2 General behavior

Chashma Jhelum Link canal tends to undergo problems of scouring. In 1978, the bed level was 2 feet (61 cm) lower than the design bed level in several parts and almost 1 foot lower in average.

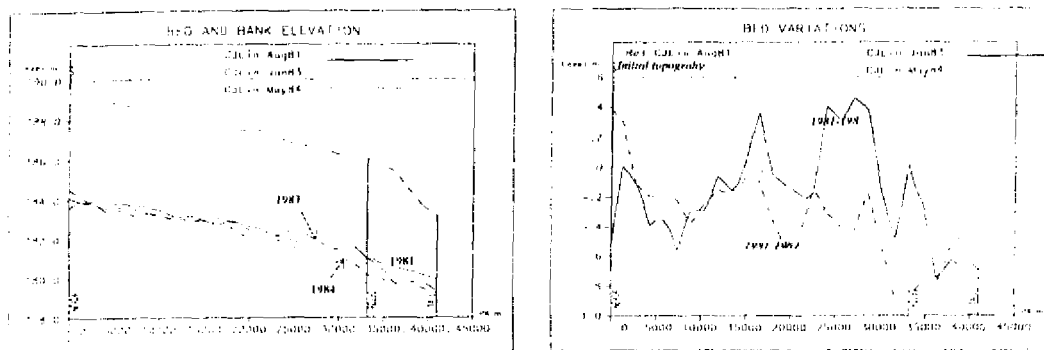


Figure 2.4-2: medium bed evolution between 1981 and 1984

In 1981, the bed level was 1 to 3 feet (0.3 to 0.9 m) below the design level, and from 2 to 5 feet (0.6 to 1.5 m) in May 1984 for the last reach. One major reason was the lowering of the tail crest.

We observe an important raising of the bed level in May 1924 at the tail (3 feet, 0.9m). Such important modifications largely affect the rating curve at the tail regulator (downstream condition for SIC model).

2.4.2.3 Characteristic variables

* Discharges: the discharges are measured every day at the head regulator of CJ Link Canal (RD0). The are represented in appendix 3.

* Strickler calibration

date	RD180-RD290	RD290-RD315
25/09/81	38	32
03/01/82	35	35
16/02/83	34	33
18/06/84	33	40

Table 6: Strickler coefficients for CJ Link Canal

We should notice thst those coefficients are stable in the period of study. They are hardly comparable with the theoretical skin Strickler coefficient, namely $21/0.00019^{0.166} = 87.6$.

* downstream condition

It is given by the rating curve calculated from the observed discharges and levels at the tail regulator (RD315). Therefore, it is assumed constant between 1981 and 1984 (thus between the two stages of the tail crest lowering). It would be preferable to update it regularly in case of important bed modifications.

* sediments: the medium diameter of the bed material varied from 0.150 mm to 0.200 mm between 1981 and 1984 but can be considered uniform all along the canal in a first approximation. The average (in time and space) medium diameter is consistent with (he design one (0.190 mm).

Considering that scouring is the predominant phenomenon, the relevant grain size distribution will be the one of the bed. Bed samples at RD290 show a good homogeneity for the bed material particles.

The dispersion coefficient $(D_{84}/D_{50} + D_{50}/D_{16})/2$ varies from 1.2 to 1.6 between 1981 and 1984, which allows us to consider D_{50} as representative enough. This medium diameter varies between 0.150 and 0.216 mm

Therefore, the bed material load will be represented by the sands only. Since silt and clay are not available in the bed material, they will be classified in the wash load and their concentration will be assumed constant.

- Evaluation of the bed forms and type of transport

The following table gives the values of average variables for a range of discharges:

Discharge Q (m^3/s)	Area A (m^2)	Hyd. rad. R_h (m)	Width/ depth	$1000.I$	Shields γ	n^*/w	C^* (g/l)
100	210	1.73	69	0.11	0.56	1.25	0.031
200	307	2.47	49	0.12	0.90	1.60	0.070
300	385	3.02	40	0.13	1.20	1.84	0.112
400	451	3.47	35	0.14	1.49	2.05	0.161
500	511	3.88	31	0.15	1.76	2.22	0.208
600	565	4.22	28	0.16	2.03	2.39	0.265

Table 7: Characteristic variables for a range of discharges.

NB: C^* is a capacity a transport calculated with Ackers-White formula.

According to the criterion of Ramette (ref. [19]), we should observe sand waves (dunes and ripples) and both suspension and bed load should be present.

In the same way, w/u^* is in the range 1 to 2.5: suspension should be dominant according to the criteria of Bagnold or Van Rijn.

- width/depth ratio: the width/depth ratio is always superior to 20 which may suggests the possibility of sand banks (Yalin 1992, ref. [24]). It is confirmed by the observation of the cross sections.

2.5 Summary

2.5.1 data

- we dispose of a large set of data for the two studied systems. Yet, the period of observation for Chashma Jhelum Link Canal (three years) is quite short.

- we are not able to associate an accuracy to the sedimentologic data, but this inaccuracy might be very high for the concentrations which are not easy to assess in natural conditions, especially in case of high sediment loads (high temporal variability).

- the accuracy on the topographies is probably much better. However, we cannot expect a centimetric accuracy. Since the cross sections are measured at a length step of 5000 feet (1524 m), bed variations at a shorter length step will not be analyzed.

2.5.2 Modeling

- the sediments encountered in Chashma Right Bank Canal and Chashma Jhelum Link Canal are very fine. For Chashma Right Bank Canal, both sands and silts seem to deposit, whereas only sands seem to be scoured in Chashma Jhelum Link Canal.

We will fix a limit of 62 μm for wash load for Chashma Jhelum Link Canal (as usually done in Pakistan); this limit will be calculated according to an energetical criterion for Chashma Right Bank Canal.

- in both canals, the sediments seem to be transported mainly in suspension: we will prefer a model of concentration.

3. Presentation of the simulation tool

This part presents the different components of the sediment transport model. In the first paragraph, the general algorithm is presented. Each of the different components of this algorithm are presented **afterwards**. Paragraph 2 deals with the hydraulic model whereas paragraph 3 presents the modeling of the concentration calculation. Paragraph 4 deals with the bed evolution. In paragraph 5, we show **how the** grain size distribution is utilized in the model. Finally, this part is ended by **a** sensitivity analysis.

3.1. *Combination of the hydraulic and sedimentologic models*

3.1.1. required outputs of the model

The sediment transport model **should be** able to predict:

- the evolution of **the** bed, so as to observe changes in **the** conveyance capacity;
- **the** volumes that would deposit in a reach, since the costs for maintenance are directly linked to **the** volumes to be dredged out.

The concentration in itself is not as essential for the water manager (**but might be** for the farmer who may prefer to receive a high amount of silt in plot). However, the concentration has to **be** known if we want to integrate **the** sedimentologic problem to a whole irrigated perimeter.

Let us remark that both quantities (concentrations and volume of sediments) **are** linked, but one is instantaneous and local (concentration) whereas the other one is integrative (in time and space).

3.1.2. General algorithm

In this work, we have chosen to consider **a** period of simulation as a succession of periods of steady flow, in which the sedimentologic and hydraulic data are assumed constant. The **geometry** of the channel is updated at the end of each period of steady **flow**.

The main reason of this choice **is** its feasibility from an operational point of view. First, we **want** to simulate long terms (several years): technically, it is not easily feasible with the **unsteady flow** model right now. Second, we **do** not dispose of sufficient data to have a realistic picture of **the** imposed discharges: we have no choice but to use **averages**, thus **to** assume the existence of steady **flow** periods. Nevertheless, **we** expect realistic tendencies through this simplification, which will be checked after the computation of the unsteady flow model in the future.

The following scheme summarizes the procedure of calculation for one simulation:

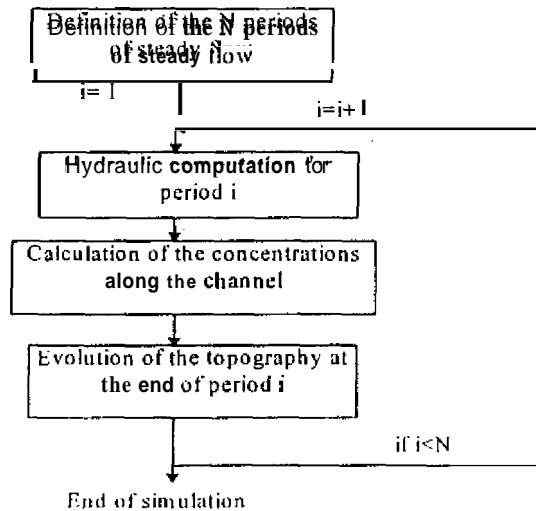


Figure 3.1-1: General algorithm for the bed evolution modeling

Thus the hydraulic and sedimentologic models are only **partially combined**: for each **period** of steady flow, the hydraulic variables are **first calculated** (from downstream to upstream of the studied [each], and these variables are used then for **the sediment transport calculation** (which is made **from upstream to downstream**). The simulated geometry is used for the hydraulic computation of the next period.

3.2. Presentation of the hydraulic model SIC

In the following, the hydraulic resolution will only deal with free surface and tranquil flows in canals. Shooting flows are also acceptable at the devices. Steady and unsteady flow computations are possible, but this Master study will be limited to steady flow conditions.

Because of the regularity of the irrigation canals, the flow is always assumed one-dimensional, which gives a simple and efficient hydraulic simulation tool.

3.2.1. Theoretical equations

The basic system of equations for the *water flow* are the equations of Saint-Venant ID. They are projected on the longitudinal axis x (direction of the flow):

- mass conservation:

$$\frac{\partial}{\partial t} S + \frac{\partial}{\partial x} Q = q \quad [\text{Eq. 3.2.1}]$$

where S is the wetted area, Q the discharge and q the lateral discharge

- dynamic equation:

$$\frac{\partial Q}{\partial t} + \frac{\partial UQ}{\partial x} + gS \frac{\partial h}{\partial x} = gS(I - J) + \varepsilon q U \quad [\text{Eq. 3.2.2}]$$

where U is the flow velocity (x direction) ($U=Q/S$), h the water depth, g the acceleration due to gravity, I the slope of the bed, J the slope of the energy line (hydraulic gradient) and ε being equal to 1 if the lateral discharge is positive, 0 otherwise.

In steady flow and for a uniform canal, this system can be simply written as follows:

$$\frac{dh}{dx} = \frac{I - J}{1 - Fr^2} \quad [\text{Eq 3.2.3}]$$

where Fr is the Froude number of the flow $Fr = \sqrt{Q^2 L / gS^3}$ (L width of the free surface)

I is given by Manning-Strickler formula $J = Q^2 / (K^2 S^2 R_h^{2/3})$ (R_h hydraulic radius, K Strickler coefficient)

• Geometry computation: all shapes of cross sections are acceptable but SIC transforms the geometric data into a bijective relationship between the width and the elevation:

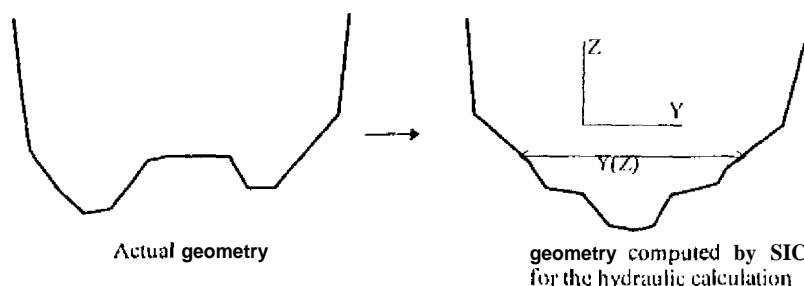


Figure 3.2-1: actual geometry computed by SIC

This procedure is appropriate for the one-dimensional hydraulic modeling but may be criticized for the sedimentologic point of view (a non-homogeneous evolution of the cross section could not be modeled properly).

3.2.2. Numerical resolution

- steady flow: the integral equation Eq. 3.2.3 of free water surface is solved according to a Gauss scheme;
- unsteady flow: the equations of Saint-Venant Eq 3.2.1 and Eq 3.2.2 are solved directly according to a Preissmann implicit scheme of resolution (finite differences).

3.3. Modeling of sediment transport

This part presents the calculation of the new topography after a period of steady flow. As explained before, we assume that all the hydraulic variables have been calculated on the geometry of the beginning of the period.

3.3.1. Physical approach

3.3.1.1. global approach

We have to calculate the concentrations and the bed evolutions. Both are linked since the decrease of the concentration produces deposition of the bed. We can observe this link from the mass conservation of the sediments:

$$\phi = (1 - p) \frac{\partial S_b}{\partial t} = \frac{\partial Q_s}{\partial x} \quad [\text{Eq.3.3.1}]$$

where S_b is the variation of the bed cross section at abscissa x , ϕ the term of sediment exchange between the bed and the flow, p the porosity

and with

$$Q_s(x) = \frac{1}{\rho_s} Q(x) \cdot C(x) \quad [\text{Eq.3.3.2}]$$

In a first step, the concentrations $C(x)$ will be **calculated** at each **abscissa**. The bed evolution will be obtained after an immediate integration with respect to the time.

3.3.1.2. Evolution of the concentrations

We assumed that the main mode of transport was suspension. As presented in the literature review, we have to take into account the presence of *wash load* which is not supposed to be in interaction with the bed.

Two options can be selected:

⇒ we assume that we know the limit for wash load: it can be defined by the user. Typically, it is fixed to 62 microns in Pakistan (limit between silt and sand);

⇒ we can use Wang criteria (ref.[22], literature review), which is the energetic criterion

$w(\text{particle}) < U_{*c}$: the particle is considered as *wash load* (NB: w is the fall velocity).

$w(\text{particle}) \geq U_{*c}$: the particle belongs to the *bed-material load*.

In this study, we will assume that:

- given hydraulic conditions and a size of sediments, there exists a capacity of transport for the bed material load: in a *uniform reach*, the concentration of bed material load should tend towards an **equilibrium concentration** (or *capacity of transport*).
- there exists a law to model the convergence towards the equilibrium concentration (*loading-law*);
- the bed material load sediments are taken in a whole and are represented by their medium diameter d_{50} .

Figure 3.3-1 shows the longitudinal evolution of the two types of sediments:

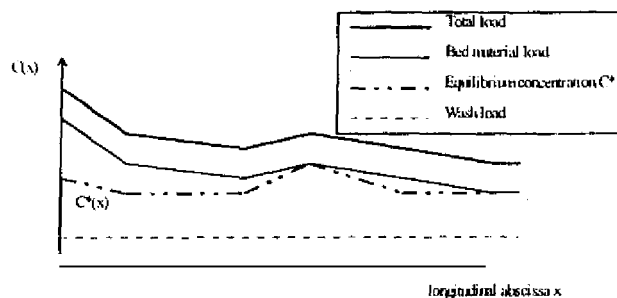


Figure 3.3-1: evolution of the concentration along the canal

3.3.2. Modeling of the concentration evolution

This part deals with the modeling of the **bed material load** concentration. The **wash load** concentration is assumed to be constant (**thus we consider that the wash load cannot flocculate**).

3.3.2.1. Convection-diffusion equation

When suspension is dominant, a model of concentration is more appropriate. This model will be **based** on the convection-diffusion **equation**:

$$\frac{\partial C}{\partial t} + V_c \frac{\partial C}{\partial x} - \frac{I}{S} \frac{a}{\partial x} \left[SK_c \frac{\partial C}{\partial x} \right] = \phi / h \quad [\text{Eq. 3.3.3}]$$

The first term represents the variation of concentration at a given abscissa, the second is the convective term, the third the diffusive term and the right side of the balance is the exchange term between the suspended phase and the bed.

This equation is not easy to address in an operational point of view since we need two boundary conditions to solve it. In the following we try to show that it is sensible to neglect the diffusion phenomenon.

[Let us note

$v = X.u$ with X longitudinal length scale

$V_c = V_0.v$ with V_0 average velocity of the flow

$C = C_0.w$ with C_0 average concentration

$S = S_0.s$ with S_0 average wetted area

$K_c = K_0.c$ with K_0 average diffusion coefficient

$h = H_0.y$ with H_0 average depth of the flow

$E = \phi/h = E_0.e$ with E_0 mean value for E .

u, v, w, s, y and e bring dimensionless variables.

To assess E_0 we can assume that the proportion k of the sediments entering a reach of length X will deposit. Under this hypothesis, we have

$E_0 = k.(Q_s \text{ entering the reach})/(\text{volume of the reach})$

thus $E_0 = k.C_0.V_0.S_0/(X.L_0.H_0)$ where L_0 is the average width.

This term reduces to $E_0 = kC_0.V_0/X$

Neglecting the temporal variations (we are still in steady conditions), the convection-diffusion equation writes as follows in a dimensionless shape:

$$\frac{dw}{du} - \frac{K_0}{X.V_0} \frac{d}{s.c.} \left[\frac{dw}{du} \right] = k.e \quad (1) \quad (2) \quad (3)$$

At this stage we can compare the orders of magnitude of the different terms.

We can easily compare (1) and (2) since they both linearly depend on $\frac{dw}{du}$ which is unknown at this stage.

After Cunge et al. (Ref. [3]) K_c can only be obtained from calibration. However, Fischer, Liu and Tackelson propose different formulae to assess K_c (refer to the literature review). These parameters are assessed for typical conditions in CRBC and CJ Link:

Canal	Q (m ³ /s)	S (m ²)	U (m/s)	u* (m/s)	W (m)	Rh (m)	K _c /U Tackelson- Frenkel (m)	K _c /U Liu (m)	K _c /U Fischer (m)
CRBC	50	116	0.43	0.034	53	2.14	2.7	63.6	152.4
CRBC	80	127	0.62	0.046	53	2.33	2.6	48.8	162.5
CJLink	300	385	0.78	0.059	121	3.02	3.2	203.3	704.3
CJLink	600	565	1.06	0.076	118	4.22	4.3	153	505.3

Table 3.3-1: different values of the diffusion coefficient

The coefficients given by Tackelson and Frenkel show that the diffusion would be significant for a length step of a few meters.

Fischer's formula (applied to CJ Link) would impose a length step of a few kilometers if we wanted to neglect the diffusion.

For both canals, we selected a length step of $X=800$ meters (for the geometry and the hydraulic computations) and we will consider that $K_c/U.X$ is negligible with respect to unity. This approximation may not be true in some cases (CJ Link for instance) and the sensitivity to the diffusion coefficient should be analyzed.

In other terms, we will say that the convection process is sufficient to characterize the evolution of the concentration, the diffusion modifying the suspended sediment distribution at a scale which is not relevant for our study.

Thus we have the very simple relationship

$$\frac{d\psi}{du} = k \cdot e^{-\psi/h}$$

In a dimensional **form**, and assuming that the **particles** have the same velocity as the flow

$$\frac{dC}{dx} = \phi / h$$

differential equation of the **first order** which needs only one boundary condition to be solved.

3.3.2.2. Equilibrium laws

Six equilibrium laws can be used to represent the capacity of transport:

- (1)- Engelund-Hansen
- (2)- Ackers-White
- (3)- Karim-Kennedy (1990)
- (4)- Karim Kennedy (1981)
- (5)- Yang
- (6)- Bagnold.

Since **these** laws were not calibrated for so fine sediments, we introduce a corrective factor β (calibration parameter) which modifies the equilibrium concentration as follows:

$$C^*(model) = \beta \cdot C^*(original formula)$$

except for Bagnold law **which** contains two coefficients to calibrate.

The normal values for β is 1. **for** the laws (1) to (5) and [$\beta_1=0.17$, $\beta_2=0.01$ when $Y>1$ and for sands $<500\mu m$]

These laws are presented in appendix and in **the** literature review.

The adjunction of other **laws** is easy.

3.3.2.3. Exchange laws

* **cohesiveless** sediments:

We will use Han's law which has been **presented** in the literature review

$$\frac{\partial C}{\partial x} = \alpha \frac{w}{u^*} [C^* - C] \quad [Eq.3.3.4]$$

$K = \alpha w / u^*$ is the inverse of a distance. $L = 1/K$ represents the adaptation **length**, namely a characteristic length for the actual concentration to reach **the** equilibrium concentration.

In the model, α **has** to be calibrated. Different parameters **for** erosion or deposition can be chosen:

- if $C > C^*$: $\alpha = \alpha_d$ (deposition)
- if $C < C^*$: $\alpha = \alpha_e$ (erosion)

Any other formulation **for** the coefficient K (or the adaptation length) **could** be easily computed.

* **cohesive** sediments:

The **chosen** models will **be** Krone and **Partheniades** models (refer to literature review). The critical shear stresses have **whatsoever** no link with **with** Shields ones

3.3.2.4. Numerical resolution

In steady conditions (for each **time step**) we have to solve the following equation which determines the concentration longitudinal distribution:

$$\frac{\partial C}{\partial x} = K(C, U, J, v, \rho, \rho_s, h, d_{50}) [C^* - C] \quad \text{(general formulation). [Eq. 3.3.5]}$$

where C^* is the equilibrium concentration.

[NB: In Han's formulation, K only depends on the shear velocity of the flow and the fall velocity of the particles]

The sedimentologic variables are calculated from upstream to downstream reach after reach.

The concentration C_0 at the head of the reach is required.

Knowing the concentration C_i at location x_i we can calculate the concentration C_{i+1} at abscissa x_{i+1} :

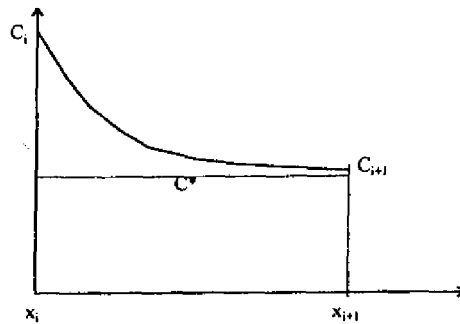
- we assume that the parameter K is uniform on $[x_i, x_{i+1}]$; K is taken as the mean value between K_i and K_{i+1}

- we assume that the equilibrium concentration C^* is uniform on $[x_i, x_{i+1}]$; C^* is taken as the mean value between C^*_i and C^*_{i+1} .

Thus [Eq. 3.3.6] can be solved analytically on $[x_i, x_{i+1}]$:

$$C(x) = C^* + (C_i - C^*) \exp(-K(x - x_i)) \quad \text{[Eq. 3.3.6]}$$

which gives the concentration at abscissa x_{i+1} :



and for the whole reach:

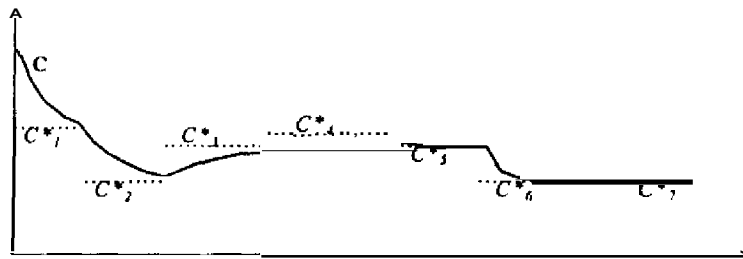


Figure 3.3-2: modelled concentration for the bed material load

3.4. Bed evolution

3.4.1. Longitudinal evolution

3.4.1.1. Equation

The integration of Eq. 3.3.1 with respect to the time for the period of **steady flow and steady concentration** writes as follows:

$$\Delta S_b(x) = \frac{T}{\rho_s(1-p)} \cdot \frac{d}{dx} [Q(x) \cdot C(x)] \quad [\text{Eq.3.4.1}]$$

where **T** is the duration of the period, **p** the porosity of the sediments, **Q** the discharge, **C** the total concentration (thus $Q(x) \cdot C(x)$ is the solid discharge in weight), ρ_s the specific weight of the sediments.

3.4.1.2. Numerical resolution

From Eq.3.3.2 and Eq 3.3.6 we can calculate the volumetric solid discharge at abscissas x_i , x_{i+1} and x_{i+2}

From Eq. 3.3.1 we calculate the deposition velocity ϕ_{i+1} at x_{i+1} with the centered derivative

$$\phi_{i+1} = \frac{1}{2} \frac{Q_{i,i+1} - Q_{i,i+1}}{\Delta x} + \frac{1}{2} \frac{Q_{i,i+1} - Q_{i,i}}{\Delta x} = \frac{1}{2} \frac{Q_{i,i+2} - Q_{i,i}}{\Delta x}$$

Thus from Eq. 3.3.1 we deduce the variation of section during the period of steady flow:

$$dS_i = \phi_i \cdot \Delta t / (1 - p)$$

This is the global variation of area for section i .

Another method would be to solve explicitly Eq.3.4.1:

$$\rho_s \frac{\partial Q}{\partial x} = C \frac{\partial Q}{\partial x} + Q \frac{\partial C}{\partial x}$$

Both terms can be calculated separately. In particular, the second term can be directly obtained from Eq. 3.3.6 (without discretization). The first one is also obtained directly if the loss by **seepage** is known. However our formulation gives a greater flexibility in the choice of the loading law (for further improvements).

3.4.2. distribution of scouring or siltation in the cross section

3.4.2.1. Method

The previous calculation gives a global variation for each section. This variation must be distributed on the whole bed and this is a complex problem since it depends on various factors:

- alternate sand banks can appear on the minor bed (cross sections will be shown in appendix);
- the ability for the particles to deposit on a surface depends on the slope of this surface. Therefore the characteristics of the banks or the presence of bed irregularities should be taken into account;
- the mechanisms of deposition or erosion depend on the lateral distribution of the shear stresses, of the suspended sediments... For instance, the coarsest particles will preferentially move in the lowest parts of the bed whereas the finest ones will tend to deposit near the banks where the flow velocity is lower.
- berms may artificially be provoked to stabilize the banks...

Taking into account all **these parameters would go** beyond the **purpose** of this study. As a consequence, **we have chosen** a simplified modeling based on visual considerations.

From the visualization **of the evolution** of **the cross sections** of Chashma **Right Bank Canal** and **Chashma Jelhum Link Canal** (ISRIP data), **we can** make a few remarks:

- (1) deposition and erosion **occur** on the whole wetted perimeter, even on the banks;
- (2) the bed variations are **most** of the time higher in the lowest **parts**;
- (3) alternate sand banks **can** appear even on initially flat **cross** sections.

We will not try to **reproduce** remark (3). To represent remarks (1) and (2), we will **spread the variation of area** in the cross section *proportionally to the water depth*. **If we note** y the transverse abscissa, $h(y)$ the water depth during the period of steady flow (from time t_i to time t_{i+1}), $z(y)$ the bed elevation at **abscissa** y , then **we will assume**

$$\Delta z(y)_{i+1}^{i+1} = \alpha \cdot h(y)$$

which is illustrated on the following **figure**:

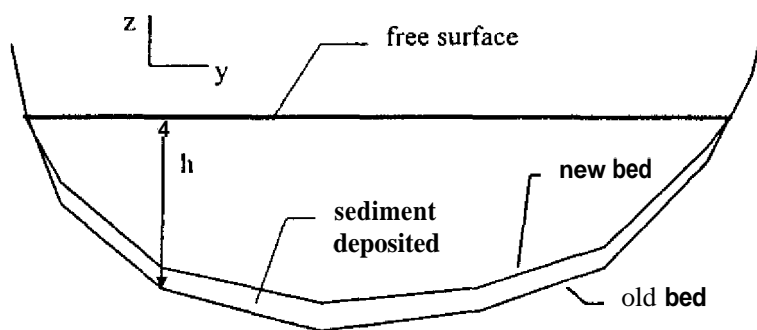


Figure 3.4-1: distribution of the sediments over the cross section

Integrating **over** the whole **cross** section,

$$\int_{y_{\min}}^{y_{\max}} \Delta z(y) \cdot dy = \int_{y_{\min}}^{y_{\max}} \alpha \cdot h(y) \cdot dy$$

and we finally obtain

$$\alpha = \Delta S/S$$

and

$$\Delta z(y) = h(y) \cdot \Delta S/S \quad [\text{Eq. 3.4.2}]$$

[If we had to justify our assumption, we would just say that

- we consider that the flow velocity is homogeneous in the cross section;
- scouring is proportional to the total shear stress thus to the water depth;
- deposition at the transverse abscissa y is proportional to the quantity of sediments available at this abscissa thus to the water depth $h(y)$ also]

3.4.2.2. suggestions for validation of this hypothesis

3.4.2.2.1 sensitivity analysis

To validate the consistency of the chosen method, we could apply different procedures of modification of the geometry, described on the following figures, such as:

- spreading the variation of section uniformly on the **wetted** perimeter (1);
- Filling the lowest part of the bed (in case of deposition) (2);
- spreading the variation on half of the **bed** (creating sand banks) (3);

...

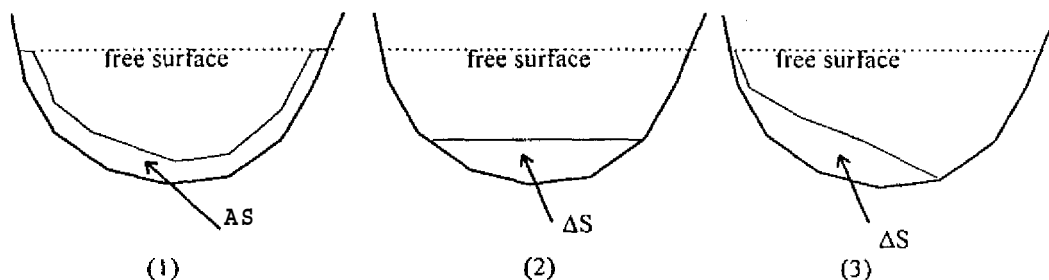


Figure 3.4-2: different types of distribution

3.4.2.2.2. empirical approach

Let us **assume** that we are looking for a relationship $\Delta z = F(X_1, X_2, X_3, \dots)$ where the variables X_i are **supposed** to be linked to the process of evolution (typically the water depth, the **wetted area**, the shear stress...) under the **constraint** of material conservation, The simplest form for F will be:

$$F(X_1, X_2, X_3, \dots) = \lambda X_1^{a1} X_2^{a2} X_3^{a3} \dots$$

Disposing of a **large set** of cross sections for a given canal but **at** different dates, we could plot the bed elevation variations Δz with respect to the **variables** $\ln X_i$, and **determine** the coefficients $\lambda, a1, a2, a3 \dots$ thanks to a multiple regression.

Here, for instance, we could **plot** the bed variations with respect to the products $h \Delta S / S$. This procedure is quite long (identification of the water level for each pair of compared cross section, calculation of the ratios $\Delta S / S \dots$) and **has not** been done in this study.

3.4.2.3. Numerical resolution

The relationship $\Delta z = \Delta S / S$ is also valid in the finite elements context and produces a simple algorithm for the modification of geometry:

- first we **create** two new points on the old geometry, at the **water** surface elevation;
- the elevation of each point located below the water surface is **moved** by dz , calculated from Eq. 3.4.2.

3.5. Definition of the bed material load concentration

3.5.1. General

Two options are available in the model: the limit for wash load can be defined by the user, or if unknown, it can be calculated with Wang criterion (see 3.3.1.2) $w(\text{limit for wash load})=U.J$. The corresponding critical diameter is calculated from Stokes formula (refer to literature review)

$$w = \frac{g\Delta d^2}{18\nu}$$

and its reciprocal

$$d = \sqrt{\frac{18\nu}{g\Delta} w}$$

Thus we have to know the grain size distribution to determine the concentrations for wash load and for bed material load.

In the equilibrium and loading laws, the sediments (bed material load) are represented by their medium diameter, noted d_{50} . This characteristic can be easily determined if we know the grain size distribution of the bed material load:

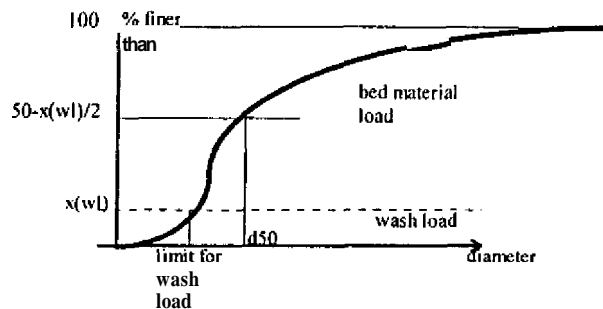


Figure 3.5-1: grain size distribution

In the following, we will note $f(d)$ the **distribution function**, namely the percentage of particles finer than the diameter d .

Let us remark that

* $f(0)=0$ and $f(d)=1$ for d superior to the maximum diameter of the sediments.

* if C_{sa} , C_{si} and C_{cl} are respectively the concentrations in sand, silt and clay, and $d_{s/si}$ and $d_{si/cl}$ the limits between these three classes, then we have the two constraints:

$$f(d_{s/si}) = (C_{si} + C_{cl}) / (C_{sa} + C_{si} + C_{cl})$$

$$f(d_{si/cl}) = C_{cl} / (C_{sa} + C_{si} + C_{cl})$$

3.5.2. Choice of the distribution functions

To be fully rigorous in our simplified approach, we should know at each time step and each abscissa the medium diameter for the bed material load (through the grain size distribution). To preserve the simplicity of the model, we will choose a constant shape of the grain size distribution function f for a whole period of simulation, in time and space, but we will respect the constraints mentioned above. Thus the full information on the grain size distribution will be given by the proportions of sand, silt and clay, which can vary in time and space.

For instance, we could choose for **f** the only polynomial function (of **degree 3**) that **respects**:

- * $f(0)=0$
- * $f(d_{silt})^3 = C_{cl}/(C_{sa}+C_{st}+C_{cl})^3$
- * $f(d_{silt}) = (C_{st}+C_{cl})/(C_{sa}+C_{st}+C_{cl})$
- * $f(d_{max})=1$

Let us assume that we also know the **medium diameters** inside each class of particles (sand, silt and clay). Then we have three more constraints to **respect**, and a sixth degree polynomial function **could** be chosen. This interpolation has the advantage **to be** infinitely smooth, but is largely dependent on the value of d_{max} which is not easy to assess and is not a representative parameter of the sediments.

In the model, we consider that **each class** of particles can be represented *independently* : we know the limits of the class and the medium diameter inside this class, so we just have to find a curve that respects these **three** constraints:

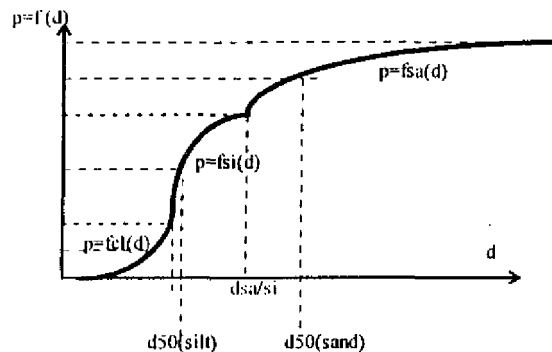


Figure 3.5-2: grain size distribution functions

* Distribution function for silt and clay:

These two classes **present** the advantage to have **well** identified upper and lower limits, noted d_{min} and d_{max} . We will **choose** for them a power function $f(d) = [\lambda(d-b)]^\alpha$ where λ and α have to be chosen so as to **respect** the three constraints inside the class. Writing these constraint, we **clearly must have**

$$b = d_{min}$$

$$\lambda = 1 / (d_{max} - d_{min})$$

$$\alpha = \ln 2 * \ln((d_{max} - d_{min}) / (d_{50} - d_{min}))$$

* Distribution function for sand:

To **avoid** fixing an arbitrary upper limit for this class, we are looking for a function that **converges** towards 1 when d is infinite. Thus we **propose**

$$f(d) = \lambda (1 - \beta \cdot \exp(-\alpha(d - d_{min})))$$

Respecting the constraints, we must **have**

$$\beta = 1$$

$$\lambda = 1$$

$$\alpha = \ln 2 / (d_{50} - d_{\min})$$

These functions are **easy to** compute but the method presents **the** drawback to be discontinuous at the limits between classes.

3.5.3. Using actual data (examples)

* analytic resolution

Some sets of data **give** concentrations for **5** classes of particles:

- C₁: 0-5 microns
- C₂: 5-50 microns
- C₃: 50-62 microns
- C₄: 62-177 microns
- C₅: above 177 microns.

Let us **show how** it is **possible** to assess **the** medium diameter for **silt** (5-62 microns) and sand:

For silt, **we are** looking for the distribution function $f(d) = ((d-5)/(62-5))^a$

But **we** know that $f(d=50\mu\text{m}) = C_2 / (C_2 + C_3)$ (percentage finer than **50** microns inside the class **5-62** microns); thus the value of **a** is given by

$$\alpha = \ln[f(d=50\mu\text{m})] / \ln[(50-5)/(62-5)]$$

The medium diameter d_{50} is then assessed **by** solving the equation $f(d_{50}) = 0.5$

For **sand**, we have

$$f(d) = 1 - \exp(-\alpha(d-62))$$

For $d = 177$ microns, **we** must have $f(d=177\mu\text{m}) = C_4 / (C_4 + C_5)$

which **gives**

$$\alpha = -\ln[1 - f(d=177\mu\text{m})] / (177-62)$$

which allows to calculate d_{50} such as $f(d_{50}) = 0.5$

This procedure appears complicated but is actually easy to compute. It allowed to use all the information **from** a set Concentration data.

• if **we** have **more** information inside a class

We can also determine analytically the polynomial function that best fits the different informations. Practically, it is simpler **to** represent the grain size distribution and to determine **the** medium diameter graphically:

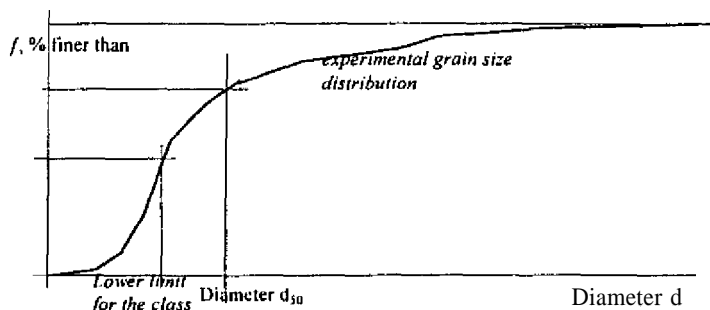


Figure 3.5-3: graphical determination of the medium diameters

3.6. Sensitivity analysis

3.6.1. Objectives and method

The objective of this part is to analyze the response of the model to errors on some input data. We have limited the study to the following parameters:

- discharge;
- water surface levels at a tail regulator;
- Strickler coefficients;
- head concentrations;
- grain size distribution.

The method consists in modifying one input data by a relevant quantity, and observing the influence of this modification on the bed evolution. We assume the linearity of the response:

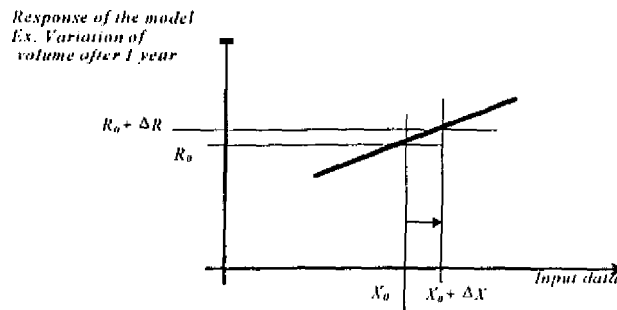


Figure 3.6-1: response of the model in the linear approximation

To correctly observe the influence of one parameter, the influence of the other ones must be minimized, thus assumed constant.

In the following, the response will be observed through the variation of volume for the reach (eroded or deposited) after one year of simulation (considering that it is a relevant quantity for the canal manager).

We will use a simplified canal dimensioned similarly as Chashma Right Bank Canal (so that we have consistent outputs). This theoretical canal will also be used in part 5 for water management strategies. The characteristics of this theoretical canal are the following:

- design discharge : $Q_{\max} = 130 \text{ m}^3/\text{s}$
- initial slope : $1=1/8000$
- length: 41 km
- downstream regulator: located at the reduced distance 40 km
adjustable gate in order to control the water level
- design cross section:

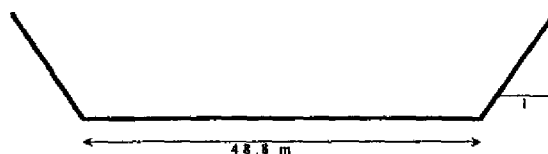


Figure 3.6-2: cross section of the flume

- Strickler coefficient: 50
- average concentration at head: 0.650 g/l (0.200 g/l for silt and sand, 0.250g/l for clay);
- average discharge: 70 m³/s
- **reference** level at the regulator :3.10m
- equilibrium law: Engelund Hansen
- loading law: Han; parameters: $\alpha_d = \alpha_c = 0.001$
- medium diameters: 2 μ m for the class 0-5 μ , 20 μ m for the class 5-62 μ m and 150 for coarser particles
- porosity: 0.30; specific weight of the sediments: 2650 kg/m³; kinematic viscosity: 10⁻⁶ m²/s
- time step: 32 days (for the updating of the geometry)
- space step: 1000m

<i>Variable</i>	<i>initial value</i>	<i>modified value</i>	<i>Modification (input)</i>	<i>volume variation after one year</i>	<i>% of modification (output)</i>
none			none	241.000 m ³	0 %
discharge	Q=70 m ³ /s	Q=77 m ³ /s	+10 %	229.000 m ³	-5.9 %
regulated level	Z=3.10 m	Z=3.00 m	-10 cm	227.000m ³	-6.0 %
Strickler	K=50	K=45	-10 %	220.000m ³	- 12.5 %
Concentration	C=0.650g/l	C=0.715g/l	+10 %	281.000m ³	+15.4 %
Variability of the head concentrations	average on 320 days	average on 32 days	/10	124.000m ³	-105 %
medium diameters	2, 20, 150 μ m	1.5, 15, 120 μ m	-20 %	223.000m ³	-8.7 %

Let us consider the bed variation over one period of steady flow:

$$\Delta S_b(x) = \frac{1}{\rho_s(1-p)} \cdot \int_{t_0}^{t_0+T} \frac{\partial}{\partial x} [Q(x,t) \cdot C(x,t)] dt$$

If Q is steady, then we can write:

$$AS_b(x) = \frac{T}{\rho_s(1-p)} \cdot Q(x) \left\langle \frac{\partial}{\partial x} C(x,t) \right\rangle \quad (\text{Eq.3.6.1})$$

where $\langle \cdot \rangle$ designs the average on the period $[t_0, t_0+T]$,

which is different a priori from

$$AS_{,,}(x) = \frac{T}{\rho_s(1-p)} \cdot Q(x) \frac{d}{dx} \langle C(x,t) \rangle \quad (\text{Eq. 3.6.2})$$

Eq 3.6.1 and 3.6.2. would be rigorously equivalent if the evolution law for C(x) was independent on the time during the steady flow. It is not the case in our approach, since the medium diameter can vary significantly with respect to the time:

- the variation of d_{50} changes the capacity of transport of the flow;
- it also modifies the adaptation length in the loading law.

One way to minimize this aspect would be to model separately the evolution of the different classes of particles, inside which the medium diameter would remain constant in time. For each of the classes, the evolution laws would be steady and average concentrations (over a given steady flow period) would be equivalent to varying ones. The sensitivity to the measurement errors on the concentrations would probably be minimized.

3.7. Summary

We have defined a simple model where several major assumptions will have to be justified or modified:

- succession of steady flow periods;
- suspension is the main mode of transport;
- the bed material load can be represented in a single class of particles;
- one-dimensional modeling is sufficient to represent the global sediment transport and the bed evolution;
- the deposited and eroded particles are of same characteristics: the bed composition (memory of the previous stages of deposition) is not considered.

The next developments of the model will consist in validating these different assumptions. In a first step, we preferred to keep the model simple but test it on actual cases. The observation of the results should allow to orient the future improvements.

4. Calibration and validation

4.7 Integrative or instantaneous calibration?

4.1.1 Instantaneous calibration

The instantaneous calibration would **consist** in calibrating the parameters of the laws with instantaneous data. In our **case**, we would calibrate the evolution laws for the concentrations using the actual concentrations at different abscissa but at the **same** time:

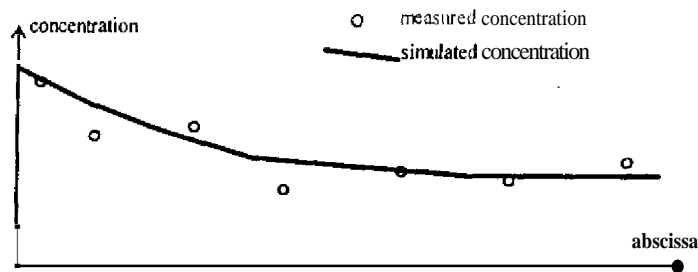


Figure 4.1-1: Fitting simulated concentration to measured data

In practice;

- 1) we define a period of steady flow (hydraulic variables, concentrations and topography are constant);
- 2) for this period, we know the concentrations at different abscissas;
- 3) if the equilibrium stage is reached, the **parameter** for the equilibrium law is easily calculated, and then the parameter for the deposition law (if the concentration is decreasing) or the erosion law (if the concentration is increasing).
- 4) if not, we have to determine the sets of parameters that minimize the distance between the measured and the simulated data.

4.1.2 Integrative calibration

This procedure consists in calibrating the parameters of the laws (which deal with concentrations) with the topographic data. This calibration is related to a period of evolution: it **consists** in minimizing the difference between two geometries, **one** obtained by simulation **from** time t_0 to time t_1 , the second one being the measured geometry at time t_1 . For example, we will compare the bed variations in terms of variation of volume per unit length, which is time integrative:

$$\frac{d\Delta V}{dx} = \Delta S_b(x) = \frac{1}{\rho_s(1-p)} \cdot \int_{t_0}^{t_0+T} \frac{\partial}{\partial x} [Q(x,t) \cdot C(x,t)] dt$$

4.1.3 Choice of a method

Both procedure were used in the preliminary study (Vabre, ref[21]) but they gave significantly different results. It has been concluded that the integrative calibration **was** much more reliable:

- the variability in time for the concentrations can be very high (due to physical variations as well as measurement accuracy), but the variations of volumes are **supposed to** integrate this variability;

Indeed, let us come back to Eq. 3.6.1 for a period of steady flow, but with a variable concentration. We have

$$\Delta S_b(x) = \frac{T}{\rho_s(1-p)} \cdot Q(x) < \frac{\partial}{\partial x} C(x,t) >$$

Thus **if the** quantity $C(x,t)$ is highly variable in time (typically during the periods of high concentrations), the time averaging has the effect to minimize the influence of this variability.

- it **is** not reliable to calibrate two parameters using a low number of measured data (typically three measures of concentration per period of steady flow for the first 30 kilometers of CRBC). When we use one **topography**, we integrate a large set of measurements.

- **even if** it is more logical to calibrate a model of concentration with concentration data, the **important** variables for the managers and **the users** of the systems are the bed evolutions and the volumes to dredge out in case of maintenance, which justifies the relevance of our choice (in other terms it is more relevant to minimize the errors on topography than those on concentrations as far as the users of the systems are concerned).

4.2 Procedure of integrative calibration

4.2.1 Principle

Using the formalism "equilibrium law/loading law", we have three parameters to determine:

- β , multiplicative coefficient for the equilibrium law;
- α_d constant for deposition;
- a constant for erosion.

The best set of parameters is **the** one that minimizes the difference between two geometries, one simulated (S_1) and one measured (M_1).

The comparison between these two geometries is made through a quadratic error function $J(M_1, S_1(\beta, \alpha_d, \alpha_e))$.

The problem consists in finding $(\beta, \alpha_d, \alpha_e)$ that minimize

$$J(M_1, S_1(\beta, \alpha_d, \alpha_e))$$

Graphical representation:

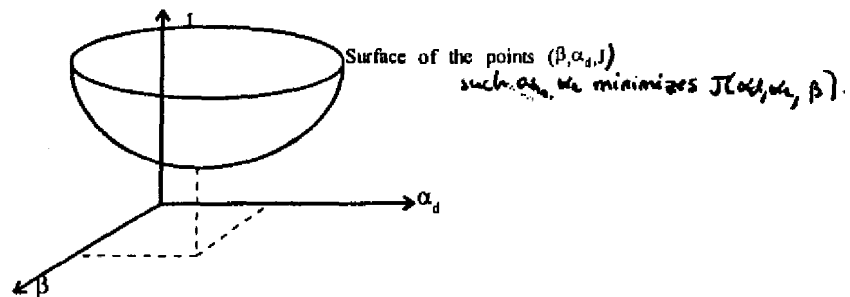


Figure 4.2-1: Minimization of the error function

Comments:

- in practise, **the** parameters **will** be obtained with an inaccuracy $\Delta\beta$, $\Delta\alpha_d$, $\Delta\alpha_e$ (variation steps for the parameters).
- there is a risk to obtain a local minimum for J.

- the method of calibration seems to **be** long because for each pair of parameters β and α_c (for instance), **we** should find α_d that minimizes **J** before trying another pair of parameters β and **a**. Actually, physical interpretations and practice accelerate the process of convergence towards the minimum.
- the automation of the procedure would be possible through simple algorithms (gradient algorithms...) and **even** necessary in a practical point of view, but technically uneasy in the actual shape of the software. It has **not** been done also because this study is more a feasibility analysis than a research of accurate parameters.
- we could **also** introduce the constraint of equality of the deposited volumes (simulated and measured), namely $\Delta V(M_0, M_1) = \Delta V(M_0, S_1)$, considering that the deposited **volumes** are important criteria in terms of maintenance costs.

4.2.2 Definition of the calibration functions

* quadratic error function:

Let us call $x_{i,i-1}$ the abscissae of the cross sections i , $i=1..n$; ΔS_i (respectively ΔM_i) the **difference** of area between the simulated cross section i and the initial cross section i (respectively between the measured final and initial cross sections i).

The error function **J** is defined as follows:

$$J = \frac{\sum_{i=1}^n \left[(\Delta S_i - \Delta M_i) \left(\frac{x_{i+1} - x_{i-1}}{2} \right) \right]^2}{\sum_{i=1}^n \left[\Delta M_i \left(\frac{x_{i+1} - x_{i-1}}{2} \right) \right]^2}$$

[NB: in this **formulation**, we consider $x_0 = x_1$ and $x_{n+1} = x_n$]

Through its denominator, which normalizes the error function, this function **depends** on the initial geometry.

J is equal to **1** if the simulated and the initial geometries are the **same**.

* **volume** verification:

$$\Delta V = \sum_{i=1}^n \left[(\Delta S_i - \Delta M_i) \left(\frac{x_{i+1} - x_{i-1}}{2} \right) \right]$$

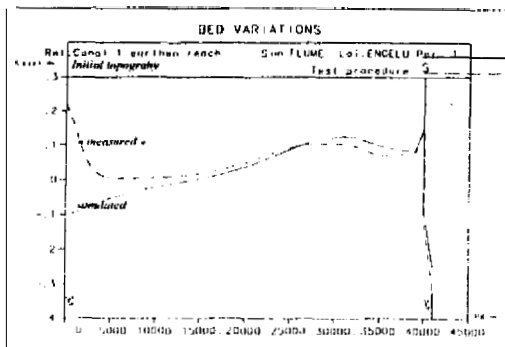
should be as close as possible to 0.

4.2.3 Illustration of the procedure

Here **we** will take a very simple case: after selecting **some** parameters for the **laws**, we **make** a simulation with these parameters. The result **will** be called the "**measured**" topography. We suppose these parameters **unknown** and we want to **apply** the calibration procedure to find them.

step 1 : **we** choose $\beta = 1$, $\alpha_d = \alpha_c = 0.001$ (as typical values for the parameters)

The simulated variations and the "**measured**" one are visualized below:

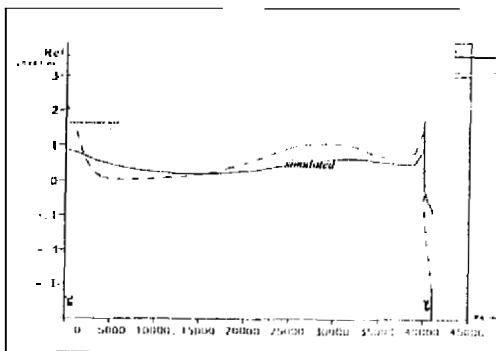
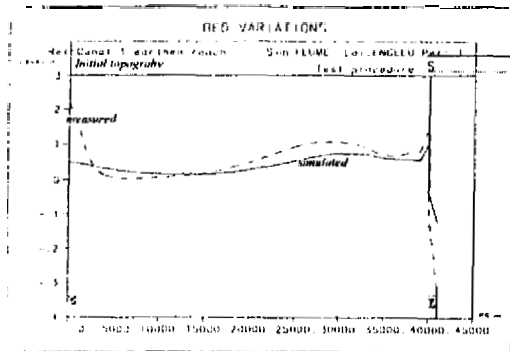


β	α_d	α_c	ΔV	J	comments
0.8	0.001	0.001	-34	0.379	scouring at head
0.7	0.001	0.001	-30	0.311	no scouring, no deposition at head
0.6	0.001	0.001	-25	0.293	deposition at head
0.5	0.001	0.001	-20	0.324	deposition at head
0.4	0.001	0.001	-15	0.401	deposition at head

Visualizations:

$\beta=0.6$

$\beta=0.5$

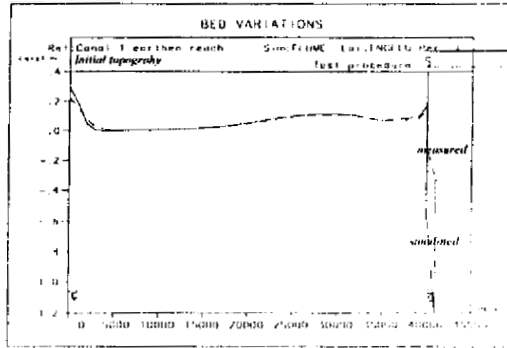
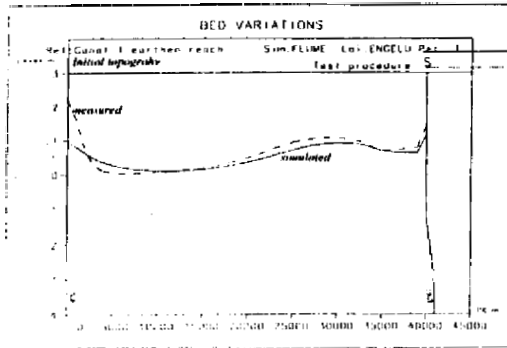


β	α_d	α_c	ΔV	J	comments
0.6	0.002	0.002	-15	0.089	the amplitude increases
0.6	0.004	0.004	-18	0.085	the amplitude increases
0.6	0.01	0.01	-25	1.405	good fitting at head but not at tail (scouring)

Visualizations:

$$\alpha_d = \alpha_e = 0.002$$

$$\alpha_d = \alpha_e = 0.01$$



The calibration is improving but the volumes are not conserved and we have too much scouring at the tail. We should reduce the erosion parameter.

β	α_d	α_e	ΔV (%)	J	comments
0.6	0.01	0.003	+0.3	0.093	
0.6	0.008	0.003	-1.9	0.073	
0.6	0.006	0.003	-5.0	0.060	
0.6	0.006	0.002	-0.2	0.007	best fitting for $\beta=0.6$
0.6	0.006	0.001	+5.3	0.072	
0.6	0.005	0.002	-0.9	0.013	
0.6	0.004	0.001	+1.5	0.120	
0.5	0.006	0.002	+5.3	0.115	modification of β
0.5	0.005	0.002	+3.2	0.082	
0.5	0.004	0.002	+0.6	0.063	best fitting for $\beta=0.5$
0.5	0.003	0.0015	-1.2	0.110	

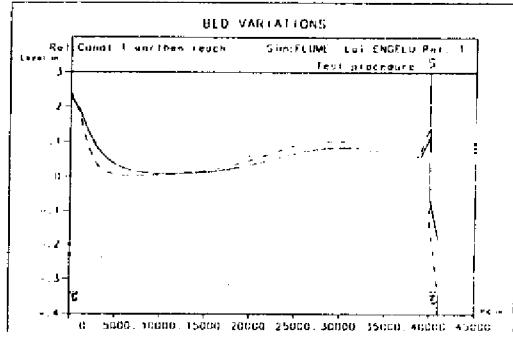
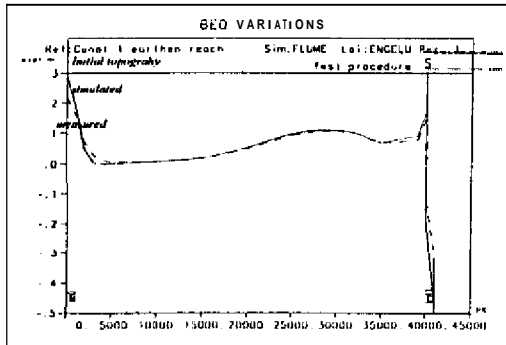
We will conclude from this table that the best parameters are $\beta=0.6$, $\alpha_d=0.006$, $\alpha_e=0.002$. (NB: the actual values were $\beta=0.58$, $\alpha_d=0.0057$ and $\alpha_e=0.0023$). The value of the error function J is very low.

However, most of the simulations above produced acceptable results: the errors on the medium bed elevation is low (most of the time inferior to 1cm), which may suggest that the model has a low sensitivity to the parameters and thus a high accuracy is not necessary.

Visualizations:

$$\beta=0.6, \alpha_d=0.01, \alpha_e=0.003$$

$$\beta=0.5, \alpha_d=0.004, \alpha_e=0.002$$



4.3 Calibration on Chasma Right Bank Canal

4.3.1 input data

The provided data were presented in part 2 (analysis of the problem). Some of **them** need to be combined for the input data of the model.

- sediment data:

For the suspended sediments, the medium diameters were assessed according to the procedure presented in 3.5.3 according to the daily data from WAPDA. The medium diameters (used in SEDt) were the following:

Average for year	silt (5-62 μ m)	sand (>62 μ m)
1987	16 μ m	153 μ m
1988	18 μm	151 μm
1990	26 μ m	188 μ m
1991	27 μ m	160 μ m
1992	30 μ m	138 μ m
1993	45 μ m	128 μ m

- April 1987-January 1989
- January 1989-July 1990
- July 1990-February 1993.

The model **was** also tested on shorter periods (July 1990-January 1991 and **January 1992-February 1993**) but the laws could not be calibrated properly (discussed **later**).

- * verification of the consistency

period	type of data	Input of sediments (transformed in volume)	Deposited volume
04/1987-01/1989	WAPDA (daily), total concentrations	1.200.000	1.700.000
04/1987-01/1989	WAPDA (daily), sediments >2 μ m	940.000	1.700.000
01/1989-07/1990	WAPDA (daily), total concentrations	986.000	900.000
01/1989-07/1990	WAPDA (daily),	680.000	900.000
07/1990-02/1993	WAPDA (daily), total concentrations	2.237.000	571.000
07/1990-02/1993	WAPDA (daily), sediments >2 μ m	1.851.000	571.000

Table 4.3-2: verification of volume conservation for CRBC

NB: all the volume were calculated with a porosity of 0.3 and a specific weight of 2650 kg/m³.

- for **1987**, we do **not** have enough sediments at head compared to the actual deposited volumes. Thus we will not expect a high accuracy on the deposited volume for the calibration. **Moreover**, we observe here the total input of sediments. **However**, it is sensible to suppose **that not all** these sediments deposit in the **first** reach (that is why we also present the input for sediments coarser than 2 μ m [as an arbitrary limit for **wash** load]). In the calibration, **we** will probably have to reduce the capacity of transport and force the deposition (high deposition parameter).

- definition of the periods of steady flow: they were defined according to the head **discharges** and to **the** concentrations. The maximum **duration** of the period is **30** days **but** shorter **periods had to** be considered when **the** variability of the concentration was too high, the scouring and the deposition at head **was** too important (high discharge, low concentrations or high concentrations).

The sedimentologic **data** files for the different simulations are given in appendix.

4.3.2 Results of calibration

The following table gives the parameters **we** obtained for the three periods of simulation:

Laws	04/1987-01/1989	01/1989-07/1990	07/1990-02/1993
Engelund-Hansen Han	$\beta=0.4$ $\alpha_d=0.02$ $\alpha_c=0.01$	$\beta=0.8$ $\alpha_d=0.005$ $\alpha_c=0.003$	$\beta=1.$ $\alpha_d=0.0006$ $\alpha_c=0.0008$
Karim-Kennedy (1990) Han	$\beta=2.0$ $\alpha_d=0.02$ $a_s=0.015$	$\beta=1.2$ $\alpha_d=0.003$ $\alpha_c=0.005$	$\beta=2.5$ $\alpha_d=0.0006$ $\alpha_c=0.0005$
Karim-Kennedy (1981) Han	$\beta=0.7$ $\alpha_d=0.015$ $\alpha_c=0.008$	$\beta=1.2$ $\alpha_d=0.003$ $\alpha_c=0.003$	$\beta=1.3$ $\alpha_d=0.0006$ $\alpha_c=0.0006$
Yang Han	$p=0.15$ $\alpha_d=0.01$ $\alpha_c=0.005$	$\beta=0.5$ $\alpha_d=0.003$ $\alpha_c=0.001$	$\beta=0.5$ $\alpha_d=0.0006$ $\alpha_c=0.0006$
Bagnold Han	$\beta_1=0.17$ $\beta_2=0.01$ $\alpha_d=0.01$ $\alpha_c=0.005$	$\beta_1=0.17$ $\beta_2=0.008$ $\alpha_d=0.003$ $\alpha_c=0.005$	$\beta_1=0.17$ $\beta_2=0.013$ $\alpha_d=0.0008$ $\alpha_c=0.001$

period	04/1987-01/1989		01/1989-07/1990		07/1990-02/1993	
Laws	AV	J	AV	J	AV	J
Engelund-Hansen	-32%	0.137	-5%	0.250	7%	0.208
Karim-Kennedy (1990)	-33%	0.142	-11%	0.233	-4%	0.165
Karim-Kennedy (1981)	-28%	0.146	-12%	0.282	8%	0.183
Yang	-30%	0.146	-13%	0.299	4.5%	0.170
Bagnold	-33%	0.115	-14%	0.271	0.33%	0.126

Table 4.3-4: error function values and volumes for the calibration of CRBC

4.3.3 Comments

- the order of magnitude for the parameters of the equilibrium laws are consistent with the original ones (1.0) and they are quite stable in time for a given law.

- the best calibration is generally obtained with Bagnold's law but all the laws give very similar results (see graphical results in appendix. Moreover, the parameters of the loading law are equivalent for a same period of simulation but different equilibrium laws.

This means that the model has a low sensitivity to the equilibrium law.

- on the contrary, the parameters for the loading law are not stable with respect to the time, and they seem to be linked to the volumes to be deposited.

As said before, we have a tendency to force the deposition in 1987 and 1989 because of the low entrance of sediments compared to the measured variation of volume: our parameters are high.

In 1990-1993, the deposited volume is much lower and high constants of deposition are not acceptable.

The sensitivity to the loading law is high.

4.4 Calibration on ChasmaJhelum Link Canal

period	type of data	Input - output of sediments (transformed in volume)	Deposited volume
08/1981-01/1982	total concentration	-86.000 m ³	+77.000 m ³
08/1981-01/1982	sand only	-72.000 m ³	+77.000 m ³
01/1982-01/1983	total concentration	+3.000 m ³	-600.000 m ³
01/1982-01/1983	sand only	+2.000 m ³	-600.000 m ³
01/1983-05/1984	total concentration	-477.000 m ³	-900.000 m ³
01/1983-05/1984	sand only	-270.000 m ³	-900.000 m ³

4.4.2 Results of calibration

The following table gives the parameters we obtained for the three periods of simulation:

Laws	01/1982-01/1983	01/1983-05/1984	01/1982-05/1984
Ackers-White Itan	$\beta=1.3$ $\alpha_d=0.001$ $\alpha_e=0.001$	$\beta=1.$ $\alpha_d=0.001$ $\alpha_e=0.001$	$\beta=1.$ $\alpha_d=0.001$ $\alpha_e=0.001$
Engelund-Hansen Han	$\beta=0.9$ $\alpha_d=0.001$ $\alpha_e=0.0012$	$\beta=0.5$ $\alpha_d=0.0012$ $\alpha_e=0.0005$	$\beta=0.5$ $\alpha_d=0.001$ $\alpha_e=0.001$
Karim-Kennedy (1990) Han	$\beta=1.3$ $\alpha_d=0.0008$ $\alpha_e=0.0016$	$\beta=1.$ $\alpha_d=0.001$ $\alpha_e=0.001$	$\beta=1.$ $\alpha_d=0.001$ $\alpha_e=0.001$
Karim-Kennedy (1981) Han	$\beta=1.$ $\alpha_d=0.001$ $\alpha_e=0.0015$	$\beta=0.8$ $\alpha_d=0.001$ $\alpha_e=0.001$	$\beta=0.8$ $\alpha_d=0.001$ $\alpha_e=0.001$
Yang Itan	$\beta=1.3$ $\alpha_d=0.001$ $\alpha_e=0.001$	$\beta=1.2$ $\alpha_d=0.0008$ $\alpha_e=0.0012$	$\beta=1.3$ $\alpha_d=0.001$ $\alpha_e=0.001$
Bagnold Han	$\beta_1=0.17$ $\beta=0.05$ $\alpha_d=0.0008$ $\alpha_e=0.0012$	$\beta_1=0.17$ $\beta=0.04$ $\alpha_d=0.001$ $\alpha_e=0.0012$	$\beta_1=0.17$ $\beta=0.04$ $\alpha_d=0.0008$ $\alpha_e=0.0012$

Table 4.4-2: calibrated parameters for CJ Link Canal

The graphical results are presented in appendix.

Error functions and volumes:

period Laws	01/1982-01/1983		01/1983-05/1984	
	ΔV	J	ΔV	J
Ackers-White	+14%	0.397	-5.5%	0.336
Engelund-Hansen	+11%	0.450	-20%	0.357
Karim-Kennedy (1990)	+16%	0.362	-1.3%	0.336
Karim-Kennedy (1981)	-0.3%	0.458	-10%	0.413
Yang	-10%	0.420	-26%	0.365
Bagnold	-6%	0.442	-2.6	0.332

Table 4.4-3: error function values and volumes for CJ Link Canal

4.4.3 Comments

- no calibration was acceptable for 1981.
- like for CRBC, the parameters for the equilibrium laws are closed to 1. with an exception for Bagnold law which seemed to underestimate the capacity of transport.
- the parameters for the loading law are stable over the two years and for the different laws, which allows prediction scenarios from 1983 to 1984. This can be explained by the stability of the canal behaviour over the period of study.
- all the laws produce comparable results.
- the scouring at the tail of CJ Link is always overestimated for the period 1983-1984.
- scouring is always predicted at abscissa $x=25000m$ for 1982-1983 but the actual topography did not seem to change during the period. Scouring occurred during the year 1983.

The model does not take into account the possible variability of the bed composition, which might be an essential factor in case of erosion: local problem could be expected.

4.4.4 Confrontation measured/simulated concentrations

The following table compares the simulated total concentrations to the measured ones for 1982-1984, and Bagnold law. A comparison between the different simulations is given in appendix.

NPer	1	2	3	4	5	6	7	8	9	10	11	12	13	14	15	16
Q	175	283	198	198	170	433	170	133	369	99	595	85	140	180	350	200
<i>Total computed concentrations</i>																
RD180	0.065	0.070	0.140	0.140	0.339	0.221	0.260	0.301	0.335	0.254	0.294	0.245	0.247	0.247	0.280	0.187
RD290	0.210	0.259	0.294	0.294	0.456	0.479	0.396	0.413	0.553	0.351	0.625	0.339	0.360	0.378	0.470	0.318
RD315	0.177	0.274	0.268	0.268	0.417	0.609	0.328	0.340	0.603	0.276	0.847	0.256	0.287	0.313	0.488	0.262
<i>Total measured concentrations</i>																
RD180	0.065	0.070	0.076	0.139	0.339	0.221	0.260	0.301	0.335	0.254	0.294	0.245	0.247	0.247	0.330	0.187
RD290	0.062	0.135	0.101	0.086	0.187	0.195	0.172	0.160	0.166	0.186	0.178	0.187				
RD315	0.059	0.063	0.144	0.173	0.261	0.250	0.245	0.274	0.284	0.269	0.267	0.270	0.270	0.270	0.360	0.178

NPer	17	18	19	20	21	22	23	24	25	26	27	28	29	30	31	32
Q	284	425	255	115	397	615	615	615	615	283	580	615	113	615	400	200
<i>Total computed</i>																
RD180	0.435	0.241	0.268	0.325	0.325	0.455	2.200	0.700	0.455	0.130	0.250	0.350	0.280	0.340	0.327	0.327
RD290	0.583	0.468	0.409	0.398	0.525	0.621	0.540	0.540	0.641	0.208	0.521	0.537	0.193	0.495	0.532	0.428
RD315	0.557	0.552	0.383	0.336	0.595	0.857	0.674	0.670	0.759	0.130	0.594	0.634	0.114	0.586	0.493	0.349
<i>Total measured</i>																
RD180	0.435	0.241	0.268	0.325	0.325	0.455	2.200	0.700	0.455	0.130	0.250	0.350	0.280	0.340	0.327	0.327
RD290																
RD315	0.459	0.278	0.273	0.323	0.323	0.860	1.100	0.215	0.860	0.400	0.225	0.670	0.056	0.191	0.383	0.383

Table 4.4-4: confrontation of measured and computed Concentrations

• comments:

Both sets of data are consistent but the model over estimates the concentrations at the tail (which is normal since we calibrated on the topography evolutions and the sediment outflow was too low to fulfill the volume conservation). This overestimation is often for the low values of the head concentrations (see the six first periods).

4.5 Example of application: validation and prediction strategies

4.5.1 Prediction strategies

Let us suppose that we have calibrated the model for 1990, 1991,... 1995. We want to apply the model in prediction scenarios for 1996 in order to minimize the maintenance costs for our system (acting on maintenance or regulation processes).

• we can calibrate the model over 1990-1995 and use the parameters to simulate 1996 from the topography of 1995. Advantage: the bigger the variations of topography are, the lower are the relative errors.

Condition: the parameters should be stable over the different periods of simulation (which was not the case for CRBC).

• we can use the parameters obtained for 1995. Advantage: we can suppose that the behaviour of the canal was stable between 1995 and 1996.

Drawback: the volume variations may be low and the relative errors high (situation encountered for CRBC in 1990 and 1992, and CJ Link in 1981).

4.5.2 Quantification of the error on prediction

In an objective of maintenance, the relevant quantity to analyze would be the variations of volumes to recover the initial bed topography.

But the distribution of the sediment over the reach should also be analyzed through its consequences on the hydraulic functioning of the channel.

In the following, we observed the errors of prediction on the volumes, as well as the error function defined for calibration. It could have also been possible to identify the consequence of our prediction on some water levels for instance (water levels being linked to the water distribution).

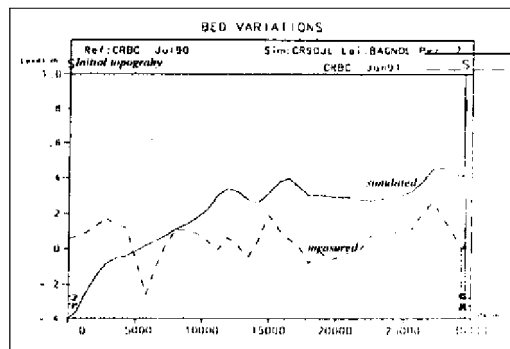
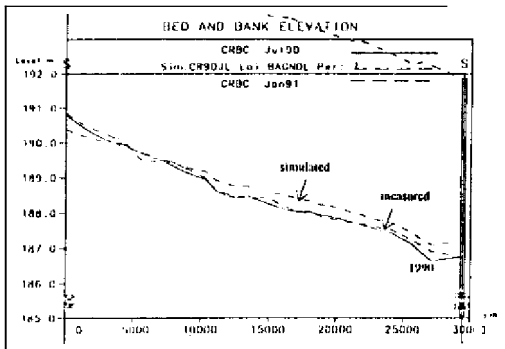
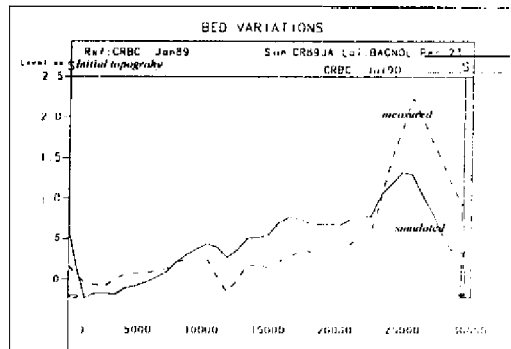
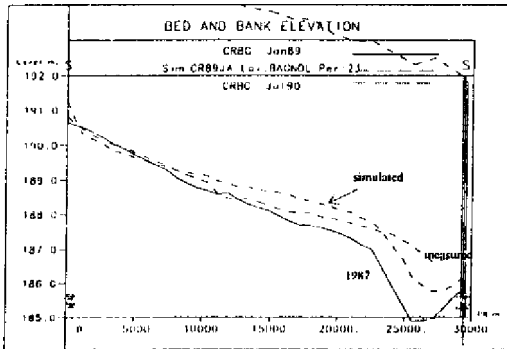
4.5.3 Application to CRBC

Laws	Parameters	Predicted volume 1000 m ³	Error on volumes with measured data	Error function value
Engelund-Hansen Han	$\beta=0.4$ $\alpha_d=0.02$ $\alpha_e=0.01$	765	+8%	0.484
brim-Kennedy (1990) Han	$\beta=2.0$ $\alpha_d=0.02$ $\alpha_e=0.015$	709	0.5%	0.394
Karim-Kennedy (1981) Han	$\beta=0.7$ $\alpha_d=0.015$ $a_r=-0.008$	762	7.8%	0.528
Yang Han	$\beta=0.15$ $\alpha_d=0.01$ $\alpha_e=0.005$	741	5%	0.534
Bagnold Han	$\beta_1=0.17$ $\beta_2=0.01$ $\alpha_d=0.01$ $\alpha_e=0.005$	697	-1.3%	0.285

Laws	Parameters	July 1990-Jan.1391			July 1990-1a		1992	July 1990- Feb. 1993		
		V	%	J	V	%	J	V	%	J
Engelund-Hansen Han	$\beta=0.8$ $\alpha_d=0.005$ $\alpha_e=0.003$	355	345	8.36	763	64	0.96	1012	77	0.73
Karim-Kennedy (1990) Han	$\beta=1.2$ $\alpha_d=0.003$ $\alpha_e=0.005$	328	311	4.42	753	62	0.61	1014	77	0.66
Karim-Kennedy (1981) Han	$\beta=1.2$ $\alpha_d=0.003$ $\alpha_e=0.003$	315	294	8.13	722	56	0.69	997	74	0.64
Yang Han	$\beta=0.5$ $\alpha_d=0.003$	308	286	7.91	719	55	0.55	993	74	0.64
Bagnold Han	$\beta_2=0.8$ $\alpha_d=0.003$ $\alpha_e=0.005$						0.56	962	68	0.56

Table 4.5-2: results of validation for CRBC 1990-1993

The results obtained with Bagnold Law (best prediction) are presented below:



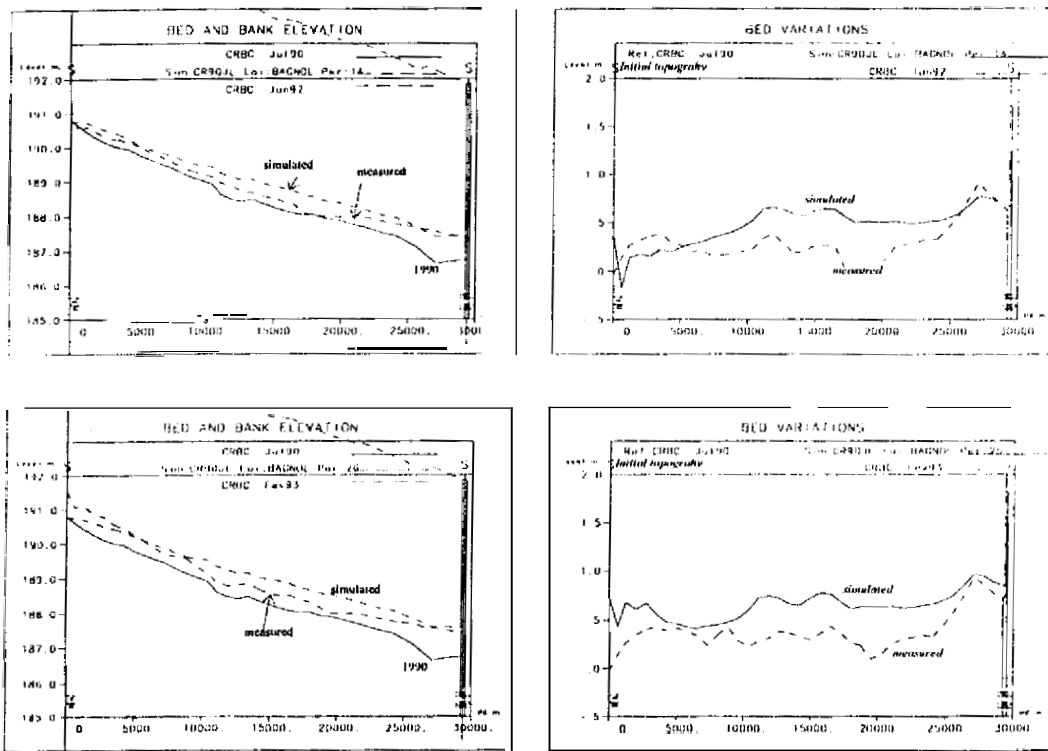


Figure 4.5-1: predicted bed evolutions with Bagnold law for CRBC

4.5.1.1 Interpretation

- Here again the predictions are similar with the different laws but Bagnold is still the best one.
- The validation for 1989-1990 is acceptable in terms of volumes.
- For 1990-1993, we predict far too much deposition (which is expected when we observe the difference between the calibrated parameters and the ones we used).
- The error for January 1991 is very high. This is consistent with the fact that no satisfying parameter could be found for the calibration on this short period.
- In 1992 and 1993, the prediction is improving in terms of topography evolution but the error on deposited volumes still remain above 50%. The prediction is generally better for 1992 than for 1993

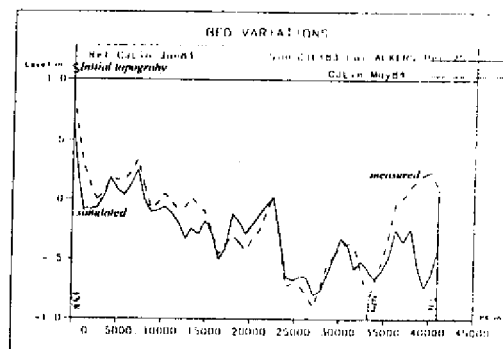
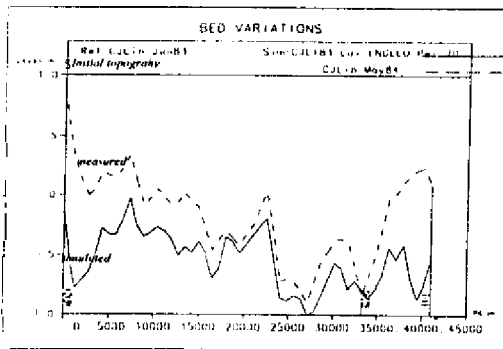
It would be interesting to compare other strategies for prediction. For example, we could calibrate the model on 1989-1991, and predict a topography for 1992 and for 1993. The strategies of prediction could then be compared. Then we could also calibrate on 1989-1992 and predict the topography for 1993.

4.5.4 Application to CJ Link Canal

4.5.4.1 Results of predictions

As for CRBC, we used the parameters calibrated on 1982-1983 for predicting the bed evolution for May 1984. The errors of prediction are presented below, as well as the results of simulations for Engelund-Hansen (worst prediction), Ackers White and Yang (best predictions).

Laws	Parameters	Predicted volume 1000 m ³	Error on volumes with measured data	Error function value
Ackers-White Han	$\beta=1$, $\alpha_d=0.001$ $\alpha_c=0.003$	-1280	-52%	0.385
Engelund-Hansen Han	$\beta=0.9$ $\alpha_d=0.001$ $\alpha_c=0.0012$	-2386	-183%	1.199
Karim-Kennedy (1990) Han	$\beta=1.3$ $\alpha_d=0.0008$ $\alpha_c=0.0016$	-1324	-57%	0.453
Karim-Kennedy (1981) Han	$\beta=1$, $\alpha_d=0.001$ $\alpha_c=0.0015$	-1821	-116%	0.670
Yang Han	$\beta=1$, $\alpha_d=0.001$ $\alpha_c=0.006$	1130	-34%	0.366
Bagnold Han	$\beta_1=0.17$ $\beta=0.05$ $\alpha_d=0.0008$ $\alpha_c=0.0012$	-1130	-34%	0.397



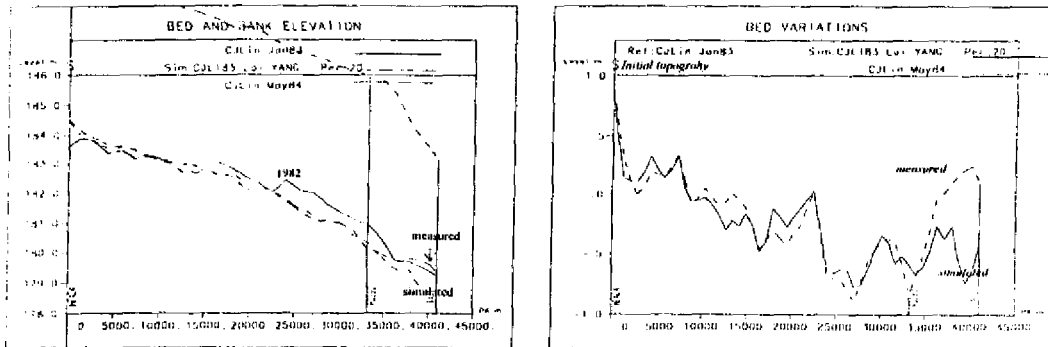


Figure 4.5-2: predicted bed evolutions for C.I Link Canal

4.5.4.2 Comments

- the different law give very different predictions. Bagnold, Yang and Ackers-White are the best ones, but Engelund-Hansen predicts too much scouring (the capacity of transport seems to be too high).

One possible explanation is the quality of the calibration for 1982, which has been made on a very short period and for low bed variations.

- the results of the prediction with Yang's formula are very close to the results of calibration.
- anyway the bed variations are generally well reproduced in the middle of the reach but problems appear at the head of the channel.
- but we overestimate the bed scouring at the tail, with all the laws; the bed variations at the tail cannot be reproduced by the model and the volume conservation is far much better from RD180 to RD290.

4.6 Conclusion

Using the model in prediction is its main interest but we cannot expect a high accuracy on the predicted volumes (at least 50% in the previous simulations).

First of all, we must mention that such an error is not unexpected in sediment transport problems.

Second, this error must be linked to the inaccuracy on the input data and the sensitivity analysis. We have shown that 10% of error on the concentrations could increase the volume variation by 15%. Thus an error of 60% on the deposited volumes could be explained by an error of 40% on the concentration (linear hypothesis), which is not unrealistic. Let us also mention that we are all the more sensitive to the errors on concentrations as we are close to equilibrium conditions, which could explain that the error of prediction is much higher from 1990 to 1993 than from 1990 to 1993.

Finally, taking into account longer series would certainly improve the reliability of the prediction. The relative error will probably decrease when the variations of volume will be high.

With a large set of topographies on long periods, different strategies of validation should be tested.

5. Example of application: strategies for water management

5.7. Introduction

The purpose of this part is to illustrate how we could use a sediment transport model to answer a problem of siltation or scouring in an irrigation canal.

New strategies of water distribution are being debated today. Currently, most of the irrigation systems in Pakistan are supply-driven: water is used by farmers if it is available in the feeding canal (and not the contrary). The simplest strategy of water distribution consists in providing a constant discharge in the main canal (when possible), and operating the secondary canals according to a defined calendar. This strategy needs few operations and limits the human influence.

But this management rises some problems. Few systems are correctly equipped with tail escapes and the lack of drainage induces waterlogging and sometimes soil degradation through salinity (uprising of the saline water table) when the delivery is higher than the requirements. Secondly, water is scarce in Pakistan whereas new irrigated areas should be developed: wasted water should be avoided. Then water shortages can sometimes appear (typically just before the monsoon, when the cropping intensity is the highest).

Pilot projects are now oriented towards a greater flexibility, consisting in adapting the water supply to the crop-water requirements. Chashma Right Bank Canal is one of these projects. Such strategies are not so simple to address because the present systems were not designed for them, and their consequences are not well identified.

In the following, we will try to present simplified strategies of operation at the main canal level, for one reach ended by a regulator able to control the water surface level:

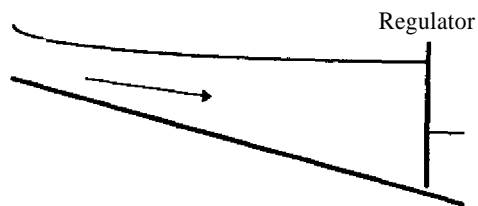


Figure 5.1-1: schematic plan of the theoretical canal

We will observe the influence of schematic strategies on the canal bed evolution, upstream from the regulator, predicted by the model SIC-SEDI.

5.2. Definitions

5.2.1. Definition of relevant strategies

To have an idea of the variability of the discharge requirements, we present two crop-water requirements charts, established for CRBC and Lower Swat Canal (LSC) (ref. [1]):

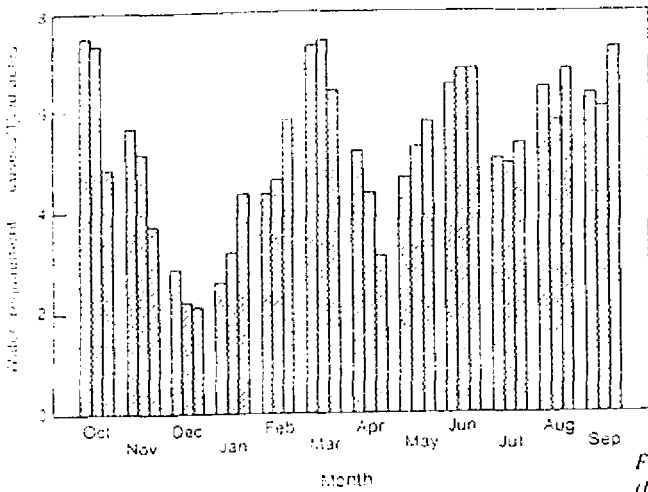


Figure 1. Irrigation water requirements at watercourse head - Chashma Right Bank Canal (CRBC).

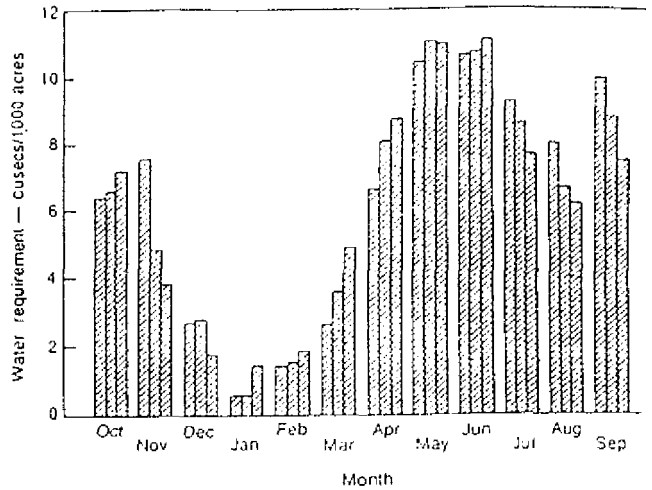


Figure 2. Irrigation water requirements at watercourse head, Lower Swat Canal (LSC)

Figure 5.2-1: irrigation water requirements for CRBC and LSC (from ref. [11])

To define management strategies, we will keep in mind that:

- a full discharge has to be supplied a certain percentage of the year;
- to feed the secondary canals (distributaries) upstream from the regulator, minimum levels are also imposed at some moments of the year.

* strategy 1: the main canal is functioning at his full discharge. What is the influence of the imposed water level on the bed evolution?

* strategy 2: the discharge balances the crop-water requirements. Keeping the same constraints on the water levels as in strategy 1, what will be the new evolutions?

Many other management strategies could be defined (like closing the canal when the concentrations are too high...)

5.2.2. Simulation canal

The simulation will use the schematic canal presented in part 4 (sensitivity analysis), designed according to Lacey's rules for a natural slope of 1/8000 and a discharge of 130 m³/s:

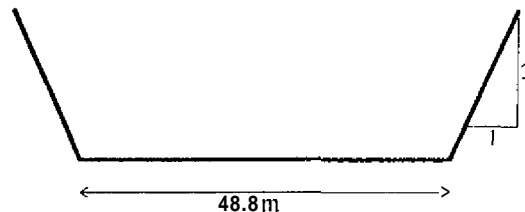


Figure 5.2-2: schematic cross section

Strickler coefficient: 50

Uniform depths (Strickler formula) :

Discharge Q	Uniform depth H
50 m ³ /s	1.45 m
90 m ³ /s	2.08 m
130 m ³ /s	2.60 m

5.3. Strategy 1: maximum discharge

5.3.1. feasibility

Lacey's rules are supposed to be appropriate for the full supply discharge. When the discharge Q decreases (the level at the regulator remaining constant), the velocity also decreases, thus the capacity of sediment transport, and sedimentation can occur. That is one of the reasons why this strategy has been privileged for a long time. However, as shown before, the needs are not constant over the year and to avoid the excess of water, escapes are necessary. This point has to be considered when comparing two solutions. The following figure presents a schematic example of network design for a full discharge supply:

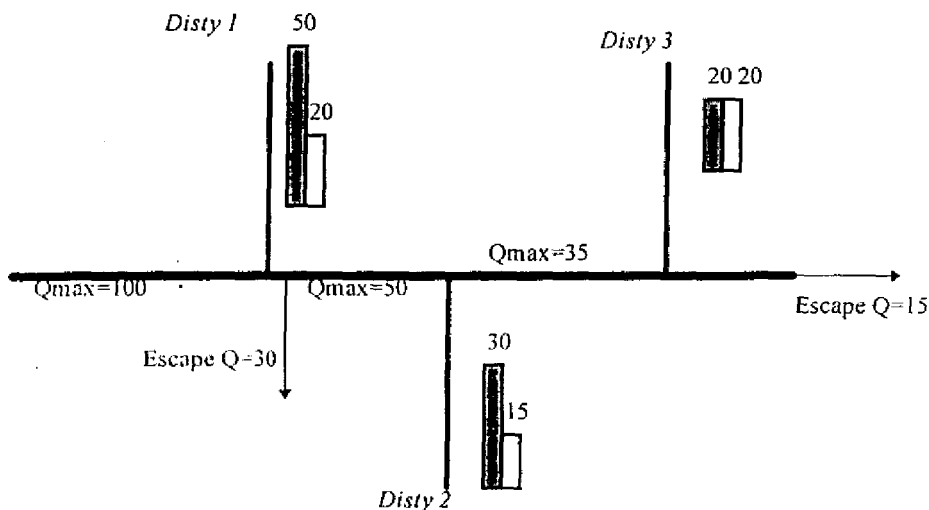


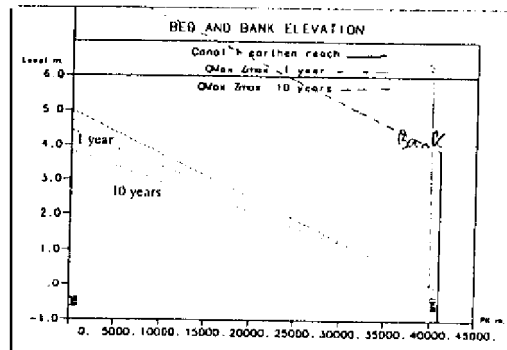
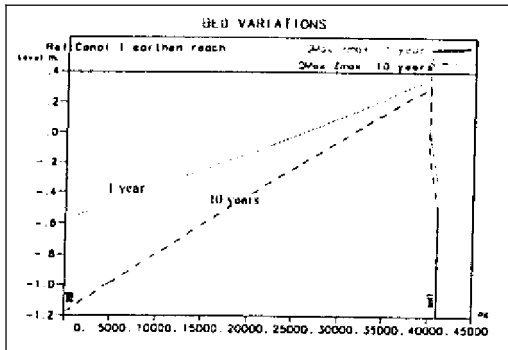
Figure 5.3-t: schematic plan of a network

For each of the distributaries (disty 1, 2, 3), the water requirements are presented for two periods of the year. Two escapes are dimensioned according to these requirements.

5.3.2. Comparison between three operating strategies at the regulator

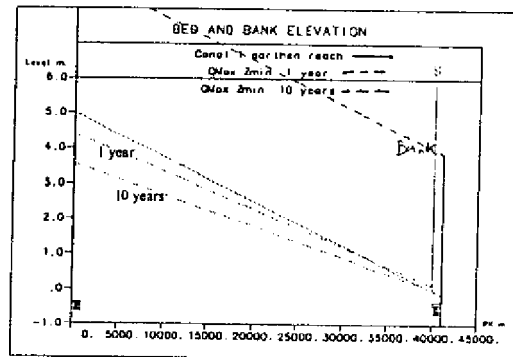
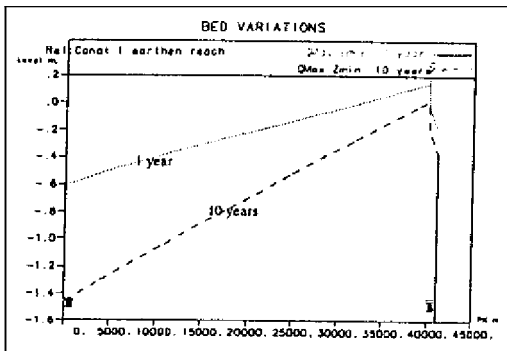
strategy 1a: the water level Z is maximum all over the year. This level is 50 cm higher than for the uniform regime (3.10 m).

Bed evolutions after 1 and 10 years:



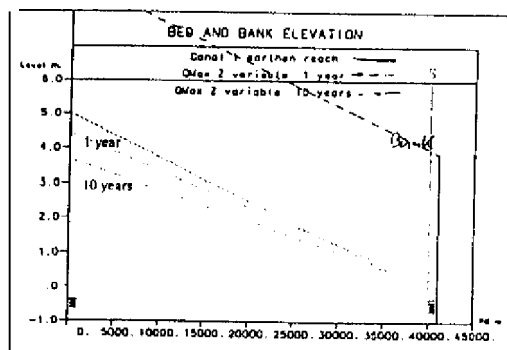
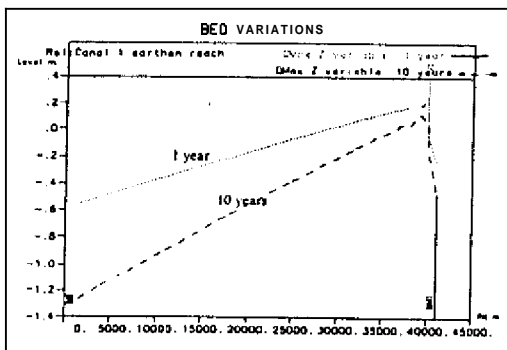
We can observe that scouring first occurs at the head. The flow is loaded with sediments and deposition occurs at the tail. Then erosion takes place all along the canal to reach the equilibrium profile. This equilibrium profile corresponds to the uniform depth of the flow.

strategy Ib: the water level Z is minimum (2.80 m) and close to the uniform depth. The bed evolutions are presented below:



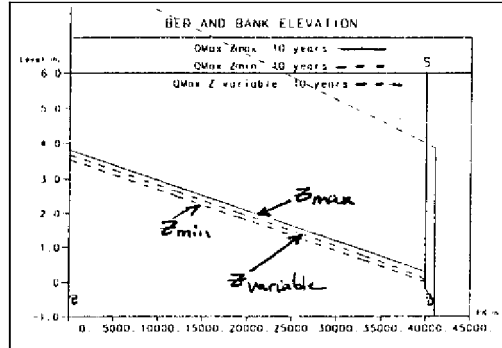
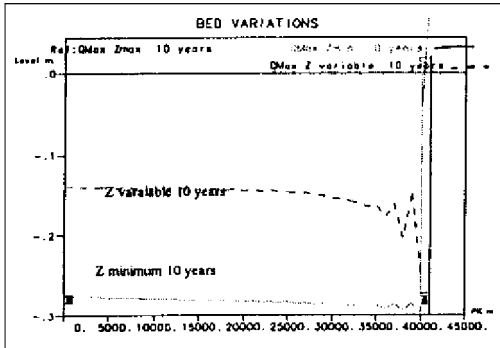
Here again we observe a lot of scouring at head but almost no more deposition at the tail. The equilibrium profile (after 10 years) also corresponds to uniform depth (after stabilizing).

strategy Ic: the water level is maximum in the high requirement period (April to September or *Kharif*) and minimum during the rest of the time.



An equilibrium profile is still reached even though the water level is changing each year.

strategy	parameters	variation of volume after one year	variation of volume at equilibrium
1a	Q=130 m ³ /s Z=3.10 m	-275 .10 ³ m ³	-917.10 ³ m ³
1b	Q=130 m ³ /s Z=2.80 m	-470.10 ³ m ³	-1497.10 ³ m ³
1c	Q=130 m ³ /s Z=2.80 & 3.10 m	-372.10 ³ m ³	-1215.10 ³ m ³



Thus we can observe that the level of the regulator has a direct influence of the bed topography:

- the three **new** equilibrium profiles are almost parallel; the **flow** has become uniform for **all** the strategies.
- the equilibrium bed for Z=3.10 m is almost 30 cm higher than the equilibrium bed for Z=2.80m: the differences between the water levels and the equilibrium beds are of same order of magnitude.

⇒ **The imposed** water level is directly **linked** to the bed elevation but not to its equilibrium slope. **It** means that we can raise or decrease the bed level just **by** an action **on the tail** regulator.

5.4. Strategy 2 variable discharge

The following chart presents the hydrogram that we used for the simulations. It was established according to CRBC head hydrogram.

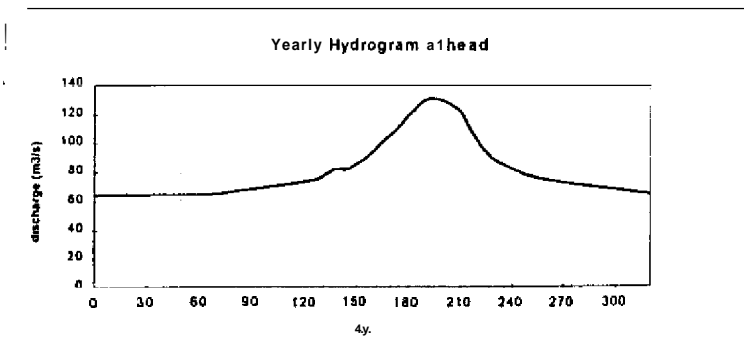
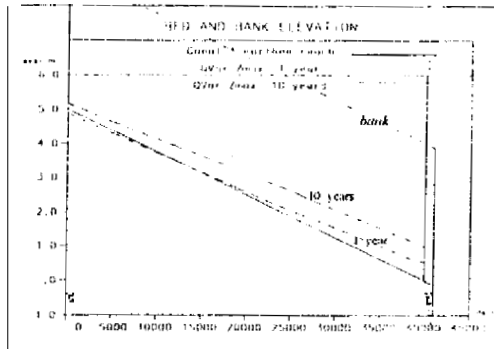
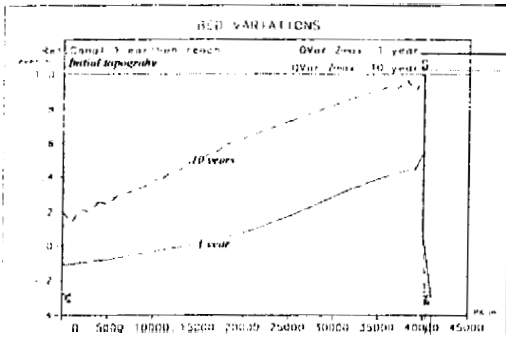


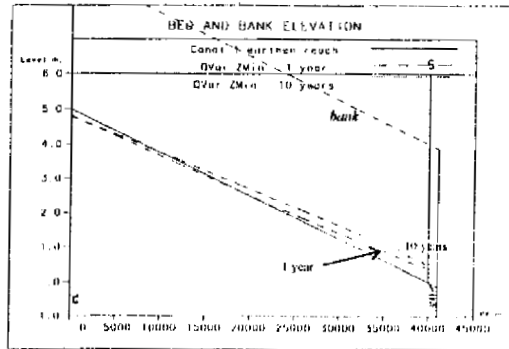
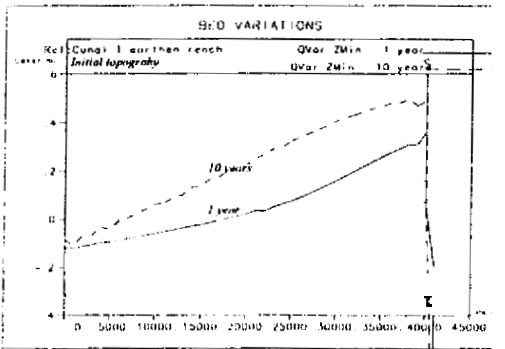
Figure 5.4-1: yearly head discharge hydrogram

Using this head discharge, we define three strategies:

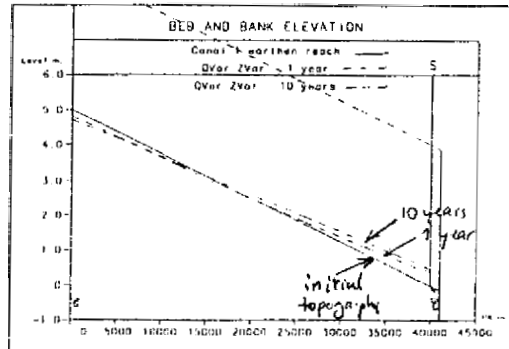
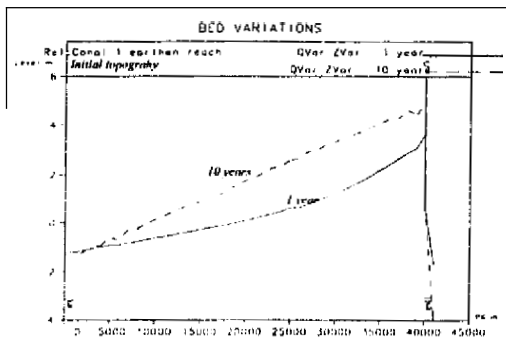
- strategy 2a: the level Z is kept constant and maximum ($Z=3.0$ m) (the distributary upstream from the regulator is also fed at his maximum);



- strategy 2b: the level Z is constant but as low as possible ($Z=2.80$ m);

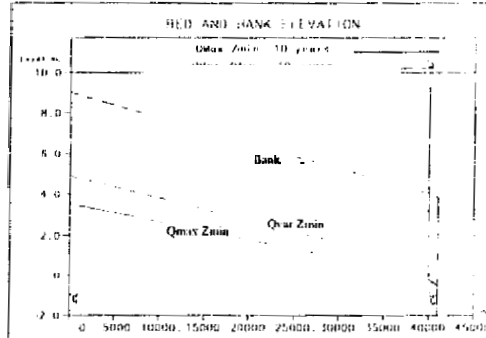
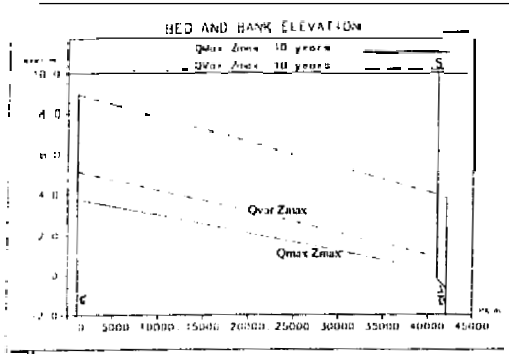


- strategy 2c: the level is variable and taken 50cm above the uniform level. This strategy seems to be the most rentistic (the distributary upstream from the regulator is fed according to the available water in the canal).



We can observe that

- now we have mainly deposition:
- the equilibrium slope is not exactly the same:



strategy	parameters	variation of volume after one year	variation of volume at equilibrium
2a	Q variable Z=3.10 m	+260 .10 ³ m ³	+1231.10 ³ m ³
2b	Q variable Z=2.80 m	+116.10 ³ m ³	+474.10 ³ m ³
2c	Q variable Z=Zunif+0.5m	+84.10 ³ m ³	+361.10 ³ m ³

The variable discharge with the highest level produces more siltation.

5.5. Example of application

5.5.1. summary

The tested strategies are compared in the following table, classified from the most "deposition-inductive" to the least one:

strategy	parameters	variation of volume after one year	variation of volume at equilibrium
2a	Q variable Z=3.10 m	+260 .10 ³ m ³	+1231.10 ³ m ³
2b	Q variable Z=2.80 m	+116.10 ³ m ³	+474.10 ³ m ³
2c	Q variable Z=Zunif+0.5m	+84.10 ³ m ³	+361.10 ³ m ³
1a	Q=130 m ³ /s Z=3.10 m	-275 .10 ³ m ³	-917.10 ³ m ³
1c	Q=130 m ³ /s Z=2.80 & 3.10 m	-372.10 ³ m ³	-1215.10 ³ m ³
1b	Q=130 m ³ /s Z=2.80 m	-470.10 ³ m ³	-1497.10 ³ m ³

Table 5.5-1: comparison of the different operation strategies

5.2. Example of interpretation:

Let us imagine that we are managing a canal with a variable discharge, and we try to adapt the levels to the requirements at each distributary (strategy 2c). We observe sedimentation in the reach.

(1) Diagnosis: in a first step, the consequences of sedimentation *must* be clearly identified

We are applying the strategy 2c. According to the table 5.5-1. we observe that our regulation strategy is not optimal from the sedimentologic point of view.

(2) Analysis of possible solutions:

We could reduce the deposition either :

a- by lowering the average level (ex $Z=Z_{unif} + 0.40m$). This would probably not satisfy the feeding of the distributaries;

β- by increasing the discharges, so that to tend towards strategies 1a, 1b or 1c. Thus we also have to consider escape channels.

α needs the construction of escapes to avoid drainage problems.

β may penalize the users upstream **From** the control regulator.

Here again, this example is very schematic since we could also observe many other strategies (flushing, temporary closure of the canal during the periods of high concentrations...)

(3) Definition of feasible strategies:

We will test the first strategy (**α**); to minimize the dimensions of the escape, we will increase the discharge by the same quantity all over the year, with a threshold of $130 m^3/s$:

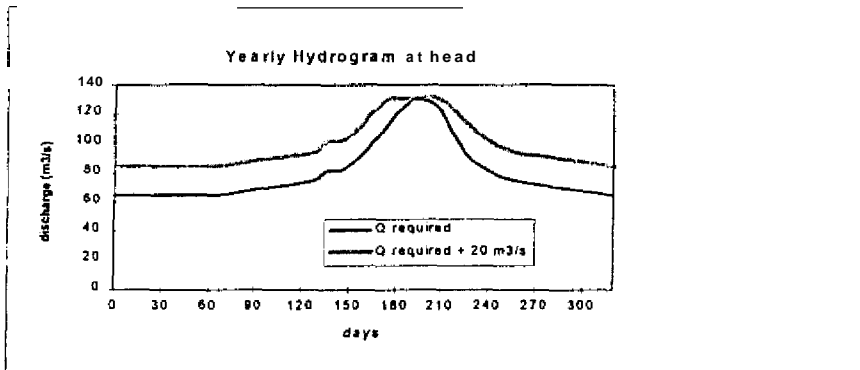


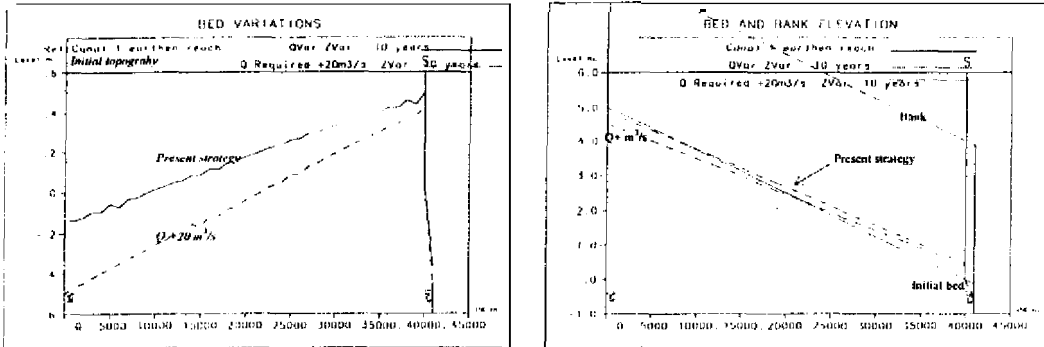
Figure 5.5-3: modified head discharge hydrogram

(4) simulation of the chosen strategies:

Here are the deposited volumes for two new strategies (increase by $10 m^3/s$, then by $20 m^3/s$):

Increase for Q	Variation of volume after 1 year	Variation of volume after 10 years
$10 m^3/s$	$+84.10^3 m^3$	$+146.10^3 m^3$
$20 m^3/s$	$-48.10^3 m^3$	$-76.10^3 m^3$

and the bed topographies:



(5) Analysis of the results:

Increasing the discharge by $20 \text{ m}^3/\text{s}$ would prevent the canal from sifting *up* in its first reach

However, we can notice that the bed profile would be **significantly** modified, with scouring at the head and deposition upstream from the regulator.

Thus, now, **we** have to **analyze** the benefits of this **new** strategy: is it **able** to address the **problems** determined during the diagnosis (1)?

It is also necessary to think **of** the quality of the prediction when analyzing the results: if the present topography **is** inside the margin of error of the simulation, then the **new** management strategy may be useless.

(6) Comparison of different acceptable strategies (economical, hydraulic, political ... points of view)

5.6. Summary

In this part, **we** have shown how the simulation tool **could** be used to analyze the impact of simple water management strategies on the siltation in a reach. The cases that are presented are very schematic **but** the same approach could be used for more complex systems, more elaborated strategies **and** a more reliable simulation tool.

5. Conclusion

5.1 summary

The objective of this work was to test a simulation tool for the topographic evolutions of irrigation canals. For that, two systems were analyzed: one main canal of irrigation, Chashma Right Bank Canal, and one link canal, Chashma Jhelum Link canal. It was concluded that the sediment transport should mainly take place in a suspended mode

A model of sediment transport was combined to the hydraulic model SIC. Among the data requirements, the model needs the definition of periods of steady flow, sediment inputs at the head of the canal and accurate topographies. Two classes of particles are defined: the wash load and the bed material load. For the bed material load, we selected two laws to represent the evolution of the concentration: one equilibrium concentration law and one loading law.

We wanted the model to be as simple as possible and many assumptions would have to be checked and improved. The sensitivity to the variability of the head concentrations, for which the inaccuracy can be important, is for instance very high, but considering several classes of particles inside the bed material load may reduce this sensitivity.

Part 4 defines a procedure for the calibration of the loading and equilibrium laws. This procedure is long but practice accelerates the convergence towards acceptable parameters. This procedure could be applied on the two case studies, CRBC and CJ Link canal.

On CRBC, the behavior of the canal was not stable over the three periods of simulation we defined, and the parameters of the loading law neither: the deposition rate decreased significantly. For CJ Link canal, these parameters are more stable but only two and a half years were tested. For both anyway, the different equilibrium laws give similar results despite a small preference for Bagnold law.

However, some local variations cannot be reproduced properly by the model: we have to conclude first that the model is not appropriate to reproduce all the sedimentologic processes (both because of the inaccuracy of the input data and because of the modeling simplifications), second that we cannot expect too much from the measured topographies. Low bed variations (and thus short periods) should not be considered with our approach.

In prediction, the model tends to amplify the bed variations and the error on the predicted volumes reached 50% in average with the best laws. However, the location of the zones of erosion or deposition was more or less acceptable. Anyway, such an error is expected in sediment transport problem. Let us remind that a good equilibrium concentration formula is valid with such an inaccuracy. Moreover, the errors on input data are not avoidable and they may largely affect the quality of the prediction.

As an example of application, simplified strategies of water management were tested. We observe that we can act on water levels and discharges to increase or reduce deposition: raising the levels at a regulator will raise the average bed level but will not change the equilibrium slope. The application of variable discharges increases the deposition compared to the strategy which consists in applying the full discharge for which the canals were designed and also changes the equilibrium slope. Thus increasing the average discharge tends to reduce deposition.

5.2 View on the follow up

In its present shape, we can use the model with all the reserves we summarized above. Our main objective is the reliability of the prediction of the model. It can be improved by:

- improving the model;
- dealing with long series for calibration, so as to have stable parameters.
- a better field observation, which should allow to understand local particularities that the model is not able to take into account.

Some views on the following are listed below.

5.2.1 Modeling

The representation of the bed material load as an homogeneous class of particles might be a coarse approximation. We are aware that the silts and the sands coarser than 150 microns do not behave similarly: the finer a particle is, the easier the flow is able to carry it; moreover sands will tend to reach their equilibrium concentration much quicker than silts. The concentrations for three classes of particles are generally available for the studied systems, thus it is sensible to separate their modeling in the future. As said in part 3.6, we would probably reduce the sensitivity to the head concentrations.

The composition of the bed should be the next step for improvement. Here again, a lot of data are available. This composition is important in case of scouring: it is not actually the main problem of the irrigation systems, but all the canals undergo periods of erosion even though they are globally silting up. From a technical point of view, it would allow the model to deal easily with lined canals (with an unerodible layer). The problem of bed forms was also avoided in the Master of Science study.

The distribution of the sediments over a cross sections and the modeling of singularities should also be studied in details. By singularities, we mean for example:

- what are the effects of kila bushings and berms (which may not appear on cross section spaced from 1500m); this practice is generally used either to stabilize the banks or to reduce the wetted area, thus to increase the flow velocity and prevent from siltation.
- what are the effects of a bend;
- how are the sediments transferred through an offtake...

The model will also be included in the unsteady flow model SIRENE of SIC. A higher accuracy is expected, especially in case of a high variability of the head data or of the operations at the nodes.

At last, the calibration procedure should also be improved thanks to optimization algorithms.

5.2.2 Applications

Instantaneous calibration was avoided in this work but it seems to be more physical to calibrate concentration laws on concentration data. However a high accuracy in the data used for calibration is required.

Then testing a large number of cases (and long series) would allow to define methodologies to quantify the reliability of prediction with respect to the quality of the calibration, to the duration of the simulation periods... Identifying the reliability is vital for the applicability of the model for maintenance or operation strategies. Moreover, we should properly define methods to analyze the quality of a prediction according to the use of the model: in this study, we selected the quantity of sediments deposited in a reach, but it might be more relevant to observe other variables, for instance the conveyance capacity, the water levels at some offtakes...

It is also essential to think of the integration of the sediment transport model on complex systems. We have to test it.

- at a different scale, namely the distributaries where most of the maintenance is done;
- at a global scale: where are the sediments carried; knowing the input concentrations at the head of the main canal, are we able to predict the siltation in the distributaries, the minors and the watercourses...

5.2.3 Data collection

In the present shape of the model, we have shown that we should have accurate concentrations, namely daily data. These data can be more easily integrated in order to compare them to the global bed variations (see part 4).

Then specific measurement campaigns (scheduled for 1997) should help:

- in the characterization of the sediment transport modes (wash load, part of the bed load compared to the suspension...) which was made in this study according to mathematical criteria and not physical observations;
- in the characterization of the bed material (cohesivity, porosity,,)

References

- [1] **BANDARAGORA D.J.**, **BADDRUDIN M.**, 1992, Moving towards Demand-Based Operations in Modernized Irrigation Systems in Pakistan, **HIMI Country Parer - Pakistan- No. 5**
- [2] **CARDOSO A.H.**, **NEVES G.O.**, 1994, *Prévision du transport solide. Evaluation des formules existantes*, La Houille Blanche, n°4-1994.
- [3] **CUNGE J.A.**, **HOLLY F.M.**, **VERWEY A.**, 1980, *Practical aspects of computational river hydraulics*, Pitman, London.
- [4] **DAUBERT A.**, **LEBRETON J.C.**, 1967, *Etude expérimentale et sur modèle mathématique de quelques aspects des processus d'érosion des lits alluvionnaires, en régime permanent et non permanent*, 12^{ème} Congrès AIRH, Vol. 3.
- [5] **GRAF W.H.**, 1971, *Hydraulics of sediment transport*, McGraw Hill.
- [6] **Le GUENNEC B.**, *Transport solide et morphologie fluviale*, cours ENSEEIHT version 91/97.
- [7] **HASNAIN KHAN**, 1996, *Desilting of Channel in Punjab and its subsequent effect on channel behavior*, Irrigation and Power Department, Punjab, Lahore.
- [8] **HASNAIN KHAN**, 1996, *Evolution of basic concepts in canal sedimentation /sediment transport related to design of channels in Pakistan*, Irrigation and Power Department, Punjab, Lahore.
- [9] **ISRIP**, *Monitoring of Chashma Right Bank Canal*, Vol. 1-5, ACOP 125, 129, 130, 137
- [10] **ISRIP**, *Chashma Jhelum Link, Monitoring for behavioral response to 3 feet crest lowering at tail regulator*, ACOP 107.
- [11] **KARIM M.F.**, **KENNEDY J.F.**, 1982, *A computed-based flow and sediment-routing model for alluvial streams and its application to the Missouri River*, IHR Report No. 250
- [12] **LIN H.**, 1993, *Le transport solide en collecteur unitaire d'assainissement et sa modélisation*, thèse de doctorat ENPC.
- [13] **LIN H.**, **LE GUENNEC B.**, 1993, *Mesure et modélisation du transport solide « au fond » en réseaux d'assainissement, par temps sec*, TSM N° 10.
- [14] **MAHMOOD Khalid**, 1970, *Design of Channels in alluvial soils*.
- [15] **MEIJER Th.J.G.P.**, 1985, **SEFLOW**, a program to calculate one dimensional channel flow with sedimentation, Delft Hydraulics Laboratory.
- [16] **MENDEZ N.V.**, *Suspended Sediment Transport in Irrigation Canals*, IHE Delft, Netherlands, M.Sc. Thesis 1995.
- [17] **POCHAT R.** *Hydraulique à Surface Libre*, cours ENGREF version 1991
- [18] **RAMEZ P.**, 1995, *Erosion et transport solide en rivière, tome 1: guide pour la compréhension des phénomènes*, CEMAGREF.
- [19] **RAMETTE M.**, *Guide d'Hydraulique Fluviale*, EDF-DER.

- [20] RAHUEL J.L.. 1988, Modélisation de l'évolution du lit des rivières alluvionnaires à granulométrie étendue, thèse de doctorat INPG.
- [21] VABRE A., Suspended sediment transport modeling in irrigation canals of Pakistan, rapport de stage ENSEEIHT 1995.
- [22] WANG S.. 1984, The principle and application of sediment effective power, J. of Hydraulic engineering, ASCE, vol 110.
- [23] YALIN M.S., 1977, Mechanics of Sediment Transport, 2nd edition, Pergamon Press, U.K
- [24] YALIN M.S., 1992, River Mechanics, Pergamon Press, U.K.
- [25] YANG C.T., WAN S., 1991, A comparison of selected bed-material load formulas, J. of Hydraulics engineering, vol 117.
- [26] YANG G.L., 1989, Modèle de transport complet en rivière avec granulométrie étendue. These de doctorat INPG, Grenoble, France.

List of appendices

Appendix 1 : Presentation of the studied systems

Appendix 2 : Bed evolutions for CRBC and C.J Link

Appendix 3 : Discharges and concentrations

Appendix 4 : Laws availables in SIC-SEDI Model

Appendix 5 : Graphical results of the sensitivity analysis

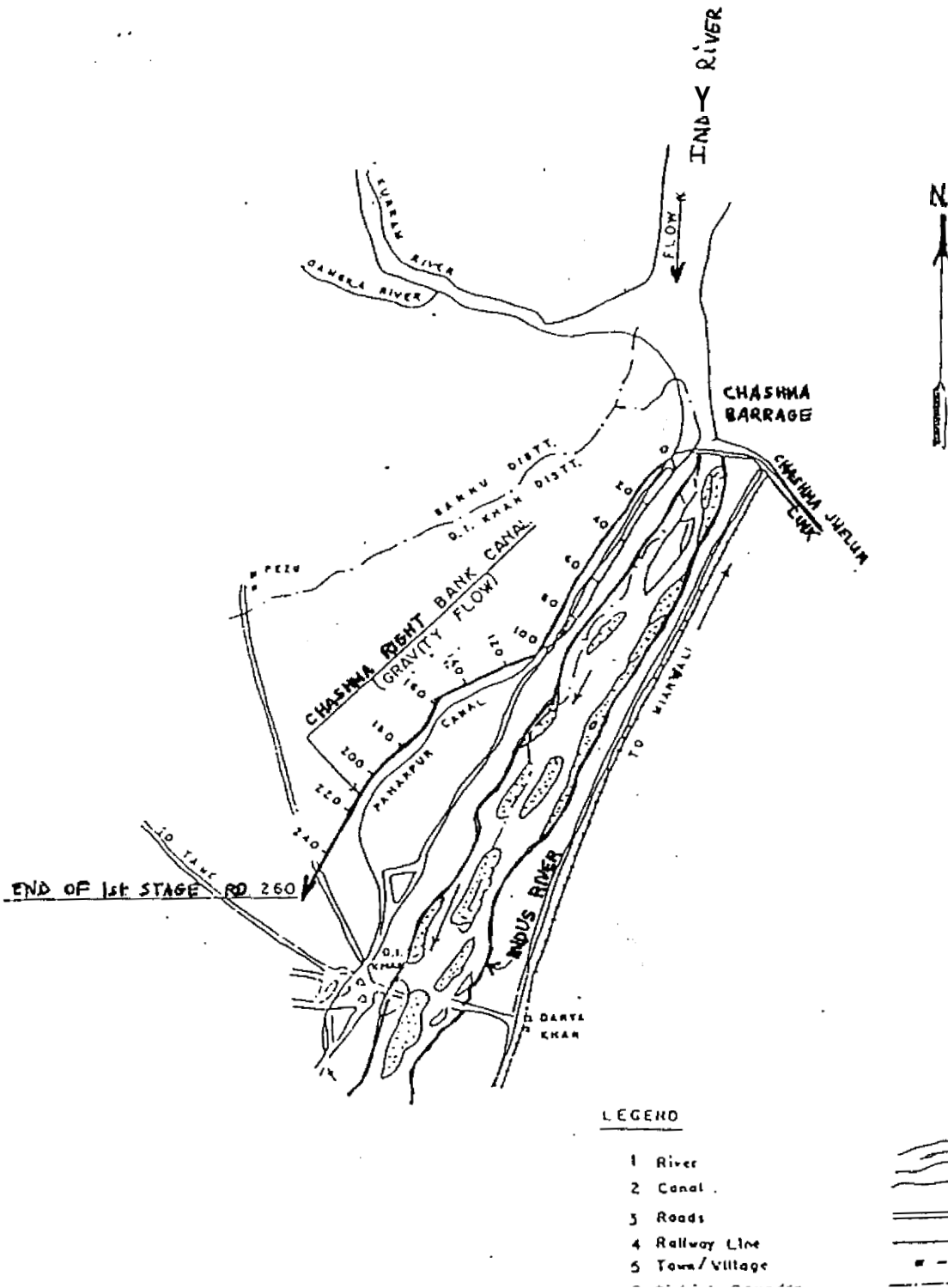
Appendix 6 : Instructions for use of SIC-SEDI

Appendix 7 : Sedimentologic data files


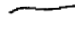



Appendix 8 : Graphical results of calibration for CRBC and C.J Link

Appendix 9 : Literature review

FIGURE A4 Map of CRBC (Stage 1)



LEGEND

- 1 River 
- 2 Canal 
- 3 Roads 
- 4 Railway Line 
- 5 Town/Village 

Appendix 1 : General presentation of the systems

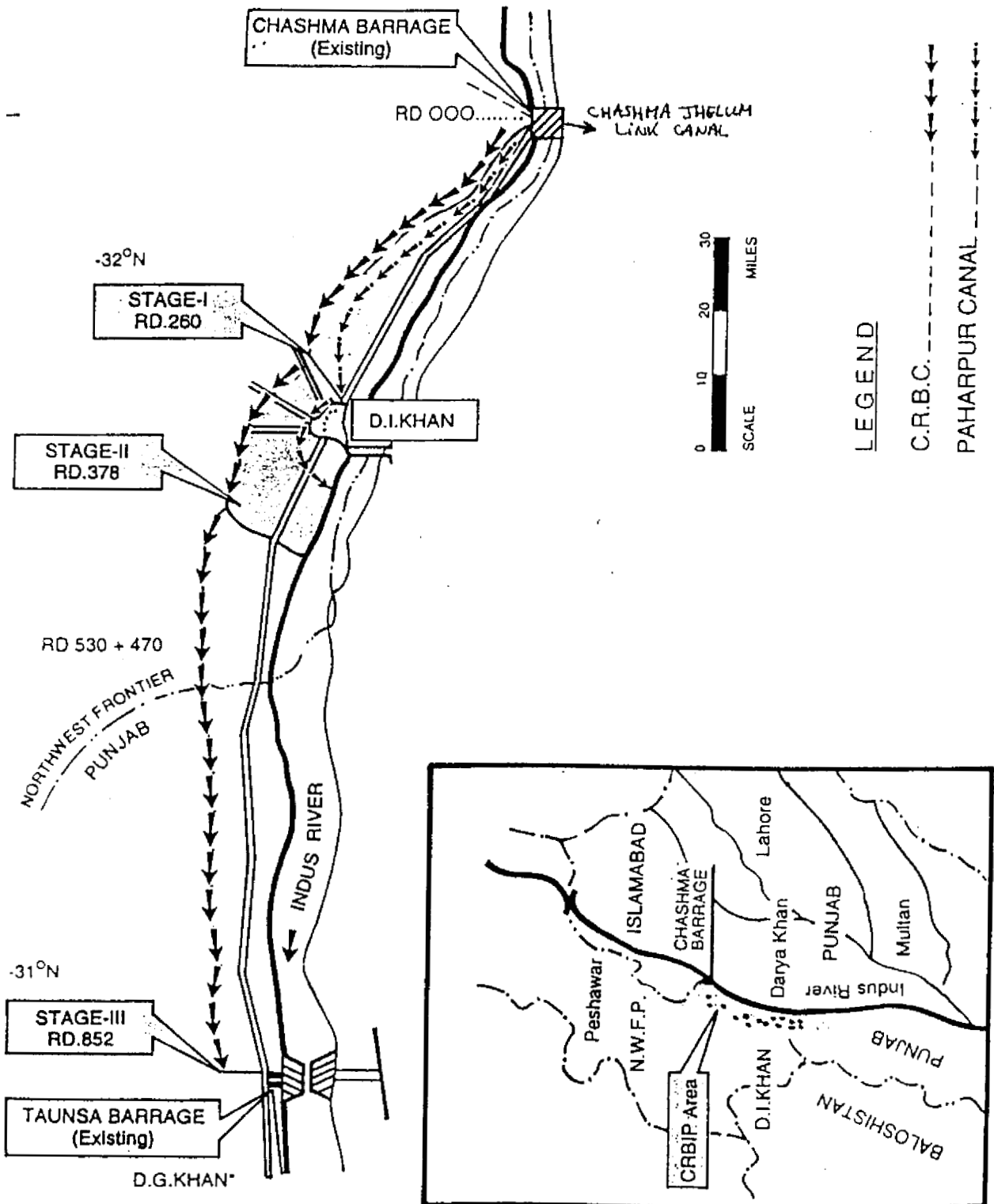
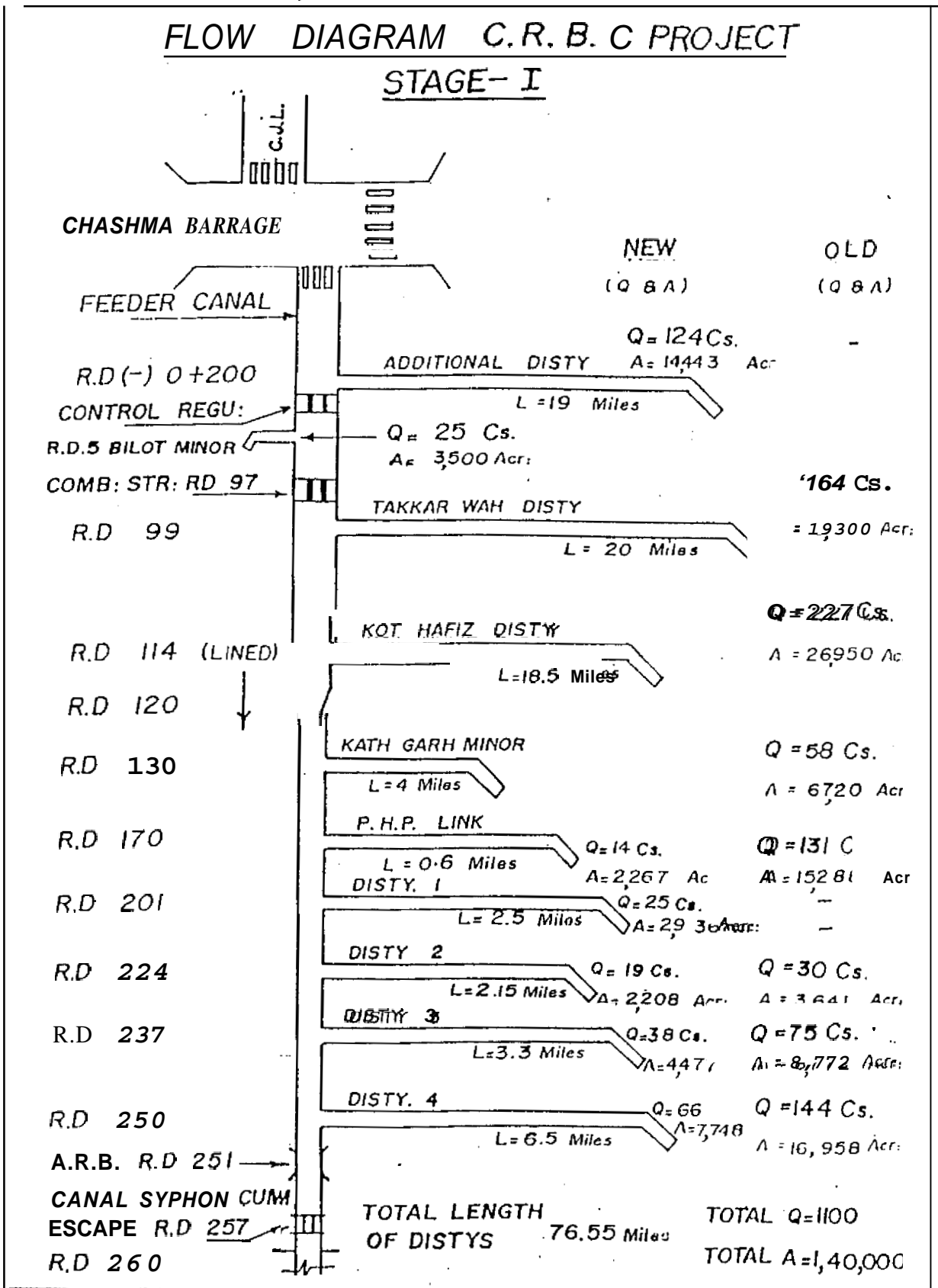
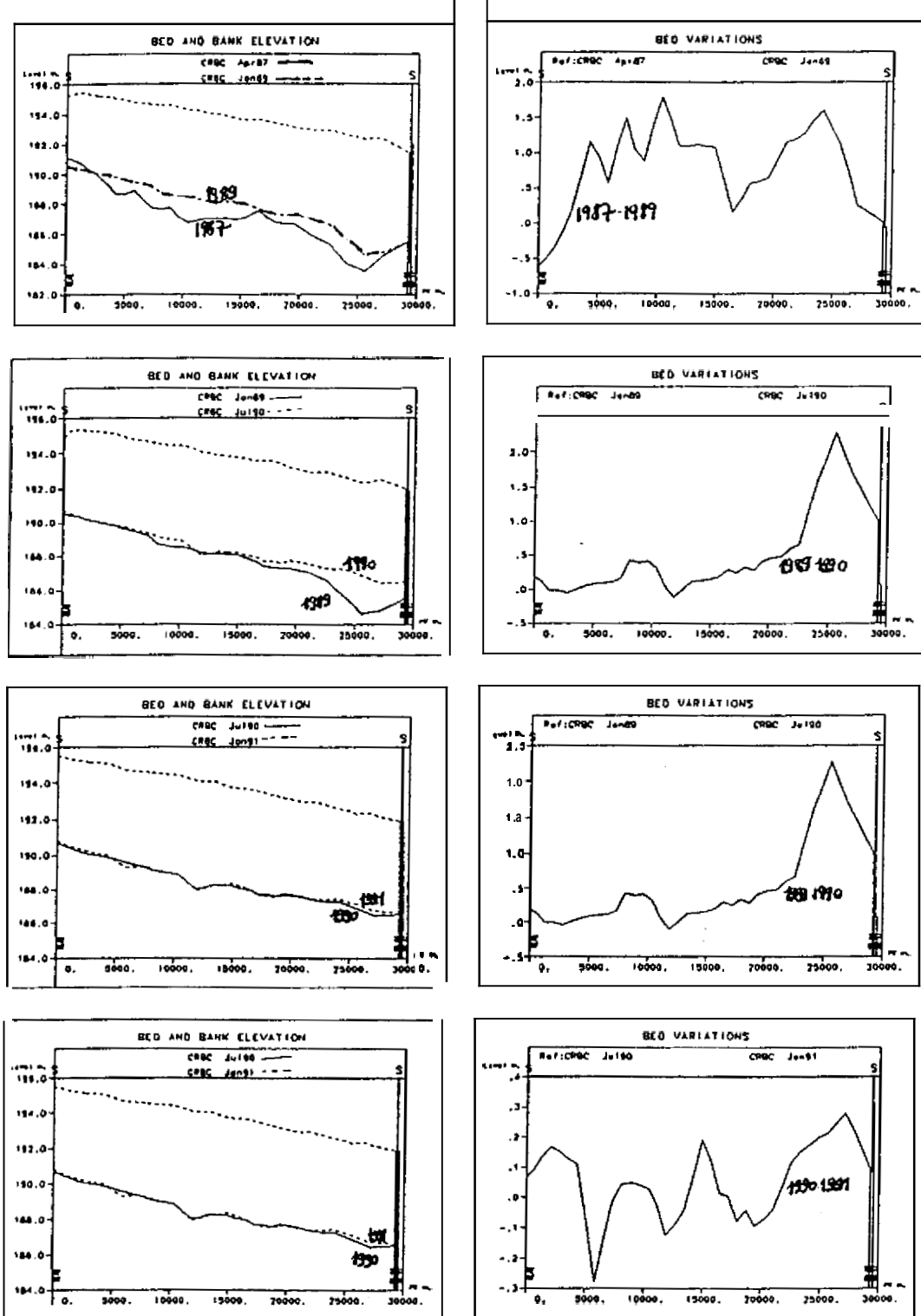


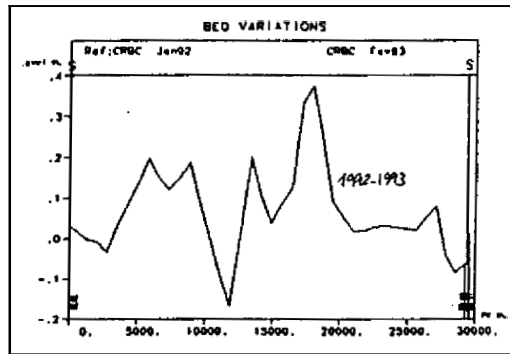
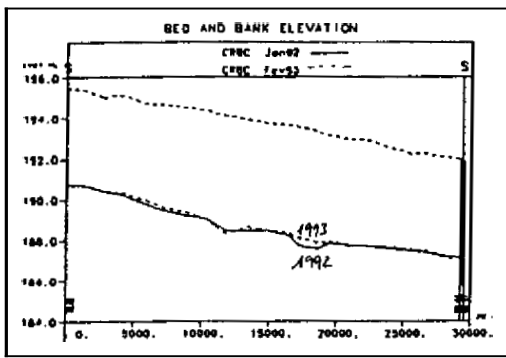
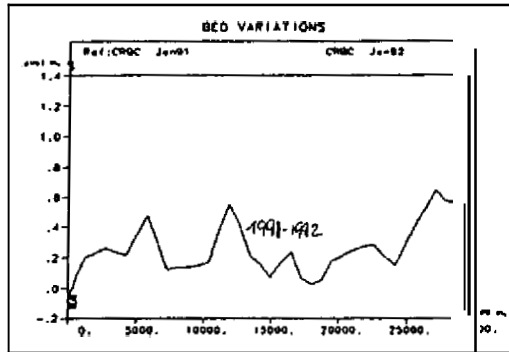
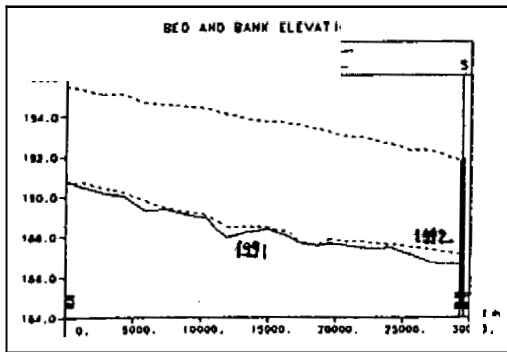
FIGURE A1 Flow diagram of CRBC (Stage I)



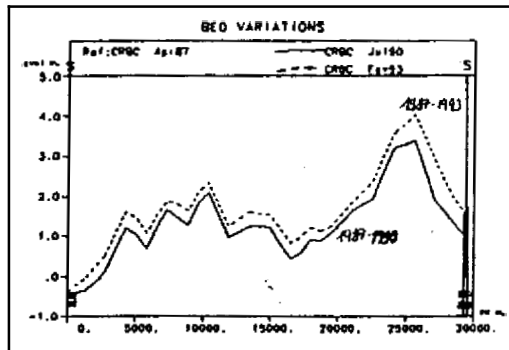
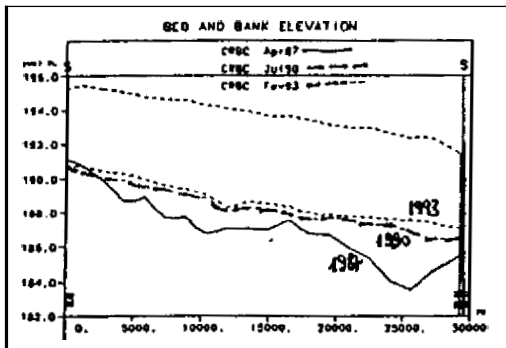
Appendix 2 : Bed evolutions for CRBC and CJ Link

Bed levels and bed variations for Chashma Right Bank Canal 1987-1993

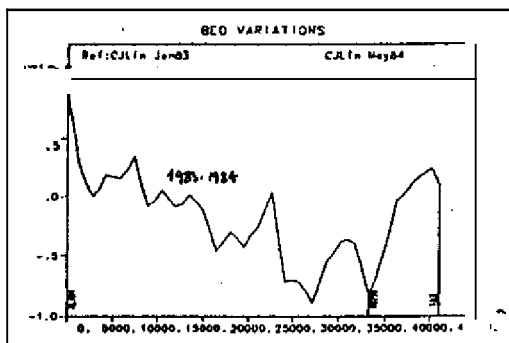
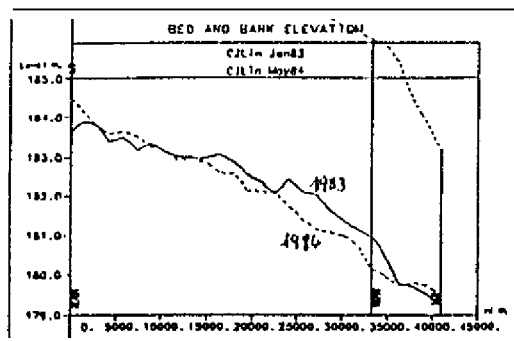
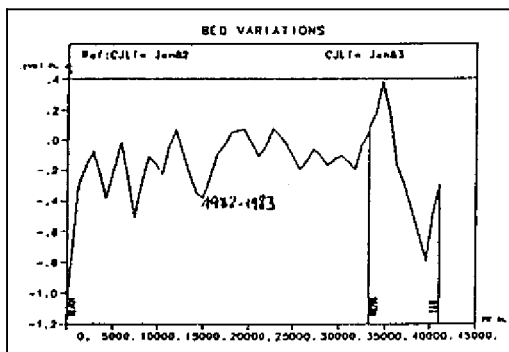
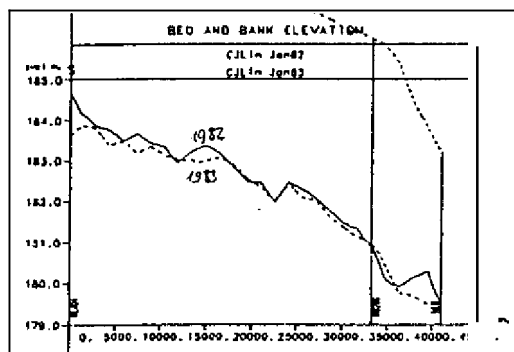
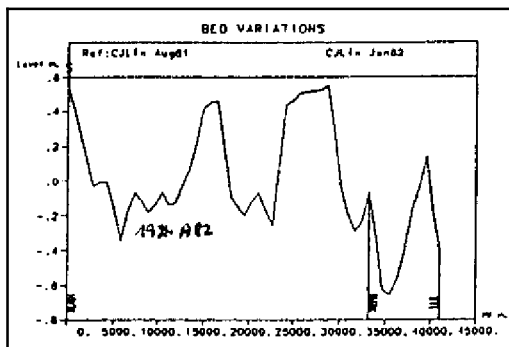
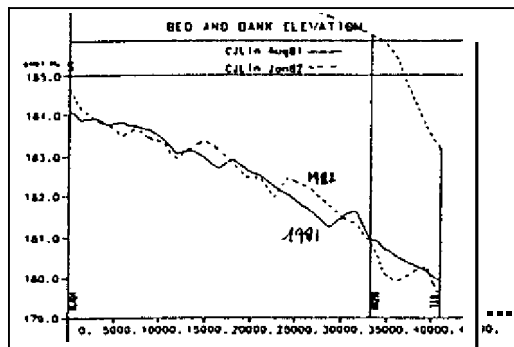


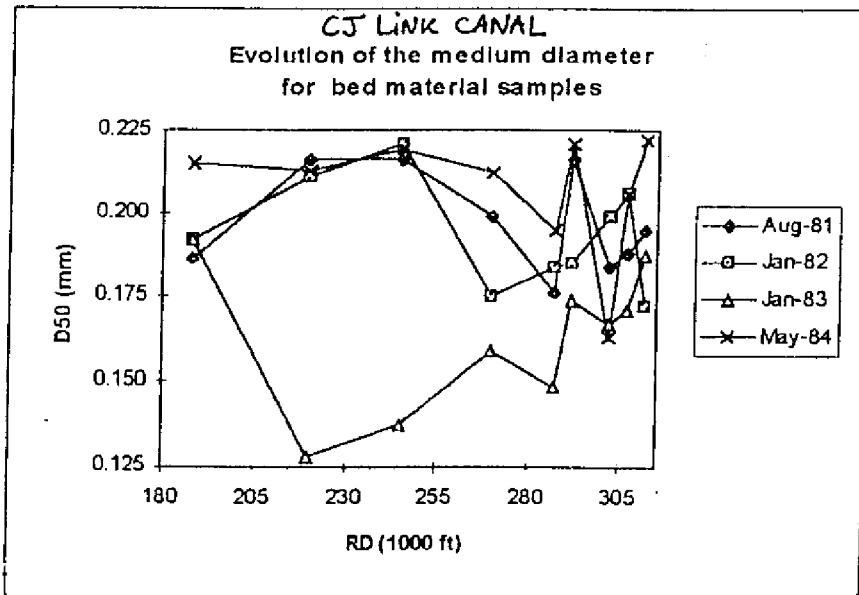
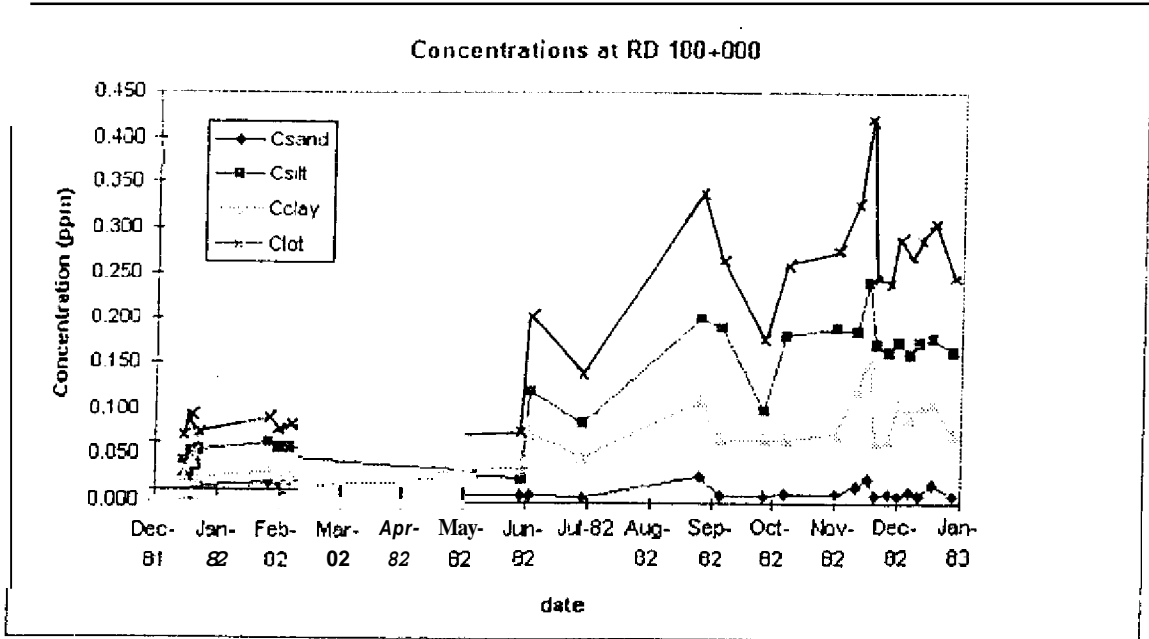


Bed evolution between 1987,1991,1993:

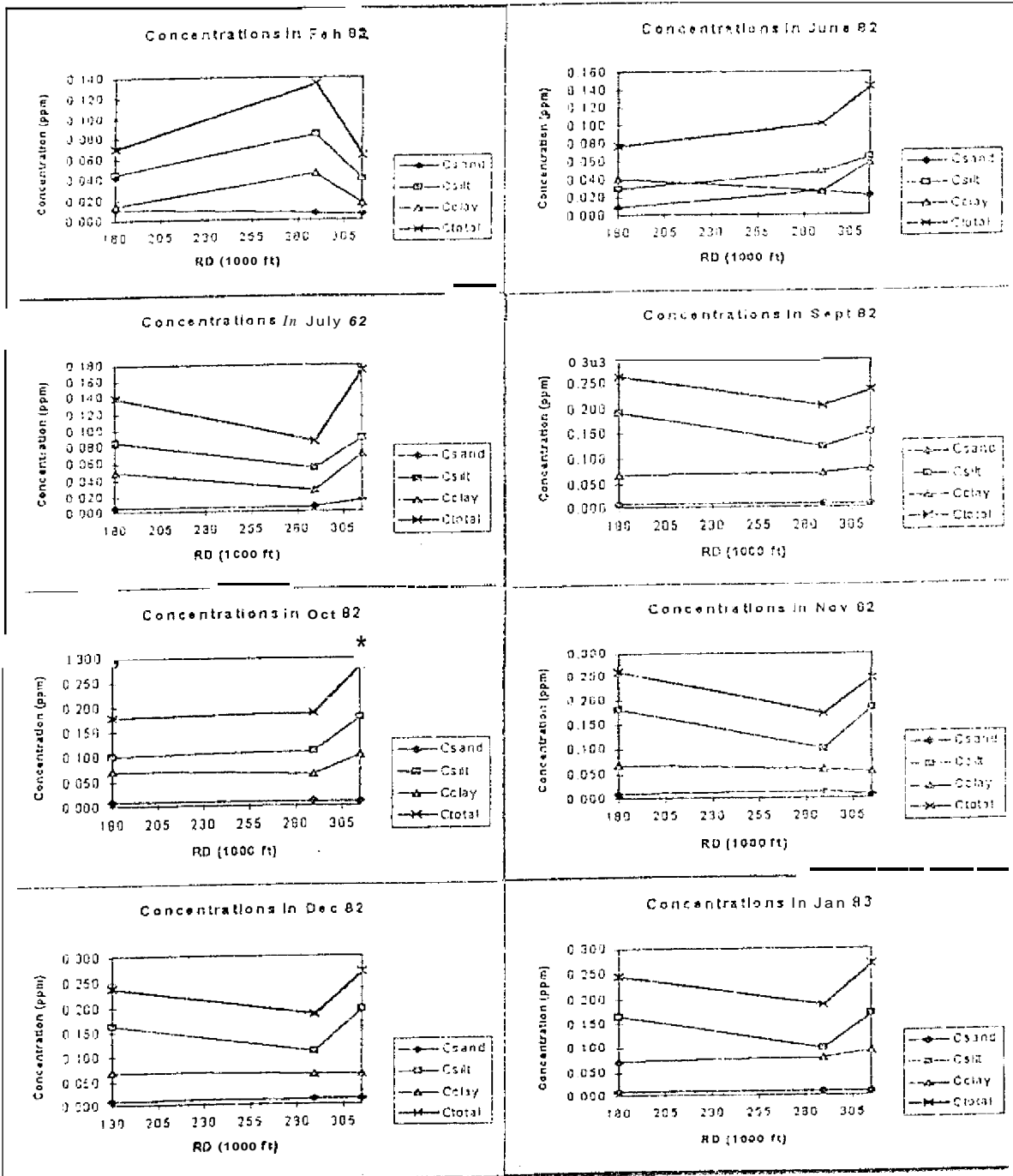


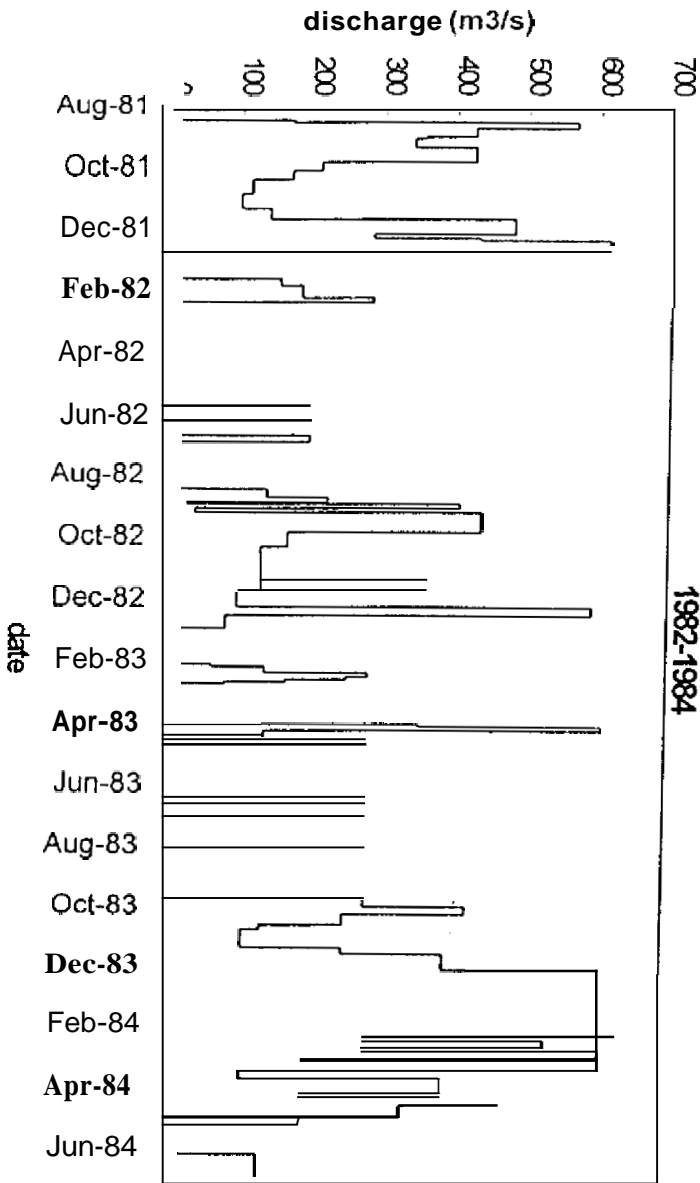
Bed levels and bed variations for Chashma Jhelum Link Canal: 1981-1984





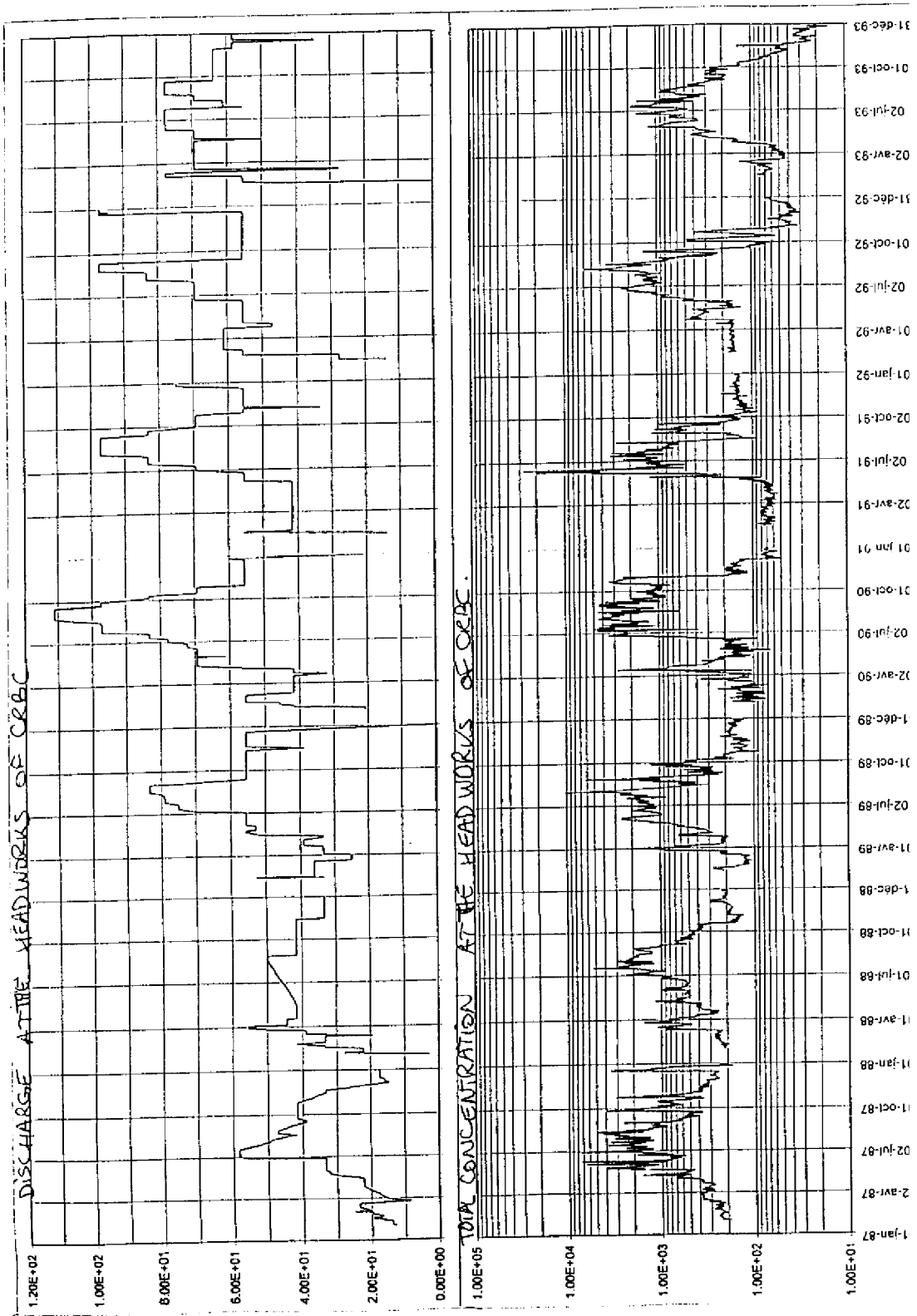
Concentrations for CJ Link 1982 at different abscissas





Discharge at the head regulator of CJ Link Canal
1982-1984

Appendix 3 : Discharges and concentrations



(a) Discharges at the head of CRBC

(b) Total Concentration at the head of CRBC

Appendix: 4 Equilibrium transport formulae (fine particles)

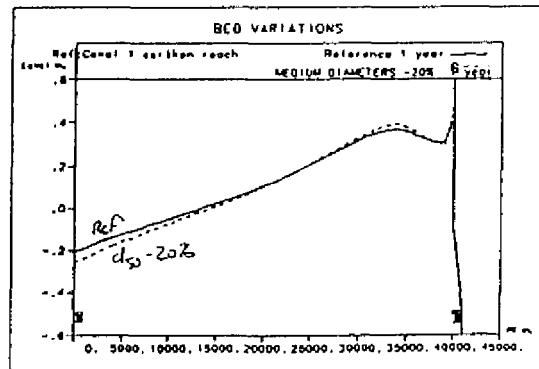
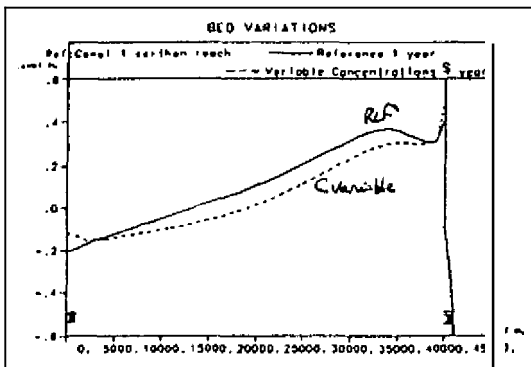
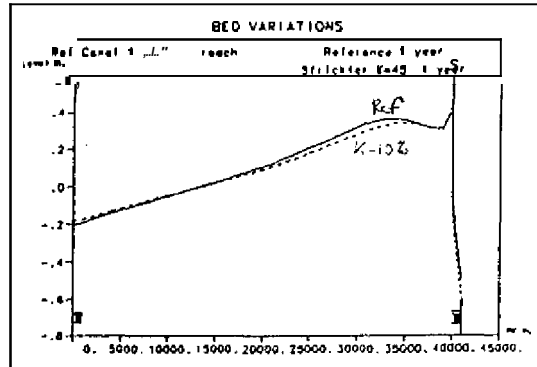
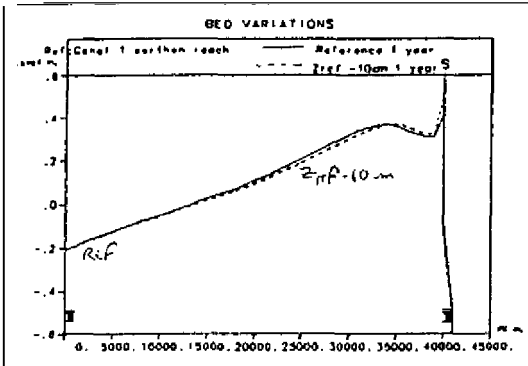
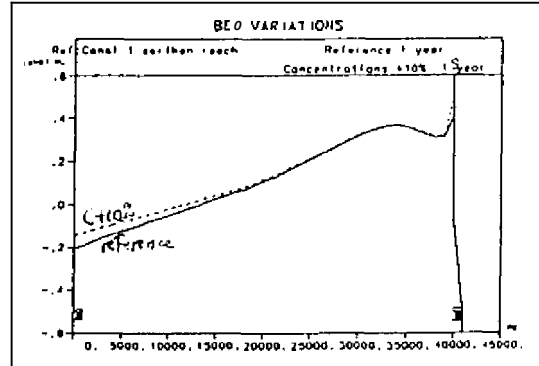
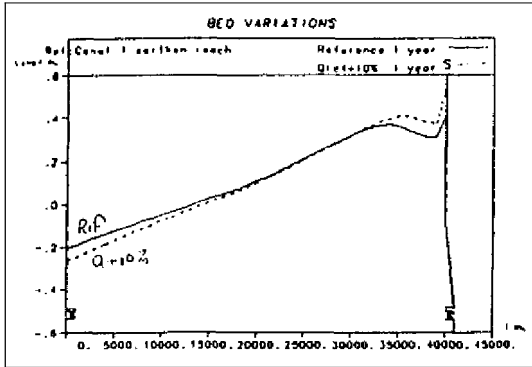
Author	Formula	Domain of validity	Opinion in literature
Engelund-Hansen (1967)	$q_s = 0.08 \sqrt{g(s-1)d}^{3/2} \left[\frac{hU}{(s-1)d} \right]^{5/2} \frac{C^2}{g}$ <p>C being here Chézy coefficient</p>	<ul style="list-style-type: none"> • total load - 190μm < d < 930μm 	<ul style="list-style-type: none"> - transport with dunes (Y > 0.3)
Bagnold (1966)	$q_s = \frac{\tau_0 \cdot U}{\rho g} \left[B_1 + B_2 \frac{U}{w} \right]$	<ul style="list-style-type: none"> - total load - based on energetical considerations 	<ul style="list-style-type: none"> - good results when suspension is present (Y > 0.4)
Ackers-White (1973)	$M = \frac{U^{*n}}{\sqrt{g(s-1)d_{35}}} \left[\frac{U}{\sqrt{32} \log \frac{12R_h}{d_{35}}} \right]^{1-n}$ $Tr = C_f \left(\frac{M}{A} - 1 \right)^m$ $q_s = d_{35} \left(\frac{U}{U^*} \right)^n \cdot Tr$ <p>with, for 1 < d* < 60,</p> $C_f = \exp(2.86 \ln(d^*) - 0.434 (\ln(d^*))^2) - 8.13$ $m = 1 - 0.56 \ln(d^*)$ $A = \frac{0.23}{\sqrt{d^*}} + 0.14$ $n = \frac{9.66}{d^*} + 1.34$	<ul style="list-style-type: none"> - total load - narrow grain size distribution particles from 0.04 to 8mm not established for $\sqrt{d} < 200$ and $d < 28$mm 	<ul style="list-style-type: none"> - obtained after field experiments - d₃₅ more representative than d - good accuracy in the domain of validity - not applicable when the particles with a diameter lower than 40μm are in majority,
Yang (1972)	$\ln C^* = 5.435 - 0.286 \ln \left(\frac{wd}{v} \right) - 0.457 \ln \left(\frac{U^*}{w} \right) +$ $\left[1.799 - 0.409 \ln \left(\frac{wd}{v} \right) - 0.314 \ln \left(\frac{U^*}{w} \right) \right] \ln \left[\frac{U}{w} - \frac{U_{*c} v}{w} \right]$ $\frac{U_{*c}}{w} = 2.5 \left[\ln \left(\frac{U^* d}{v} \right) - 0.06 \right]^{-1} + 0.66$ <p>for $1.2 < \frac{u^* d}{v} < 70$</p> $t_s = U h C^*$	<ul style="list-style-type: none"> total load - narrow grain size distribution w terminal velocity d: 150 to 1710μm h: 0.01 to 15.2m U: 0.23 to 1.97m/s f: 0.000043-0.0279 C*: 10-585000ppm 	<ul style="list-style-type: none"> good accuracy (after Yang and Molinas, 1982) be careful when the proportion of big particles is not negligible.

<p>Karim-Kennedy (1990)</p>	$\Phi = 0.0015 \left[\frac{V}{g(\rho_s/\rho - 1)d} \right]^{3.369}$ $\left[\frac{u^* - u_{*c}^*}{g(\rho_s/\rho - 1)d} \right]^{0.840}$	<p>- total load - u_{*c}^* critical shear velocity defined after Shields curve.</p>	<p>- good accuracy especially when the total shear stress is superior to the critical shear stress.</p>
<p>Karim Kennedy (1981)</p>	$X_1 = \frac{q_s}{\sqrt{e\Delta d_{30}^3}}$ $X_2 = \frac{V}{\sqrt{g\Delta d_{30}^3}}$ $X_3 = \frac{u^* - u_{*cr}^*}{\sqrt{g\Delta d_{30}^3}}$ $X_4 = \frac{h}{d_{30}}$ $\log X_1 = -2.279 + 2.972 \log X_2 + 1.060 \log X_3 + \log X_4 \log X_3$	<p>-same remarks as before</p>	<p>- good accuracy after Cardoso and Neves (Ref 1) - According to the authors, this formula is more accurate for the low concentrations of sediments</p>

Spatial Delay Effect Laws

<p>Han (1980)</p>	$\frac{\partial C}{\partial x} = K(C^* - C)$ <p>with $K = \frac{\alpha \cdot w}{u^*}$</p>	<p>- appropriate for total load</p>
<p>Krone (1962) and Parthéniades (1965)</p>	<p>For erosion (Parthéniades):</p> $\phi = M \left[\frac{\tau}{\tau_{crb}} - 1 \right] \text{ if } \tau > \tau_{crb}$ <p>For deposition (Krone):</p> $\phi = -w \cdot C_f \left[1 - \frac{\tau}{\tau_{crd}} \right] \text{ for } \tau < \tau_{crd}$	<p>- appropriate for cohesive sediments; - appropriate for total load; - empirical model where M and the critical shear stresses must be obtained by calibration. - C_f is a reference concentration, in the vicinity of the bed, at a variable distance of it.</p>

Appendix 5 : Sensitivity analysis of the model

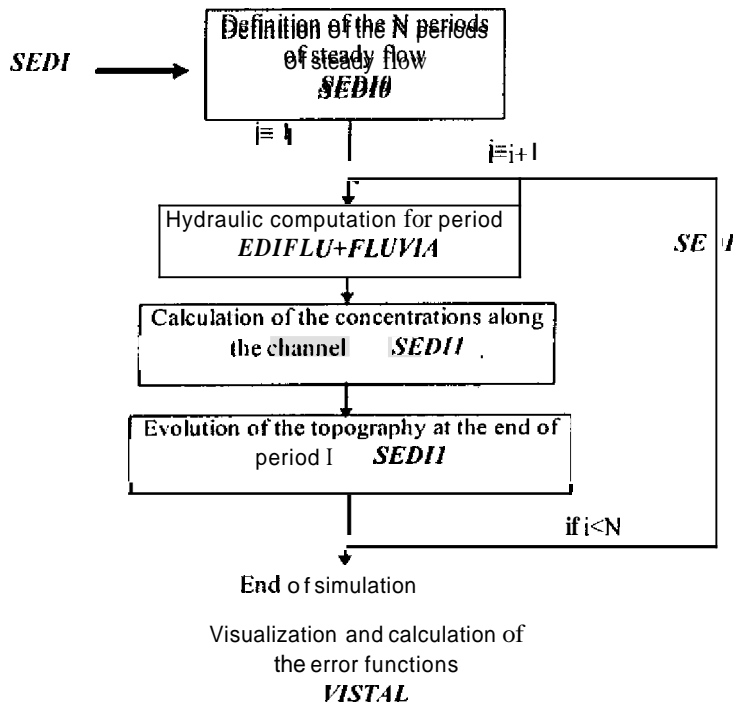


SIC-SEDI program - practical presentation

Version 03 August 1996, demonstration version IIMI-ISRIP-CEMAGREF

1. General

SEDI aims at calculating the evolution of the bed topography of a canal for a succession of steady flow periods, where the hydraulic and sedimentologic variables are constant. The geometry of the canal is updated at the end of each of these periods.



The command program SEDI is computed in Pascal for Windows. The programs SEDI0 and SEDI1 are computed in FORTRAN77.

VISTAL is the tool which allows to visualize three topographies at the same time, and to calculate the error functions between these geometries.

All these programs still have to be developed for a correct utilization (interfaces and algorithms)

2. Requirements

2.1 Geometric data

The initial geometric files must be prepared with TALWEG: files .MIN, .TIT, .DIS.

2.2 Hydraulic data

You need to create as many files .FLU (created by EDIFLU) as necessary for your whole simulation. However, the discharge at the upstream node of the canal is read at each period of steady flow. For instance, if the Strickler coefficients, the operations at the nodes, the targeted levels, the downstream condition are unchanged for the whole simulation, you need to create only one file .FLU, even though the discharge is variable.

NB: be sure that the calibration mode for FLUVIA is **not** activated.

2.3 Sedimentologic data:

They are all contained in the file .SED which must be edited manually, respecting strict format of writing.

You have to enter:

- general variables: constant due to gravity, specific weight, porosity of the sediments, kinematic viscosity
- grain size distribution. First of all, three classes have to be defined. The grain size distribution is specified for the whole period of simulation through the medium diameters for each class,
- limit for wash load: it can be user-defined or automatically calculated thanks to an energetic criterion.
- data for each period of steady flow:
 - * discharge at head
 - * concentrations for the three classes of particles at the upstream node;
 - duration of the period;
 - * medium diameter for the coarsest class [if not mentioned in the general grain size distribution]
- parameters for the laws
 - * you have to select the laws for the evolution of the bed material load
 - ⇒ model with equilibrium concentration: select a formula (Ackers-White, Engelund-Hansen, Yang, Karim Kennedy, Bagnold) as well as a loading law (Han).
 - ⇒ empirical model: for cohesive sediments especially (Krone and Partheniades)

Original values: $\beta=1$ For the equilibrium concentration, except for Bagnold law which has two parameters: $\beta_1=0.17$, $\beta_2=0.01$ for very fine particles).

Refer to the MSc study for the parameters of Han's loading law encountered for CRBC and CJ Link canal.

3. Output

- geometric files .MIN, .TIT, .DIS which can be visualized by VISTAL. NB: presently, the file .TIT is reduced and cannot be used for the steady flow computation.
- result files: for each period, a file .LST is created. Currently, the following informations are provided for each calculation section:
 - ⇒ number of the calculation section
 - ⇒ Xgeo: abscissa (m)
 - ⇒ Q : discharge (m^3/s)
 - ⇒ A: wetted area (m^2)
 - ⇒ Rh: hydraulic radius (m)
 - ⇒ J : slope of the energy line (m/1000m)
 - ⇒ DS : variation of the bed area in the section (m^2);
 - ⇒ DZB : maximum variation of the bed level (m)
 - ⇒ C_{sand}, C_{silt}, C_{clay}: concentrations for the three classes of particles (g/l)
 - ⇒ C_e: equilibrium concentration (g/l)

⇒ **D50** : medium diameter of the bed material load (μm)

⇒ **DWL** : critical diameter for wash toad (μm)

Y : Shields parameter

This list can easily be modified.

4. Restrictions

A few are listed below:

- the model was tested on simple reaches only (**earthen** portion of CRBC and CJ Link canal,
- a simulation cannot contain more than **99 periods**. For more periods, divide your period of simulation, and take care to use a complete file .TIT (titles of the geometric file), like the initial one, for the second simulation.
- the model only deals with erodible beds. If used for a lined canal, the bed may also be scoured. In the future, a special structure (extra geometric tile) should contain the nature of the bed (concrete, sand [⇒ diameter of the particles], cohesive sediments, dunes...)
- the integration to several branches was not tested: the singularities are over simplified (the concentration is supposed to totally transferred from one branch to another at the nodes, whatever the nature of the offtake).
- local phenomena (kila bushings, ...) cannot be modeled at present (see the simplification of the sediment distribution in the cross section)

...refer also to the report for the simplifications in the model.

5. Type of errors

-'Error reading file .MAC': the steady flow computation encountered some errors, such as:

- * over topping
- * targeted level not achieved
- * discharge out of range of the downstream condition
- * wrong data or format in file .FLU
- ...

Advice: change the interface mode to 'Normal' in the Option menu of SIC and run FLUVIA and EDIFLU on the initial geometry.

- 'Warning: time step should be shorter': the bed elevation variation was too important (25% of the water depth is this version). Check file .LST, reduce the time step or change the parameters of the laws.

- Windows errors : check the files .LST

...

6. Edition of the file .SED

See example.

All the line preceded by '*' are read as comments.

All the lines of data must start by a special character. The information associated to this character is read from the 11th column, except for the description of the periods.

In the following description of the formats, 'x' means character not read and benchmarks the limit between two informations.

Fxxxxxxxxx**GEOMETRY** : initial geometric **file** .MIN
FH01xxxxxxxx**HYDRAULI** : hydraulic file, valid for period 01 **and** until a new hydraulic file is read
 In the example, CR90JL1R is used for **periods 01 and 02**, CR90SE1R is valid for **period 03 to the last period**
Nxxxxxxxxxx**UPSTNODE** : upstream node name
X1 xxxxxxxx**LOWERxMEDIUM**: **lower limit** for **the finest class (0)**, then medium diameter inside the class.
X2 xxxxxxxx**LOWERxMEDIUM** : lower limit for the middle class (normally **silt**, thus 2 or 5 μm), then medium diameter inside the class.
X2 xxxxxxxx**LOWERxMEDIUM** : **lower limit** for **the coarsest class** (normally **sand**), then medium diameter inside the class. **If** this diameter **is** below the limit of the class, it will be read again at each period.
Yxxxxxxxxxx**DWL** : critical diameter for the wash load.
PiixQ0\$\$\$\$xCOSAND**xCO**SILT**xCO**CLAY**xDT\$\$\$\$x**D50**\$\$\$** : description of the period **ii**.
Some errors are generated if the periods **are** not numbered in the right order. **Q0** is the head discharge (m^3/s), **CO\$\$\$\$** are the head concentrations, **DT** is the duration of the period in days, **d50** the medium diameter of the coarse class if it is not mentioned in **the grain size distribution (μm)**.
Lxxxxxxxxxx**IEQ** : number of the equilibrium law
B1xxxxxxxxxx**B1** : first parameter for the equilibrium law, (**BxxxxxxxxxB1** is sufficient if only one parameter is needed)
B2xxxxxxxxxx**B2** : second parameter for **the equilibrium law**.
Cxxxxxxxxxx**ILOAD** : **number of** the loading law.
Dxxxxxxxxxx**D1**
D1xxxxxxxxxx**D1** : first deposition parameter;
D2xxxxxxxxxx**D2** : second deposition parameter;
Exxxxxxxxxx**E1**
E1xxxxxxxxxx**E1** : first erosion parameter;
E2xxxxxxxxxx**E2** : second erosion parameter;

7. Visualization

This is briefly presenting the program VISTAL

VISTAL allows to visualize **the geometric files** computed by TALWEG or SEDI. Three **files** can be **open** in the same time. The first one is called **the reference file**.

The structure is similar to the program VISFLU (visualization of FLUVIA results).

The file VISTAL.INI contains the proportion **X of the total** width (LMAX) on which the medium bed level will be calculated (see procedure in the MSc report) [interface to be done]. In the following, we will call this width LBED: $\text{LBED}=\text{LMAX}*\text{X}$

7.1 Description of the options

- "Longitudinal profile" : visualization of the longitudinal medium bed level or of the bed variations
- "Cross sections" : visualization of the **cross** sections used for the steady flow computation. They are symmetrical (defined in width/elevation) thus they may differ from the actual cross section entered **under** EDIFLU.
- "reference file visualization": visualization **of the medium bed levels of all the open files** (defined in part 3 of the Msc report) and **the bank of the reference file**.
- "bed variations" : visualization of the **differences** between the second **file** and the first file (reference file) (\Rightarrow continuous line) and **between** the third and **the reference file** (\Rightarrow dotted line).

The scale can be calculated automatically or user-defined.

Graphical representation: the titles are **the ones included in file .TIT** (that **is why this file is changed by SEDI**). *You* can print the result on a file .HGL which can be then inserted as a picture in WORD. However the transfer changes the long **dots** into short dots (problem of converter).

7.2 output

The output is the file VISTAL.LST which contains the **following** informations

- lowest point elevation of **each section and medium** bed level calculated on the lowest **part of** the bed (the percentage of the total **width on** which the calculation is **made** is specified in the file VISTAL.INI);

- comparison between the geometries:

first column: number of the calculation section

second column: longitudinal abscissa (**m**) from the **upstream** node

third column: difference of volume between the second file and the first file, calculated on the width of the bed I.BED.

fourth column: **same difference** but between the third and the first files.

fifth and sixth columns: differences between the total volumes (procedure to be checked when the banks **are not the same** for the files that are **compared**).

last column: percentage of **error** between column 3 and 4 (999% means **out** of range).

At the end, the **quadratic error functions** (gross and **normalized**) are calculated (see definition in the report).

Appendix 7 : sediment data files

CRBC 1987-1989 (complete file .SED)

```

*****
Sedimentologic Data for SEDI
Version 01 August, 1996
*****

* Initial geometric file (.MIN, .DIS, .TIT) without extension
* The six first characters will give the name to the simulation
XXXXXXXX
FGEOM CR87AP1R
* Hydraulic files
* ---> check consistency with periods
FH01 CR87AP1R
FH13 CR88JA1R

* Upstream node
N HEAD

* Grain size distribution
* CLASS LOWER MEDIUM DIAMETERS (MICRONS)
*I XXXXXX XXXXXX
X1 CLAY 0. 2.
X2 SILT 5. 20.
X3 SAND 62. 0.

* if D50 for sand is lower than the limit silt/sand
* its value will be read at each period

* Limit for Wash load (microns):
* Enter a negative value if you want it to be calculated with
* an energetical criterion at each calculation section
Y -1.

*****
* Description of the different periods of steady flow
*****
*PP Q0XXXX COSAND COSILT COCLAY DTXX D50XX
PO1 20.7 .019 .166 .237 30. 152.
PO2 28.2 .026 .807 .713 30. 152.
PO3 38.5 .414 .688 .635 15. 152.
PO4 38.5 .414 .688 .635 15. 152.
PO5 55.8 .728 .709 .717 15. 152.
PO6 55.8 .728 .709 .717 15. 152.
PO7 45.9 .691 .498 .672 15. 152.
PO8 45.9 .691 .498 .672 15. 152.
PO9 41.1 .453 .220 .303 30. 152.
P10 41.0 .304 .274 .320 30. 152.
P11 30.6 .021 .166 .143 30. 152.
P12 16.8 .372 .166 .127 27. 152.
P13 28.9 .018 .108 .110 30. 150.
P14 38.2 .019 .221 .433 30. 150.
P15 44.5 .016 .172 .228 30. 150.
P16 41.9 .081 .251 .274 30. 150.
P17 44.2 .126 .272 .298 30. 150.
P18 46.9 .765 .614 .586 7. 150.
P19 46.9 .765 .614 .586 10. 150.
P20 46.9 .765 .614 .586 13. 150.
P21 48.4 .370 .583 .920 15. 150.
P22 48.4 .370 .583 .920 15. 150.
P23 41.6 .020 .253 .345 30. 150.
P24 41.6 .011 .155 .160 30. 150.
P25 39.9 .008 .063 .098 30. 150.
P26 33.3 .014 .102 .108 34. 150.
P27 42.0 .012 .095 .099 9. 150.

*****
* General data
*****
G 9.81
W 1000.
V 0.000001
S 2650,
M 0.3

*****
* Choice of the laws

```

```

*****
* Equilibrium Law: 1 Engelund;
*                 2 Ackers White;3 Bagnold;
*                 4 Van Rijn;5 Karim Kennedy 1990;
*                 6 Yang; 7 Karim Kennedy 1981
*****
L           3
* Parameters for the laws
B1         0.17
B2         0.01
* B=Multiplicative coefficient for the equilibrium law
* Normal values : B=1. For the laws 1,2,4,5,6,7
                B1=0.17 0.2 around 0.01 for law 3
*****
* Non equilibrium law : 1 Han Qiwei;2 Dnubert Lebreton
                      3 Krone et Partheniades
*****
C           1
*Parameters for the laws
D         0.01
E         0.005

```

CRBC 1989-1990

*Grain size distribution

*CLASS LOWER MEDIUM DIAMETERS (MICRONS)

*I XXXXXX XXXXXX

X1 CLAY	0.	1.5
x2 SILT	5.	30.
X3 SAND	62.	188.5

'Description of the different periods

*PP	Q0XXXX	COSAND	COSILT	COCLAY	DTXX	D50XX
P01	36.5	.010	.070	.073	30.	100.
P02	30.3	.012	.246	.198	30.	100.
P03	36.1	.014	.119	.153	30.	100.
P04	52.4	.086	.608	.472	30.	100.
P05	57.9	.107	.543	.630	30.	100.
P06	77.5	1.019	.740	.721	15.	100.
P07	77.5	1.019	.740	.721	15.	100.
P08	81.6	.153	.485	.408	30.	100.
P09	56.1	.066	.131	.304	30.	100.
P10	55.5	.019	.050	.088	30.	100.
P11	52.6	.016	.060	.089	30.	100.
P12	44.4	.010	.066	.086	24.	100.
P13	45.8	.015	.038	.073	30.	100.
P14	43.2	.011	.040	.099	30.	100.
P15	41.6	.044	.193	.447	30.	100.
P16	68.0	.012	.040	.111	30.	100.
P17	71.3	.549	.157	.123	15.	100.
P18	71.3	.549	.157	.123	15.	100.
P19	86.7	.326	.708	1.310	15.	100.

CRBC 1990-1993

'Description of the different periods

*PP	Q0XXXX	COSAND	COSILT	COCLAY	DTXX	D50XX
P01	86.2	.327	.721	1.194	15.	160.
P02	102.9	.202	.708	1.716	30.	160.
P03	105.1	.177	.674	.883	30.	160.
P04	71.0	.176	.597	.901	30.	160.
P05	55.5	.011	.041	.106	30.	160.
P06	53.9	.009	.025	.046	30.	160.
* 1991						
P07	42.1	.011	.026	.035	30.	160.
P08	41.6	.008	.025	.034	30.	160.
P09	41.6	.010	.022	.036	30.	160.
P10	41.6	.015	.083	.148	15.	160.
P11	53.4	5.341	1.818	.824	4.	160.
P12	53.4	5.341	1.818	.824	4.	160.
P13	53.4	5.341	1.818	.824	7.	160.
P14	57.5	.815	.555	.370	15.	160.
P15	71.9	.419	.673	.460	15.	160.
P16	88.7	.254	.424	.369	30.	160.
P17	97.0	.021	.189	.217	30.	160.
P18	75.1	.015	.057	.135	30.	160.
P19	60.2	.011	.037	.082	30.	160.
P20	55.5	.014	.044	.092	30.	160.
P21	60.4	.014	.045	.082	30.	160.
* 1992						
P22	44.3	.018	.050	.089	30.	160.
P23	61.1	.019	.053	.093	30.	160.
P24	55.0	.019	.115	.186	30.	160.
P25	55.5	.053	.132	.145	30.	160.
P26	65.3	.329	.484	.629	30.	160.
P27	73.5	.822	.394	.570	15.	160.
P28	73.5	.822	.394	.570	15.	160.
P29	91.4	.476	.200	.372	30.	160.
P30	57.9	.097	.118	.138	30.	160.
P31	55.5	.044	.024	.047	30.	160.
P32	55.5	.010	.011	.021	30.	160.
P33	75.5	.019	.012	.025	30.	160.

```

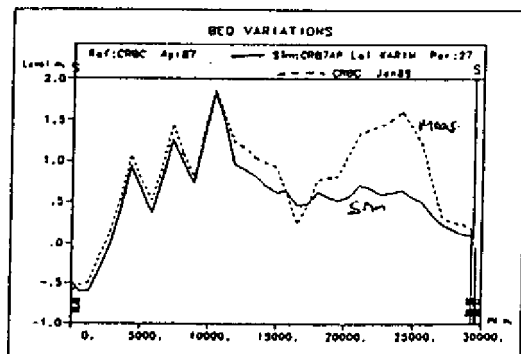
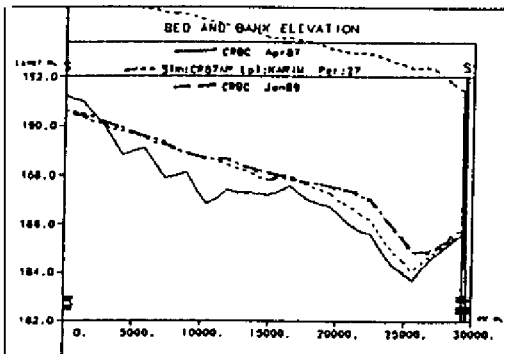
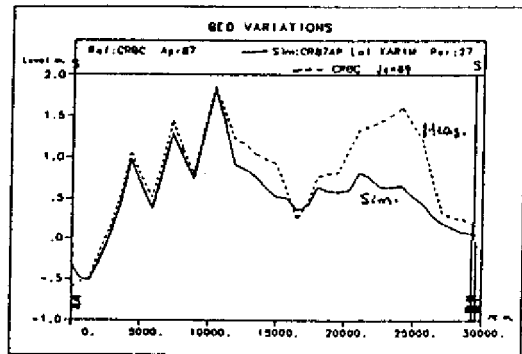
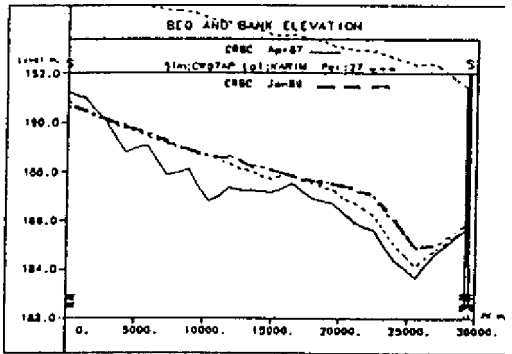
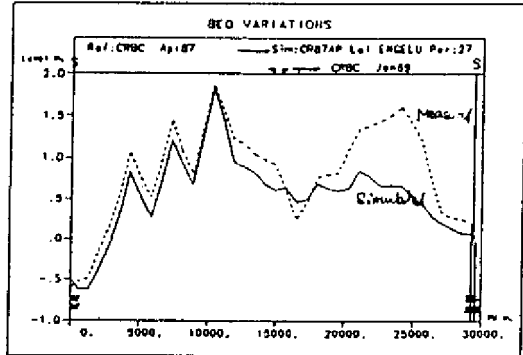
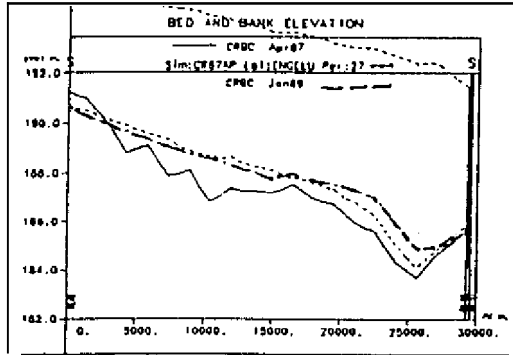
*****
• Equilibrium Law:  1 Engelund;
                   2 Ackers White;3 Bagnold;
                   4 Van Rijn;5 Karim Kennedy 1990;
                   6 Yang; 7 Karin Kennedy 1981
*****

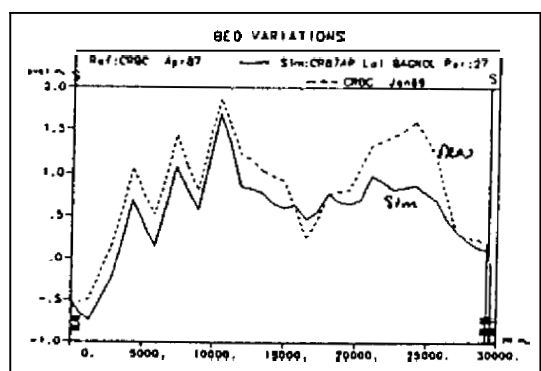
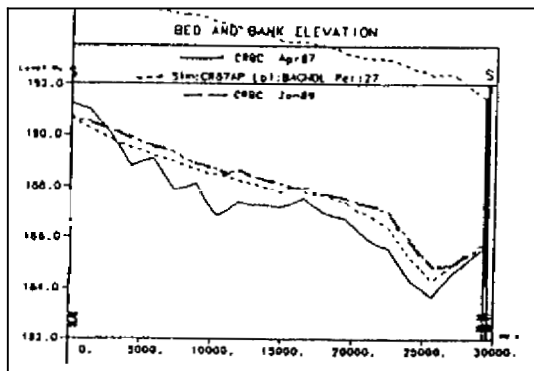
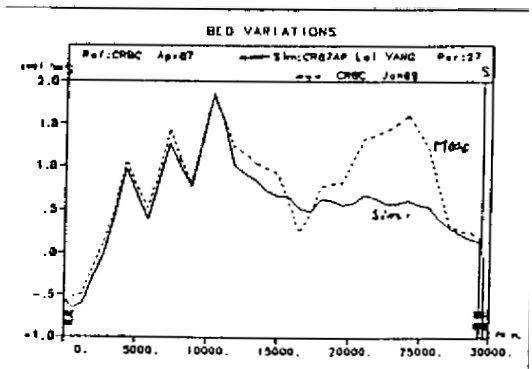
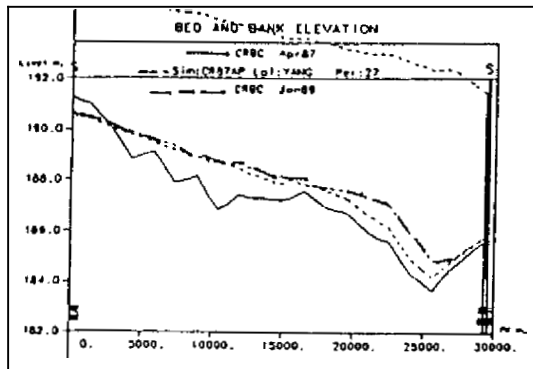
L           3
* Parameters for the laws
B1          0.17
B2          0.01
* B=Multiplicative coefficient for the equilibrium law
* Normal values : B=1. for the laws 1,2,4,5,6,7
                  B1=0.17 B2 around 0.01 for law 3
*****
* Non equilibrium law : 1 Han Qiwei;2 Daubert Lebreton;
                       3 Krone et Partheniades
*****

C           1
* Parameters for the laws
D           0.01
E           0.005
    
```

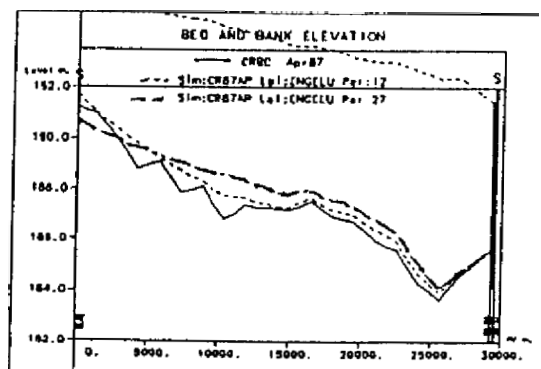
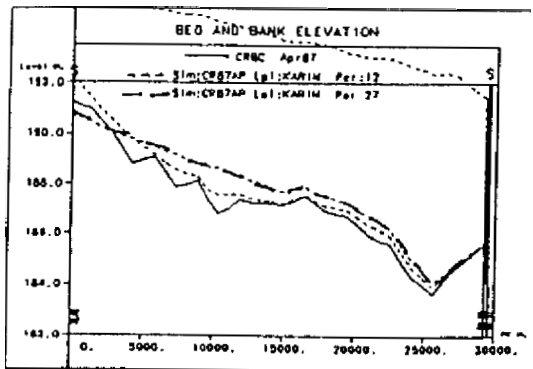
Appendix 8 : Graphical results of calibration

Results of calibration, CRBC 1987-1989

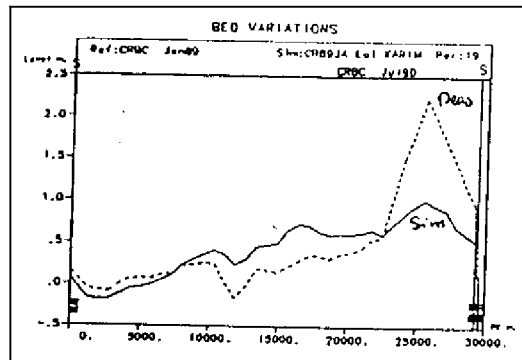
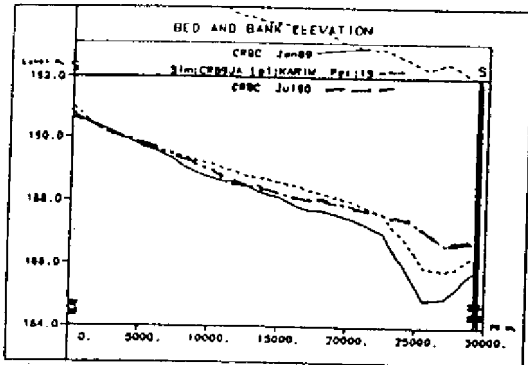
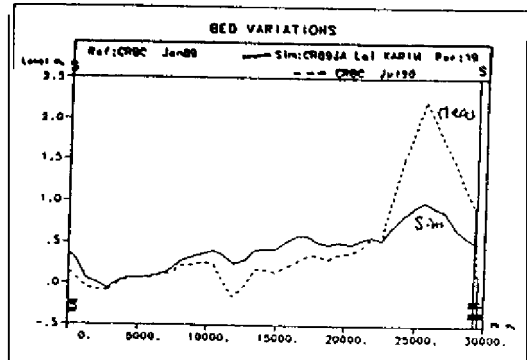
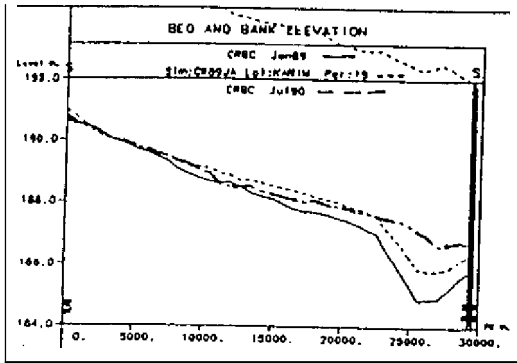
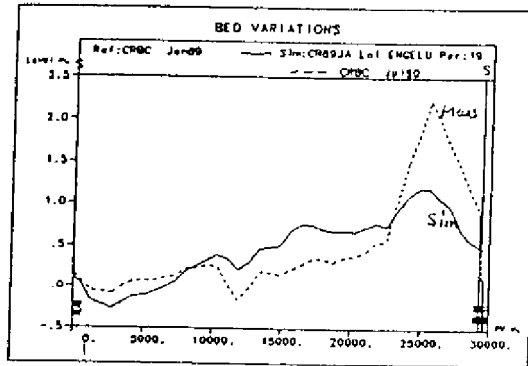
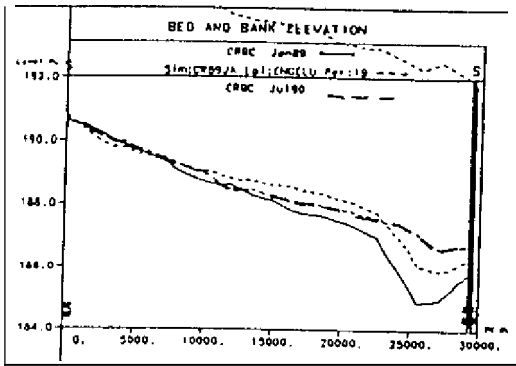


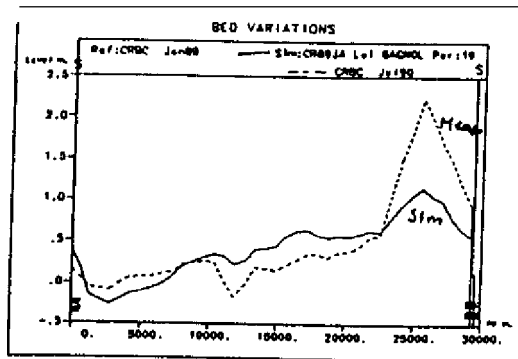
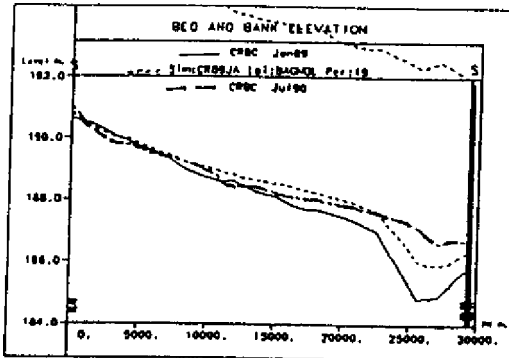
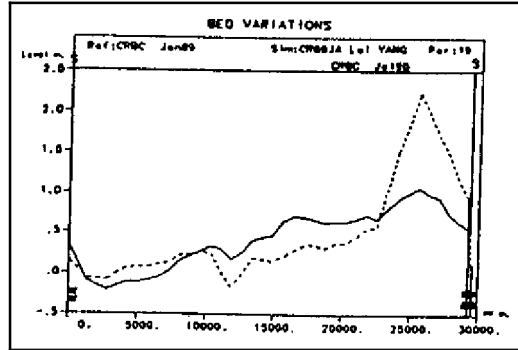
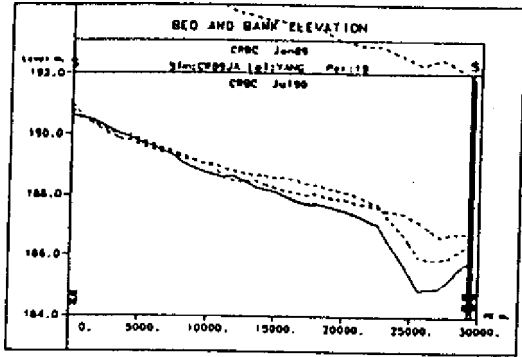


Simulated evolutions for April 1987, March 1988 and January 1989:

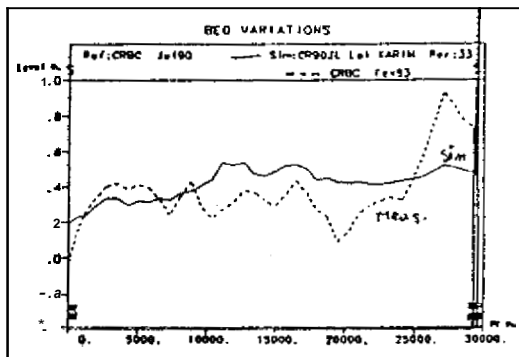
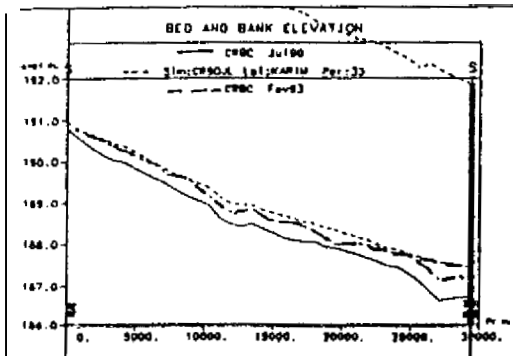
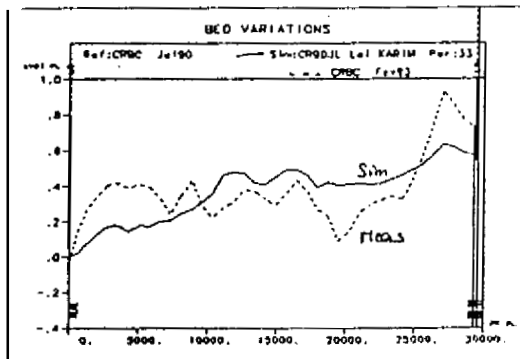
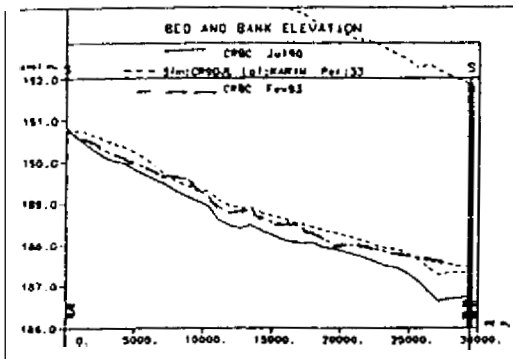
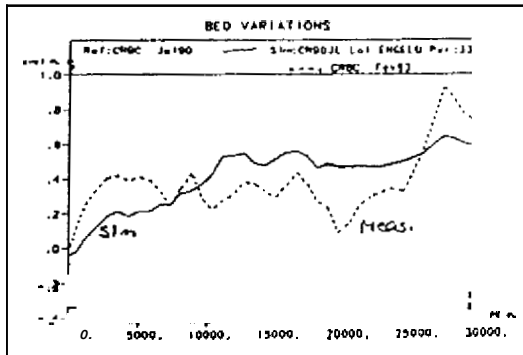
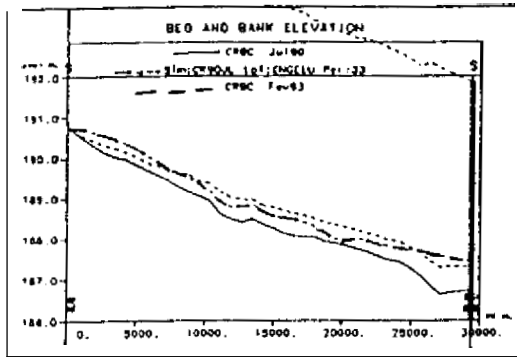


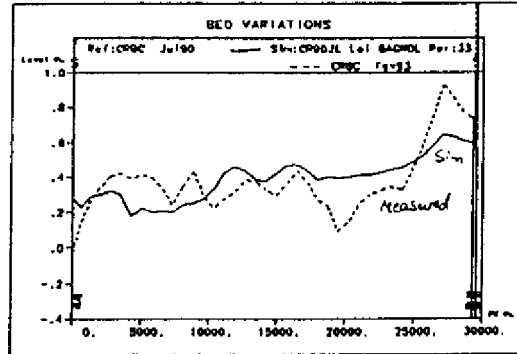
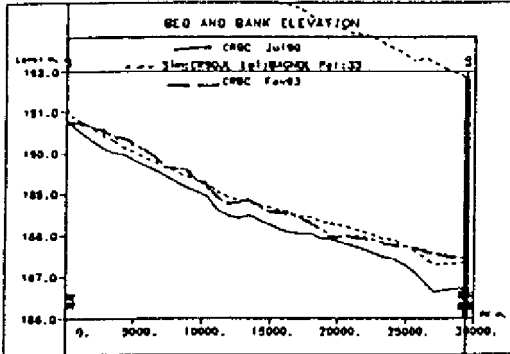
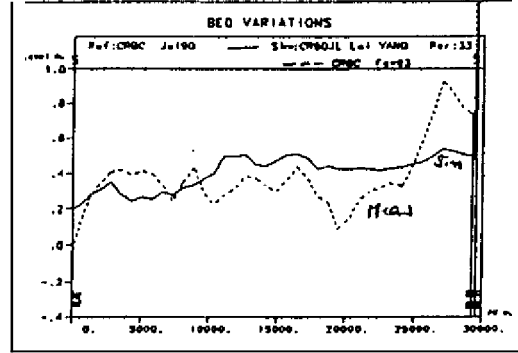
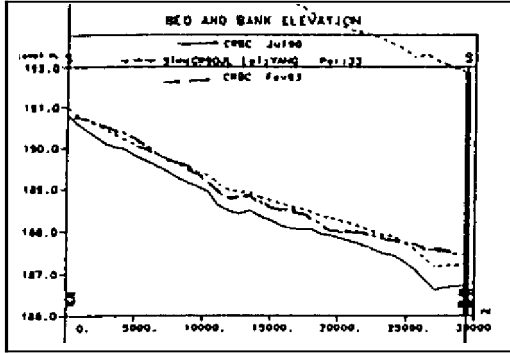
Results of calibration, CRBC 1989-1990



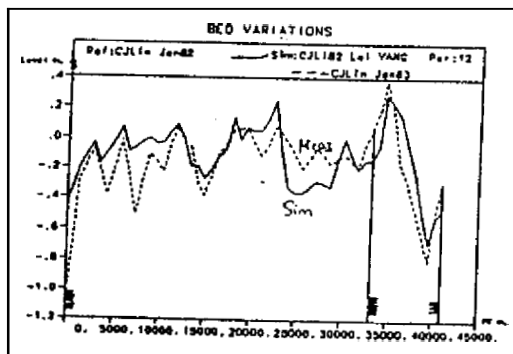
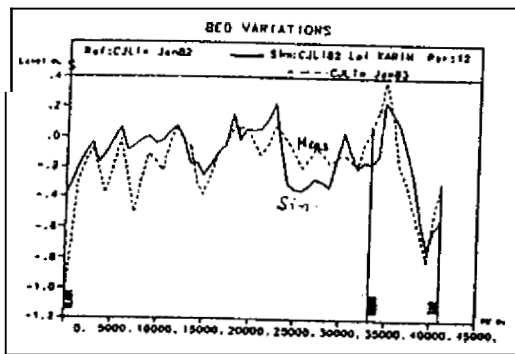
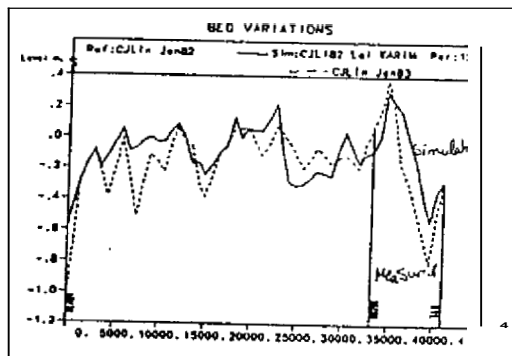
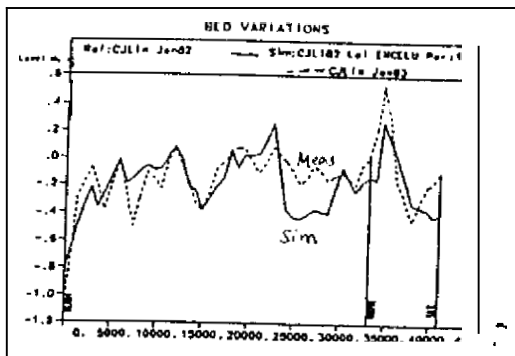
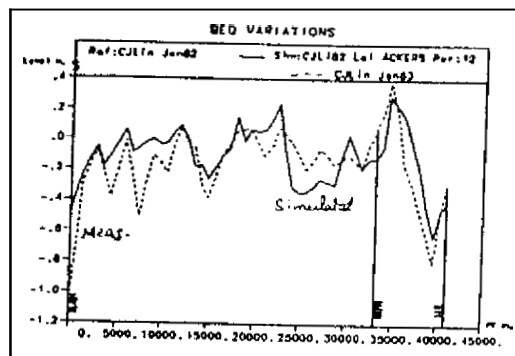
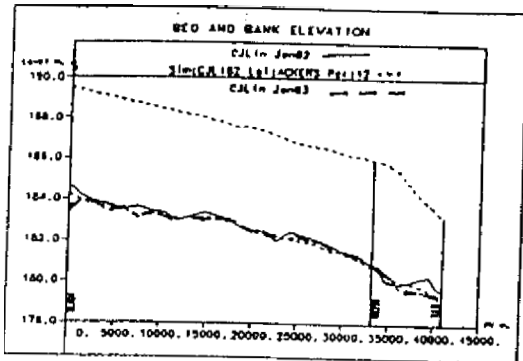


Results of calibration. CRBC 1990-1993

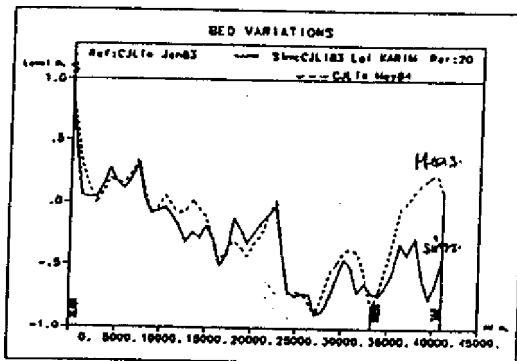
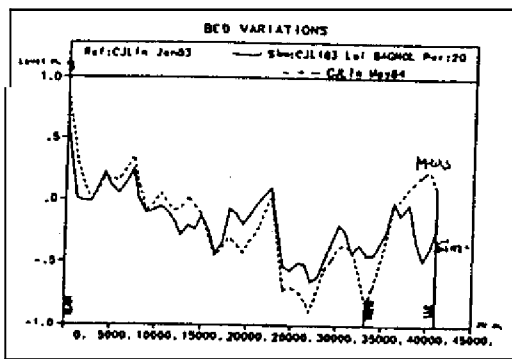
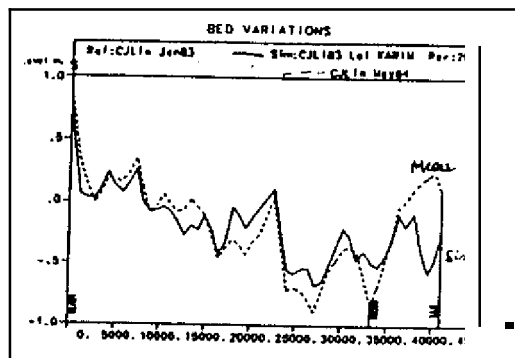
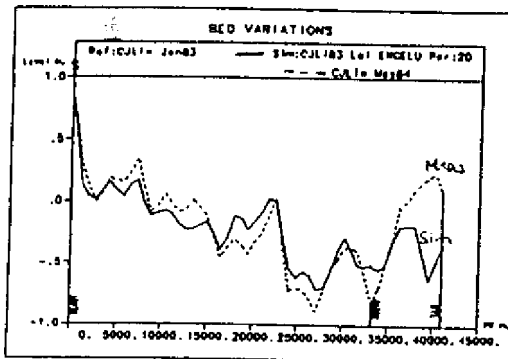
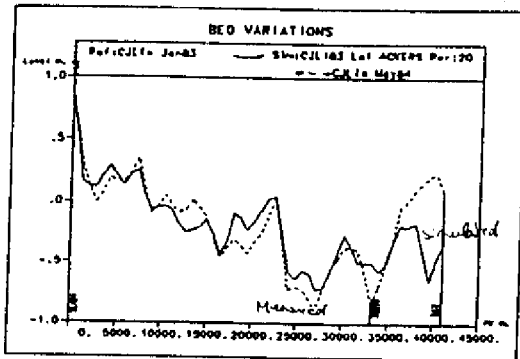
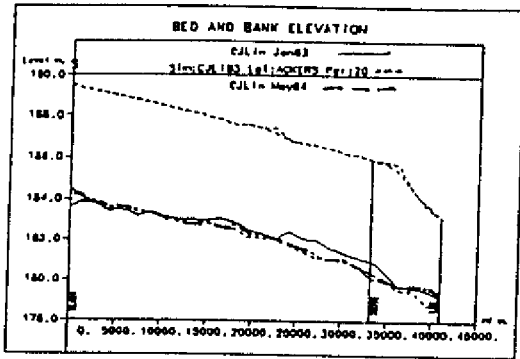




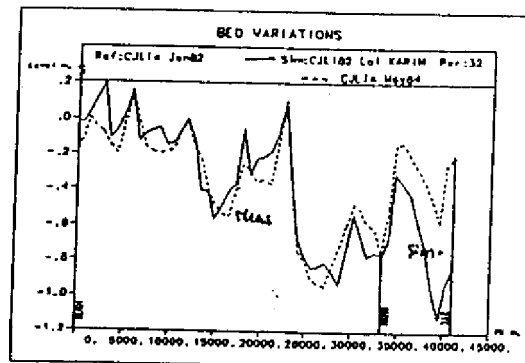
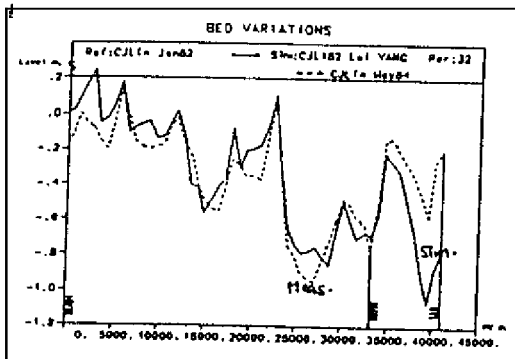
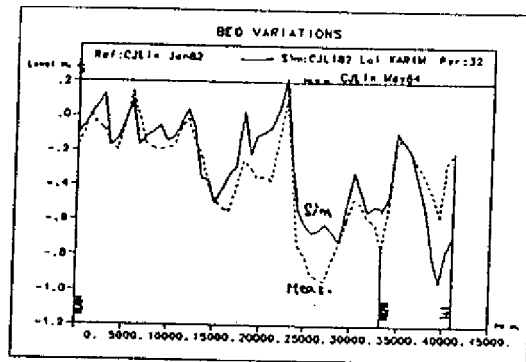
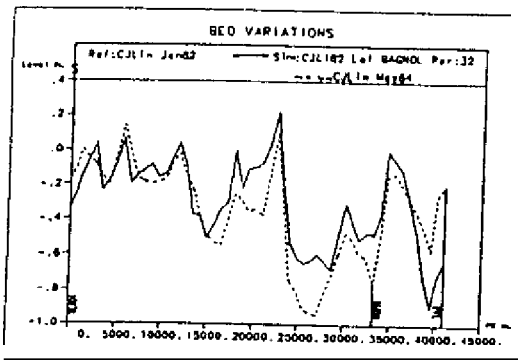
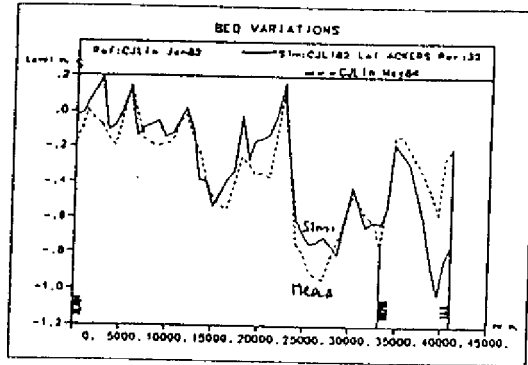
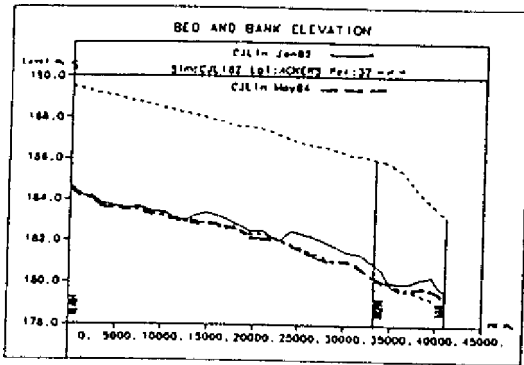
Results of calibration for Chashma Jhelum Link Canal 1982-1983



Results of calibration for 1983-1984



Results of calibration for 1982-1984



Concentrations for CJ Link 1982 at different abscissas

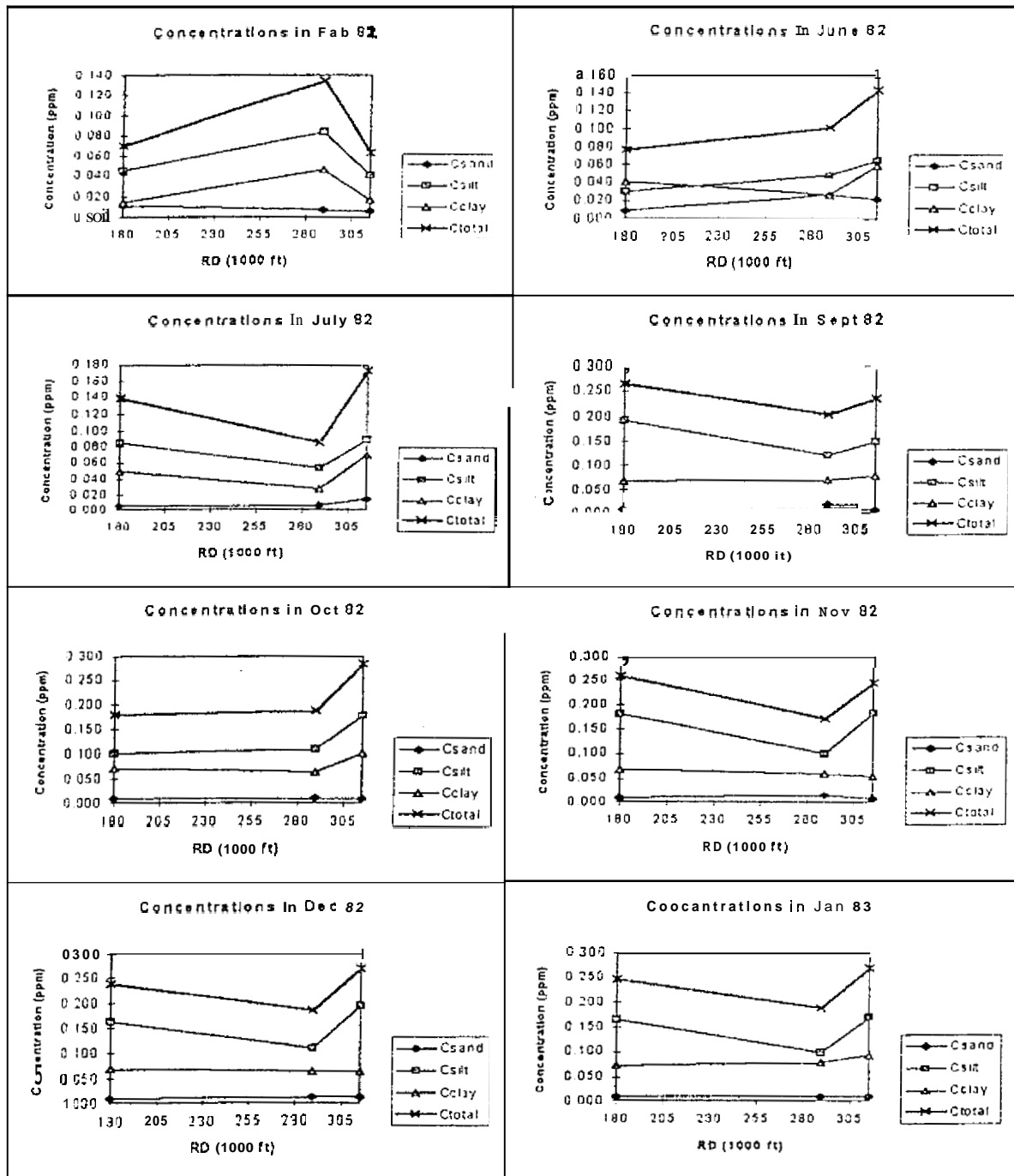


TABLE OF CONTENTS

1. GENERAL	2
<hr/>	
2. DESIGN OF IRRIGATION CANALS	3
2.1 REGIME THEORY	3
2.2 HISTORIC	3
3. PHYSICAL ASPECTS OF SEDIMENT TRANSPORT	4
<hr/>	
3.1 DIFFERENT TYPES OF TRANSPORT	4
3.1.1 BED LOAD AND SUSPENSION	4
3.1.2 BED FORMS: SAND WAVES	4
3.2 MECHANICS AT CHANNEL SCALE	4
3.2.1 FUNDAMENTALS OF HYDRAULICS	4
3.2.2 TERMINAL VELOCITY (OR SETTLING OR FALL VELOCITY)	6
3.2.3 INITIATION OF MOTION	7
3.2.4 FRICTION PREDICTION	9
3.3 SYNTHESIS: LINK BETWEEN THE FORCES AND THE SEDIMENT TRANSPORT	9
3.3.1 AT GRAIN SCALE	9
3.3.2 AT THE GLOBAL SCALE	11
3.3.3 INFLUENCE OF THE BED COMPOSITION	12
4. MODELING	13
<hr/>	
4.1 CHOICE OF THE MODELS	13
4.1.1 GENERAL	13
4.1.2 TYPES OF MODELING	13
4.1.3 CRITERIA FOR CHARACTERIZATION	13
4.2 MODELS OF TRANSPORT	14
4.2.1 CLASSICAL FORMULAE	14
4.2.2 SELECTION OF EQUILIBRIUM MODELS	16
4.3 MODELS OF NON-EQUILIBRIUM TRANSPORT	16
4.3.1 CONVECTION-DIFFUSION EQUATION	16
4.3.2 EXCHANGE (OR SPATIAL DELAY EFFECT) LAWS.	17
4.4 EULERO-LAGRANGIAN MODELS	18
4.5 A FEW OPERATIONAL MODELS	18

1. General

In rivers, granular material transport induces major modifications of topography, like thresholds or meanders. An important erosion can threaten the stability of the surrounding grounds.

In storage basins, the fine sediments, coming from upstream lands, are ineluctably deposited when the flow velocity decreases. To insure the perennity of the systems, they must be evacuated, either by mechanical dredging (not always possible), by bottom outlets (with serious environmental consequences downstream from the dam) or by hydraulic flushing (the sediments are carried away by the flow); this second process is quite new: its consequences and efficiency are not well identified at the moment.

The irrigation canals also undergo problems of erosion (earthen canals) and deposition. When sedimentation is important, the capacity of hydraulic transport can be affected, penalizing the users downstream from the networks.

In waste water networks, the deposition also reduces the capacity of transport and strategies of dredging have to be conducted.

Du Boys, in 1879, proposed the first sediment transport formula. Since that time, especially after 1950, many other theories followed, but they often rest on empirical considerations. Even though the theoretical basis have been reinforced in the present formulations of sediment transport, no law can be considered as universal today (ref. [7],[8]).

The rivers of Himalayan countries receive high loads of fine sediments (sand, silt and clay) resulting from an intensive erosion in Himalayan areas. Ning Chien and Tai Ting Chung (1981) give a few figures to illustrate the problem: the average concentration is about 4g/l in Ganges River, 2.5g/l in Indus River, 38g/l in Yellow River where concentrations of 666g/l have already been measured!

In Pakistan, Tarbela storage basin, one of the largest in the world with 13 billion cubic meters, built in the 70's on Indus River, should be filled in less than 30 years. On Indus River also, sand deposition has already caused the meandering of the river.

The irrigation canals receive high loads of fine sediments as well. When the flow velocity decreases, these sediments fall and the waterways undergo sharp problems of siltation, implying high costs of maintenance. In Chashma Right Bank Canal (CRBC), a main canal dimensioned for a discharge of 135 m³/s, the deposition layer reached half a meter in 1991, for a hydraulic radius of 2.5 meters in average.

The design and the water management have not well identified consequences on the deposition process and they are currently done according to empirical rules. The most famous ones are Lacey's one (1929) which were used for CRBC in 1987 (Mahmood 1970 [14]). These rules assume the existence of an equilibrium profile for given solid and liquid head discharges (regime theory).

When the actual head discharges differ from the conception ones, or while the equilibrium profile is not reached yet, the regime theory is not able to forecast the bed evolution. Nevertheless, we can use models of sediment transport, deposition and erosion. These models generate the concentrations in every point and at every time. The conservation laws give the bed evolution then.

Because of the important discharges variations in irrigation canals, imposed by the head conditions and the strategies of water distribution, Cemagref chose this second approach. This training period aims at understanding the process of sedimentation and computing a model of sediment transport, coupled to an existing hydraulic model, in order to observe the impact of various regulation and maintenance strategies on several irrigation systems of Pakistan.

The first paragraph gives a few notions about the current criterion of design. The second part of this literature review presents a few physical aspects of sediment transport. The last one develops a few models of transport, sedimentation and erosion.

2. Design of irrigation canals

2.7 Regime theory

Ref. [IS], [23]

The problems of siltation in irrigation canals led the engineers to define rule of conception at the end of the previous century. These rules, despite empirical, have been improved and formalized. **They** are known today as the regime theory (Blench 1957).

In an irrigation canal, the liquid discharge Q which must be transported is imposed. The classical equations (Manning-Strickler, Chézy, Saint-Venant...) define an infinity of possible geometries for the bed. However, we can observe (in flumes or actual channels) that, when the imposed solid and liquid discharges **are** constant, the channel **reaches** an equilibrium profile after a sufficiently long time (stable slope **and** cross section). The equations of sediment transport **must** be able to represent this equilibrium stage.

These equations will be:

- at each point of the bed, the total shear stress will be the same as the critical shear stress;
- a closure criterion.

This criterion is often given by the optimization of a physical function (Froude number, energy supplied by the flow, hydraulic gradient, friction coefficient...). These criteria often give slightly various results, which is consistent with the variety of equilibrium profiles observed for a same bed.

2.2 Historic

Ref. [8].

Kennedy **proposes** as early as 1895 the first rules of conception. He observes that the siltation is closely dependent on the amplitude of flow eddies thus on the water depth (for a given discharge). He proposes the first empirical formula

$$V_0 = 0.84 \cdot h^{0.64}$$

where V_0 is the critical average velocity and h the flow depth. This formula, however criticized, was largely applied and reduced the siltation process in irrigation canals of Pakistan.

With the same idea, Lindley proposed in 1919 three similar equations which link the width, the water depth and the flow velocity.

Let us also mention the regime **theory** of Lacey (1919-1928) which proposes a **more** accurate calculation of the geometry. This theory was largely used in Punjab. The Irrigation Research Institute (1933) introduced the concentration and the fall velocity in his formulae.

Many theories followed **but** they often rest on empirical considerations and Lacey's rules are still currently used (Chashma Right Bank Canal [CRBC] for example (1987), main canal designed for a liquid discharge of $160 \text{ m}^3/\text{s}$).

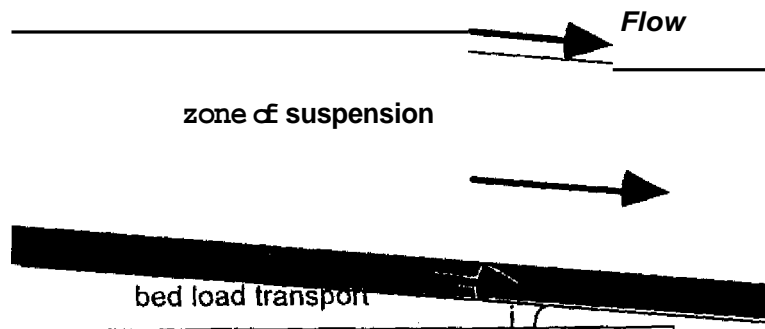
Since 1986, a procedure for redefinition of the design criteria has been launched. Sediment transport models (Engelund-Hansen, Ackers-White, Yalin, Van Rijn...) **were tested** with poor results: **none** is able to fit the measured concentrations.

3. Physical aspects of sediment transport

3.1 Different types of transport

3.1.1 Bed load and suspension

The particles of any river bed tend to be carried away by the flow. When these particles move in the core of the flow, they are in *suspension*. When they regularly remain in contact with the bed, they represent the *bed load transport*.



The *suspension* is closely linked to the *turbulence* of the *flow*; the *flow* eddies maintain the grains in motion.

The *bed load transport* is linked to the tractive *forces* (viscous forces) of the flow. Inside this *type* of transport, we can distinguish:

- sliding or *rolling*: the grains remain in the vicinity of the bed;
- *saltation* (or *skip movement*): the particles are raised by the viscous *forces* but fall under the action of their weight.

3.1.2 Bed forms: sand waves

Ref. (23), [24]).

Dunes, ripples and anti-dunes are peculiar modes of bed load transport. They appear under certain hydraulic conditions.

Antidunes appear only in *shooting flows* and their profile is *more* or less *sinusoidal*. They are in phase with the free surface deformations but move from downstream to upstream.

Dunes and ripples (small dunes) move in the same direction as the *flow*. They have a triangular shape. After Ramette (1981) (Ref. [19]) their height can reach 35% of the flow depth and their length is about 6 times as large as the flow depth.

In theory, we could link the transported bed load to the *velocity of the dunes*. Many empirical *formulae* propose to assess this velocity, but none is universal and they produce results in a very wide range (ref. [6]).

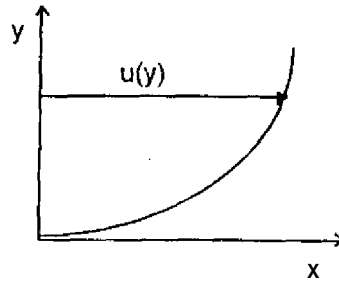
The presence of these bed forms may have a strong influence on the flow (friction, creation of bursts...) and introduce a factor of inaccuracy in the measures of topography.

3.2 Mechanics at grain scale

3.2.1 Fundamentals of hydraulics

3.2.1.1 flow velocity distribution

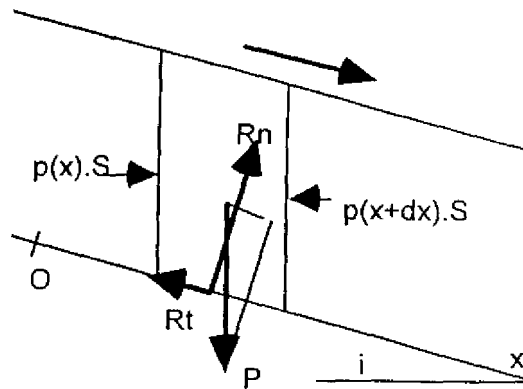
The flow velocity is zero at the bed and maximum at the free surface. The vertical distribution of the velocity can be represented as follows:



This distribution is logarithmic in a turbulent **flow** and parabolic in a laminar **flow** (cf. Yalin 1977, Pochat, Le Guennec)

3.2.1.2 Shear stress distribution: two types of forces

In a steady uniform flow, each column of water is in a dynamic equilibrium. It is submitted to its weight and to the reaction of the bed:



The resultant of the pressure forces is zero if the **flow** is uniform: $p(x).S(x)$ is independent on x .

Writing the projection of P and Rt of R on the axis Ox , we obtain: $P \sin(i) = Rt$

Considering $\sin(i) \approx i$ if i small and for a steady uniform flow, and $\tau_0 dx$, we finally obtain:

$$\rho ghJ = \tau_0$$

Here, τ_0 is the total shear stress at the bed. We can define, by the same way, the total shear stress τ in every point. τ can be divided in two terms: a viscous shear stress and a turbulent shear stress.

- the viscous force:

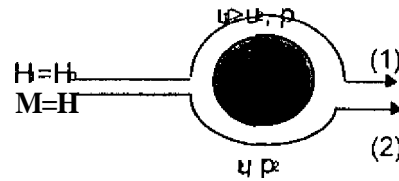
It is a friction force at the interface between two neighbouring layers of fluid which have different velocities. It is defined as follows:

$\tau_{xy} = \mu \frac{\partial u}{\partial y}$ where u is the projection of the **flow** velocity in the x direction, τ_{xy} the shear stress in the x direction on a surface perpendicular to the y direction. μ is the dynamic viscosity.

Acting on a grain, this force produces:

- the traction of the grain in the flow direction.
- the rotation of the particle if the velocity is not uniform around it.
- the traction of the grain perpendicularly to the flow direction.

[Consider indeed the flow around the particle.



The hydraulic charge H is assumed identical for both stream lines H_1 and H_2 . We have then

$$H = Z_1 + \frac{p_1}{\rho g} + \frac{u_1^2}{2g} = Z_2 + \frac{p_2}{\rho g} + \frac{u_2^2}{2g}$$

The grain is submitted, from the liquid, to the pressure force

$$F = -\iint p \cdot dS \text{ which can be divided into two terms:}$$

$$F = \iint Z \cdot dS + \frac{1}{g} \rho \iint u' \cdot dS$$

The first term is Archimed force, the second one is the lift force. Indeed, since the flow velocity increases from the bed to the free surface, this second force is also oriented from the bed downwards the free surface.

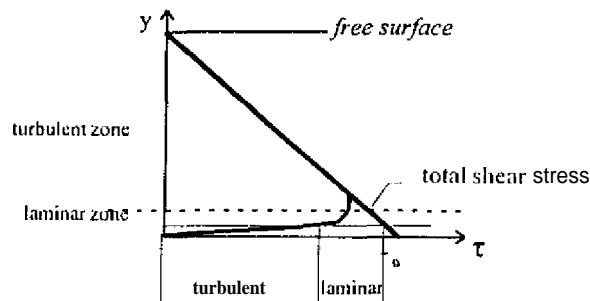
Its magnitude is all the higher as the velocity gradient is high, namely in the vicinity of the bed. (After Ref. 4)]

- Inertia forces:

They are predominant in the turbulent zone. They are linked to the fluctuations u' and v' of the flow velocity with respect to their averages u and v . The turbulent shear stress is defined as follows according to the turbulence theory (Ref. [23]):

$$\tau_t = -\rho \overline{u'v'}$$

We can draw the magnitudes of the different shear stresses on the same graph:



As we can see from the previous figure, the laminar zone is quite limited. However, the bed load transport will generally take place here, whereas the suspension will take place in the turbulent zone.

3.2.2 terminal velocity (or settling or fall velocity)

Ref. [23], [6]

This is the velocity that a particle can reach when falling in a quiet unbounded fluid, with no interaction with the other particles. This parameter is often used for the suspended phase. For example, the ratio w/u^* is often used as a criterion to separate suspension from bed load; w is intrinsic to the particle whereas u^* is intrinsic to the flow.

It is possible to calculate w in certain conditions.

[The terminal velocity is defined as the velocity that balances the forces (F) exerted by the flow on the particle and its weight. The particle is assumed spherical and its diameter is sufficient to represent its geometry. The dimensional analysis allows to assess the magnitude of F :

$$\frac{F}{\rho w^2 d^2} = \varphi\left(\frac{\rho w d}{\mu}, \frac{y}{h}\right) \quad (1)$$

When the flow around the particle is **laminar, namely when** the Reynolds number $X^* = wd/\nu$ is lower **than** unity, F reduces to the viscosity forces: F must **be** independent on the densities of **the** grains and **the** flow (F would be the same for any other density). Equation (1) implies

$$F = cste. \frac{\rho w^2 d^2}{\frac{\rho w d}{\mu}}$$

This constant, determined experimentally, is **approximately** 3π .

Thus, we have $F = 3\pi \cdot \mu w d$ (Stokes law). When the equilibrium is reached, we have

$$F = (\rho_s - \rho)g \cdot \frac{\pi d^3}{6}$$

and finally

$$w = \frac{1}{18} \cdot \frac{(\rho_s - \rho)g \cdot d^2}{\mu} \text{ for a laminar flow.}$$

When the flow is turbulent (Reynolds number greater than 1000 approximately), F is independent **on the** viscosity.

The dimensional analysis implies **the** proportionality between F and $\rho w^2 d^2$ (Newton law): $F = \frac{\pi}{20} \cdot \rho w^2 d^2$.

Hence we have $w = 1.74 \sqrt{\left(\frac{\rho_s}{\rho} - 1\right)gd}$ for a turbulent flow.

When the flow is intermediate, namely when the Reynolds number Re'' is approximately between 1 and 1000, we cannot use the previous formulae. Abacuses are presented in appendix]

The terminal velocity increases **with** the particle diameter. A **grain** tends to fall all **the** quicker as its diameter is high. **Hence** the suspension **phase** will contain the finest particles whereas the **biggest** ones **will** remain in the vicinity of the bed.

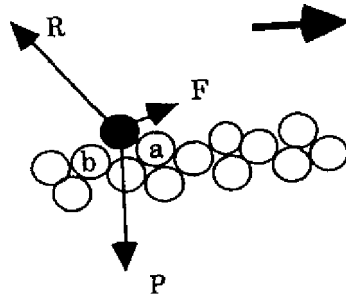
We must remain **prudent** when using the classical expressions of the terminal velocity, obtained for spherical particles in a quiet fluid: the shape might be notably essential.

3.2.3 Initiation of motion

Most of the sediment transport theories assume the existence of a threshold for the initiation of motion:

- the sediments can be cohesive (particularly the organic materials). To initiate the motion of these sediments, the flow must overcome the electrochemical forces between the bed and the particles.

- the geometry of the grains also accounts for the existence of the threshold:



by Jack

Indeed, we can see from the previous figure that the grain ~~a~~ will move if F can compensate the reaction R exerted by the grain a. Hence, if the reaction R and the weight P do not verify $R+P=0$, F will necessarily be different from zero for the initiation of motion.

In 1936, Shields tries to assess this threshold for an actual flow, working with a big number of non-cohesive particles. He introduces the parameter Y, today known as Shields parameter, mobility number or dimensionless shear stress and defined as follows:

$$Y = \frac{\tau_0}{(\gamma_s - \gamma) d}$$

and a Reynolds number at grain scale:

$$Re^* = \frac{u^* d}{\nu}$$

Here, d is the grain diameter if the granulometry is uniform or the medium diameter of the particles of the bed otherwise. Shields analyzes the initiation of motion in function of Y and Re^* . He obtains an experimental relation $Y_{cr} = \Phi(Re^*)$ (presented on the following figure) for the critical stage. If, for a given value of Re^* , Y (representing the ability for the grains to be carried by the flow) is greater than Y_{cr} , the grains will be carried by the flow; nothing will happen on the contrary.

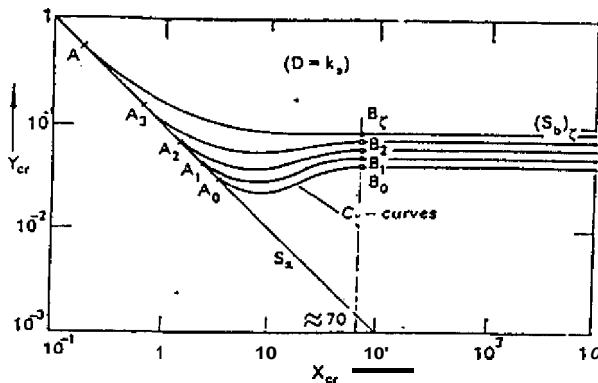


FIG. 4.11

After [16]

The shape of Shields curve is consistent with theoretical considerations (Ref. [23]).

[For very fine particles, the bed is completely smooth and the size of the grains d loses its meaning: d must vanish from the relation $Y_{cr} = \Phi(Re^*)$ and we obtain $Y_{cr} \cdot Re^* = cste$ which produces a slope of -45' on the log-log representation of the critical stage.

For a turbulent flow (Re^* high), the viscosity has no meaning and must vanish from the relation $Y_{cr} = \Phi(Re^*)$ which reduces to $Y_{cr} = cste$.]

3.2.4 Friction prediction

Ref. [6], [23].

3.2.4.1 Definitions

Friction factors are essential in hydraulics. **They** can be assessed by two methods: either by calibrating them when **we** know all the other variables of the flow, or by analysing the structure of the bed.

- Strickler coefficient **K**: it comes from **the** equation $K = Q/S.R^{-2/3}J^{-1/2}$ which is known as Manning-Strickler equation and varies from 20 (bed with vegetation) to 100 (lined bed) in a canal. $n=1/K$ is Manning coefficient.
- Chézy coefficient **C**: it is the oldest (end of 18th century) but still used currently. **C** is given by the formulae $U = C \cdot \sqrt{R_s \cdot J}$ but is not dimensionless. Yalin prefers to define $c = C / \sqrt{g}$ which is dimensionless.
- Let us also mention finally Darcy-Weisbach coefficient: $f = 8 / c^2$

3.2.4.2 smooth bed

Many empirical formulae propose to assess the roughness of a bed as a function of its granulometry (Yang [26]). It is called *skin roughness*.

For a smooth and unbounded bed, the Strickler coefficient is generally given by a relation $K = \frac{a}{d_s^n}$. **The** most classical formulae use $\alpha = 2$, $n=1/6$ and $x=50\%$ or $a = 26$, $n=1/6$ and $x=90\%$.

3.2.4.3 actual bed

For an actual bed, these coefficients can be deeply different from those obtained by calibration, namely $K = Q/S.R^{-2/3}J^{-1/2}$. This difference can generally be explained by the presence of **banks** and bed deformations. **As** mentioned before, **the** dunes and ripples may notably change the global roughness of the bed, dividing by two the Strickler coefficient in some cases. Thus, the loss of energy is **the** sum of the loss due to the grains and **of** the loss due to the bed forms. These losses are proportional to J (hydraulic gradient) thus to f .

Engelund (1966) (ref. 23)) proposes to calculate f for an actual bed as the sum of the skin roughness Factor and a bed form roughness factor.

Ramette (ref. [19]) gives a similar relation with the Strickler coefficients.

The bed forms also reduce the efficiency of the total shear stress, characterized with the ratio $\alpha = \frac{\tau_{eff}}{\tau_b}$. Meyer and Peter (1948) (ref. 18)) gave the simplest relation to assess this efficiency, obtained experimentally:

$$\alpha = \left[\frac{K}{K_r} \right]^{1/2}$$

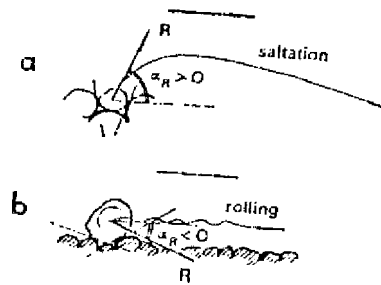
where K and K_r are respectively the actual and theoretical Strickler coefficients. In practice, α is close to 1 for a flat bed but can reach the value of 0.35 for beds with dunes.

3.3 Synthesis: link between the forces and the sediment transport

3.3.1 At grain scale

This paragraph tries to show how the forces presented above can **provoke** the different types of transport

- initiation of **bed** load transport: the viscous forces are sufficient to overcome the cohesion forces. According to **the** micro geometry of the bed, the grain can be displaced either by saltation, rolling or **sliding**:



From Ref. [23]

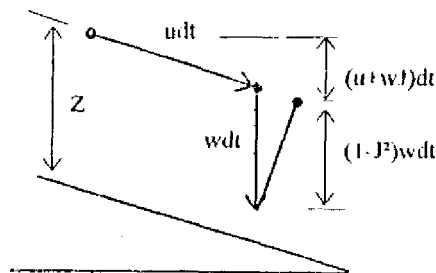
- Initiation of suspension: the grain is brought into suspension when the viscous forces are sufficient to raise it and the turbulence sufficient as well to balance the weight of the particle.
- at last, we must mention the *wash-load*, which is a form of suspension but resulting from other mechanisms.

Wang (ref [22]) defines the wash load as the portion of particles which need no energy from the flow to remain at a constant level (effective-power theory). This criterion results to the equality

$$w = u_c J$$

where w is the settling velocity. The expression of w in function of the grain diameter, gives the critical diameter for the wash load phase.

[Consider indeed the trajectory of a particle remaining at a constant height for the bed.



During the time dt , the particle was carried by the flow (with the velocity u) and should have fallen from the height $w dt$. Yet, the lift force, perpendicular to the free surface, supplied enough energy to maintain the particle in suspension. As we can see from the previous figure, this energy (per unit weight) is $w(1-J^2)dt$ and is won by the grain. In the same time, the grain has lost the gravitational energy (per unit width) $u+w)J dt$. Developed at first order, the energy received by the grain is $E = w - uJ$.

According to Wang, the particle is self suspended (or in the wash load phase) if it receives no energy from the flow, i.e. $E = 0$.

Another criterion for wash load is the homogeneity of the concentration for a given class of particles: if the flow supplies no energy to maintain the grain into suspension, there is no reason to be a gradient of concentration for the wash load phase.

The concentration distribution is generally considered homogeneous when $\frac{C(z)}{C(z_0)} \in [0.8; 1.2]$ approximately (cf. Wang, ref. [22]), where $C(z_0)$ is a reference concentration in the vicinity of the bed.

To assess the concentration, Schmidt (1925) and O'Brien (1933) (ref. [18]) write the diffusion-convection equation in which they only keep the vertical variations of the concentration. They obtain

$$w \frac{\partial C}{\partial z} + \frac{\partial}{\partial z} \left(\epsilon_s \frac{\partial C}{\partial z} \right) = 0$$

which can be integrated **once** in

$$wC + \epsilon_s \frac{\partial C}{\partial z} = 0$$

where ϵ_s is a turbulent diffusion coefficient, w the terminal velocity of the considered class of particles. This equation is known as Schmidt-Rouse one. ϵ_s is usually defined with $\epsilon_s = \frac{\nu_t}{\sigma_t}$ where ν_t is the turbulent viscosity and σ_t Schmidt turbulent number. assessed between 0.5 and 1.0 according to the authors. Writing the turbulent shear stress, we obtain the value of ν_t :

$$\tau_t = \rho \nu_t \left(\frac{\partial U}{\partial z} \right) = \rho u_*^2 \left(1 - \frac{z}{h} \right)$$

thus $\nu_t = \xi u_*^2 z \left(1 - \frac{z}{h} \right)$, ξ being Von Karman constant. Reported in Schmidt-Rouse equation, we finally obtain after integration

$$C(z) = C(z_0) \left[\frac{h-z}{z} \cdot \frac{z_0}{h-z_0} \right]^{\frac{\sigma_t w}{\xi u_*^2}}$$

At present, z_0 can only be obtained through calibration on field measurements.]

3.3.2 At the global scale

3.3.2.1 wash load:

Considering its definition, we can **easily** imagine that this type of particles is not in interaction with the bed. If the energy of the flow is constant, the wash load will remain in suspension without any contact with the bed.

Since the flow supplies **no** energy to maintain the wash load in suspension, we can also consider that **there** is no limitation for the concentration of these particles. This is not completely true since flocculation can appear for high concentration (around a few grams per litre).

3.3.2.2 bed load material:

- Equilibrium conditions

It is commonly assumed that a uniform flow **reaches an equilibrium concentration** for the bed load materials. In this case, the equilibrium solid **discharge** is also called *capacity of sediment transport* and depend on the granular material nature and the flow characteristics.

This equilibrium state does not mean that each particle is in a dynamic equilibrium. Yet, the integration of all the particles trajectories gives the equilibrium transport rate. To define rigorously the equilibrium, we could say, like Bagnold (1966) (ref. [23], [5]), that the **loss** of energy for the flow and the energy **used** to transport the sediments are equal.

However, it is not very **easy** to calculate this energy from mechanical considerations at grain scale. That is **why** many formulations of the sediment **transport** rate rest on **empirical** basis.

We will present in the next chapter several equilibrium **laws**.

- Non equilibrium conditions:

When the flow or the solid discharge is not uniform, we are *a priori* in non-equilibrium conditions. For instance, the flow discharge decreases from upstream to downstream in an irrigation canal, and thus the capacity of sediment transport as well.

When the actual concentration is lower than the equilibrium concentration, the flow will tend to erode the bed. When it is greater, the particles will tend to deposit. However, deposition and erosion will occur with a spatial and temporal delay. In order to model this phenomenon, we will present in the next chapter several laws for the sedimentation-erosion process. These laws are called *delay effect laws*.

Galappatti (1983) (ref. [16]) defines the *adaptation* length as the length necessary for a uniform flow to reach its capacity of transport. This adaptation length depends on the hydraulic variables and the granulometry of the sediments. According to Daubert-Lebreton (1967) (ref. [4]), this length can be very short for bed load transport (one hundred times the grains diameter), but is much higher for very fine particles. We could say for instance that the wash load phase has an infinite adaptation length, and therefore the equilibrium concentration would have no use for wash load.

3.3.3 Influence of the bed composition

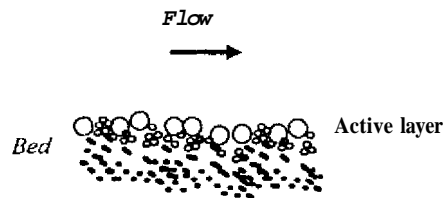
3.3.3.1 Armouring

Ref. [20], [11], [3]

When the river bed is in a stage of scouring, the medium diameter d_{50} may not be representative of the particles which can be eroded.

Indeed, several phenomena must be taken into account:

- the finest particles will be scoured first if they are available;
- the coarser ones will behave as an armour:



This phenomenon is often encountered in gravel rivers where the coarser gravels need a lot of energy to be moved

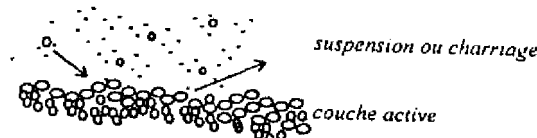
3.3.3.2 Active layer

The active layer is the upper layer of the bed (see figure). It participates in the exchanges between the bed load and the actual bed of the river. Below this layer, we can find other layers of different characteristics:

- grain size distribution;
- cohesivity;
- nature (for example the clays would become wash load if eroded whereas sand would be considered as bed material load)

Thus a model with the active layer concept should be able to predict those characteristics at each time step and each abscissa. For that, the grain size distribution of the suspended and the bed load must be known also. They will be modified according to the two following processes which occur simultaneously:

- erosion: the transported load will receive particles with the characteristics of the active layer;
- deposition: the transported load will lose a proportion of its particles.



4. Modeling

4.1 Choice of the models

4.1.1 General

Many equilibrium and delay effect laws exist for bed **load** as well as for suspension. These formulac are mast of the time empirical; they have often been obtained in steady and uniform conditions, for homogeneous materials and calibrated through flume experiments.

To apply them far actual rivers or canals, it **is** recommended to replace some coefficients proposed by the authors with parameters calibrated through actual data.

4.1.2 Types of modeling

- for the wash load, we will prefer models of concentration (convection-diffusion equation), where the term of exchange with the bed will be zero.
- for the bed load material, we can use:
 - either a model of concentration or material conservation. This model must be coupled to an exchange law. This law can be:
 - * an erosion and deposition law, such the empirical model of Krone and Partheniades (see further);
 - * an delay effect law coupled with an equilibrium law.
 - or an eulero-lagrangian model which **calculates** the trajectory of **each** particle. The concentration is calculates through integration of all the trajectories.

It is possible to separate different classes of particles, especially when **the** granulometry is wide. Nevertheless, the equilibrium laws give the solid discharge for the whole **bed** material load.

4.1.3 Criteria for characterization

4.1.3.1 characterization of the different phases

It is necessary to distinguish wash load From bed material load since the mechanisms of transport are significantly different. The wash load cannot be modelled through an equilibrium law. Let us **come** back on the criteria of separation.

- energetical approach: we have assumed that **if** the terminal velocity w of a particle is such as $w > U_c$, then it can be considered as wash load. w **is** directly linked to the diameter of the particle (see calculation of terminal velocity). Hence we can calculate a critical diameter d_{cr} below which the particles are auto-suspended (wash load) and above which the particles belong to the bed material.
- concentration distribution: this approach **needs** to **know** the profile of concentration for several classes of particles. If for one class the concentration is homogeneous, **then** this **class** can **be** considered as wash load otherwise it will be classified as bed material. This method is **therefore** more complicated and **less** accurate than **the** previous **one**.

4.1.3.2 Characterization of the bed material load

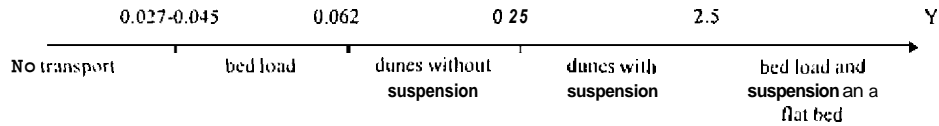
We presented **in** the present chapter the different types of transport. This **paragraph** aims at giving a criterion to be able to say if we have suspension, **bed load**, dunes...

Ramette (ref. [19]) classified the flows with Shields parameter $Y = \frac{hJ}{\left[\frac{\rho_s - 1}{\rho} \right] d}$ which is approximately the ratio between

the magnitude of the tractive force to **the** weight of the **medium** particle

The following figure gives the thresholds for:

- the initiation of motion: from 0.027 to 0.045, which is consistent **with** Shields approach.
- the appearance of dunes;
- the appearance of suspension;
- the end of appearance of dunes.



We will also use criteria **defined** by Bagnold, Engelund and Van Rijn (ref. [26]):

$$u^*/w > \lambda \Rightarrow \text{apparition of suspension}$$

λ is in the range [1; 4] after Van Rijn, its value is 0.8 for Bagnold and 0.25 for Engelund.

4.2 Models of transport

4.2.1 Classical formulae

Ref. [23], [6]

4.2.1.1 Formula of Meyer-Peter (1948) (or Swiss formula)

This (simplified formula) gives **good results when there is bed load only** ($Y < 0.25$). It is the first of the modern formulae but it is still used **with success today** (Rahuel 1988).

Hypothesis: **A critical shear stress Y_{cr} exists. Below** this value, no grain is eroded from the bed. **Y_{cr}** is determined from Shields curves but Meyer and Peter assume Y_{cr} constant and **propose $Y_{cr} = 0.047$** .

Meyer and Peter assume that the solid discharge is **only** function of the difference ($Y - Y_{cr}$). They **give** the following empirical formula

$$\Phi = 8 \cdot [Y - 0.047]^3$$

where Φ is the dimensionless solid discharge, Y Shields parameter.

Notice that the viscosity does not **appear in this formula**, which implies the non validity of Meyer-Peter formula for fine particles. The water **depth** does not appear either, like in many **bed load** formulae.

Domain of validity:

h between **1** and **120 cm**

J between **0.4‰** and **20‰**.

d between **0.4mm** and **3cm**

ρ_s between **1.02** and **$4.33 \cdot 10^3 \text{ kg/m}^3$**

For small grain diameters (**<0.5mm**) dunes can appear and the relation is not valid.

4.2.1.2 Einstein's theory (1950)

Even though Einstein made two mistakes in his **development**, his approach is particularly interesting and was used by many other authors.

He does not assume the existence of a threshold for initiation of motion, which is sometimes contested,

He makes the following hypothesis:

- the **probability for a particle** to be brought into motion is independant **on** its history;
- a particle is eroded as soon as the lift force is **superior** to **its weight** in water;

- the distance L between two consecutive points of contacts with the bed for the particle is only function of its geometry;
 - the probability p for a particle to be eroded and the exchange time T to replace the eroded particle are supposed known,
 For p , Einstein chooses a normal law and proposes $T = \alpha \frac{L}{w} = \theta \frac{d}{w}$, where d is the diameter of the particles, w their terminal velocity, α, θ coefficients of proportionality. With those hypotheses, Einstein obtains

$$\frac{A^* \Phi}{1 + A^* \Phi} = p,$$

A^* being a parameter linked to the geometry of the grains. The problem consists in giving a value for p . Since p is linked to Shields parameter Y , Einstein proposes

$$p = 1 - \frac{1}{\sqrt{\pi}} \int_{-B^*/Y - U/\eta_0}^{B^*/Y - U/\eta_0} e^{-\xi^2} d\xi$$

where A^* , B^* and η_0 are assessed experimentally. Einstein gives a smoothed form for his equation, making it practical:

$$\Phi = 32.6. Y^3$$

We can also mention Einstein-Brown's smoothing

$$\Phi = f(Y)$$

Yalin (77) (Ref. 16) followed Einstein's development in a correct way and obtained, after smoothing,

$$\Phi = [5.28Y]^{3/2}$$

4.2.1.3 Total load formula of Bagnold (1966)

This formula rest on energetical concepts. Bagnold assumes that the power necessary to transport the sediments is proportional to the loss of potential energy of the flow per unit time, which bagnold calls "available power". This power per unit area is

$$E_p = \rho g \int_0^h U \cdot u \cdot dy = \rho g h \cdot l \cdot U = \tau_b \cdot U$$

Considering on the one hand the bed load transport and on the other hand the suspension, Bagnold obtains the following theoretical formula:

$$\rho g \frac{q_s}{\tau_b \cdot U} = \frac{e_b}{\tan \psi} + e_s (1 - e_b) \frac{U_s}{w}$$

where U_s is the velocity of the sediments, e_b the efficiency of the flow for the bed load, e_s the efficiency for the suspended load, w the terminal velocity and $f = \tan \psi$ a friction factor on the bed.

Assuming $U_s = U$ and proposing numerical values to make his formula practical, he finally obtains

$$q_s = \frac{\tau_b U}{\rho g} \left[\frac{e_b}{f} + 0.01 \frac{U}{w} \right]$$

For sand finer than 0.5mm and $Y > 1$, Bagnold gives the value of 0.17 for e_b/f and special graphs to assess it otherwise (ref.[5]). This model was compared with several set of data. It produces quite satisfying results when suspension is present ($Y > 0.4$ according to Yafin).

4.2.1.4 Formula of Engelund-Hansen (1967)

This formula is empirical. It was established for particles from 0.190 to 0.930mm and produces good results for bed load as well as for suspension. It writes as follows::

$$q_s = 0.08 \sqrt{g \left(\frac{\rho_s}{\rho} - 1 \right) d_{50}^3} \left(\frac{hJ}{(\rho_s / \rho - 1) d_{50}} \right)^{\frac{5}{2}} \frac{C^2}{g}$$

C is Chézy coefficient, d_{50} the medium diameter. Using dimensionless variables, it writes

$$\Phi = 0.08 Y^{5/2} \frac{C^2}{g}$$

Engelund-Hansen formula assesses the total load and Ramette (Ref. [19]) proposes to use it when $Y > 0.3$ when suspension exists. It is valid even when dunes and ripples are present.

4.2.2 Selection of equilibrium models

4.2.2.1 Comparison of existing formulae

Ackers tried in 1980 (ref. [6]) to classify after experimental criteria the most famous of the equilibrium transport formulae. Ackers-White formula was the best one, followed by the models of Engelund-Hansen, Rottner, Einstein, Bishops, Toffaletti...

Yang and Wan (ref. [25]) also compared different models with flume and river data. In flume experiments, Yang's formula is the best one, followed by Engelund-Hansen, Ackers-White, Laursen and recommend not to use the models of Colby, Einstein and Toffaletti.

In rivers, Yang's formula is still the best one, then Toffaletti, Einstein, Ackers-White, Colby, Laursen and Engelund-Hansen.

He notices that the calculated concentrations are always higher than the actual one (up to 100%) which is normal (after him) since the bed load is seldom measured.

Cardoso and Neves also compare ten total load formulae with the support of more than 7000 measurements. They observe that the formulae of Korin-Kennedy (1981 and 1990) often give the best results, followed with Ackers-White (1973) and Shen-Hung (1971).

We must keep in mind however that most of these formulae were established after flume experiments, in steady and uniform conditions and for a controlled grain size distribution. For instance, the formulae with only one characteristic grain size will not be appropriate for gravel rivers. Furthermore, the different models will be more or less sensitive to the errors in measurements.

4.2.2.2 Models appropriate for the irrigation canals

We present in appendix 5 several models adequate *a priori* for irrigation canals. They were selected on the following criteria:

- low flow velocities;
- presence of suspension;
- mainly very fine sediments (sand, silt and clay).

The formulae we present were considered as the most reliable ones by several authors.

4.3 Models of non-equilibrium transport

4.3.1 Convection-diffusion equation

This equation writes as follows:

$$\frac{\partial C}{\partial t} + V_c \frac{\partial C}{\partial x} - \frac{1}{S} \frac{\partial}{\partial x} \left[SK_c \frac{\partial C}{\partial x} \right] = \phi / h$$

where ϕ is a term of exchange (won by the suspended load), K_c is a diffusion coefficient, V_c the mean velocity of the grains. assumed most of the time the same as the flow velocity, even though the concentration is higher in the vicinity of the bed, where the flow velocity is the lowest. K_c depends on the geometry of the grains:

$$K_c = 7.25hu^* \left[\frac{U}{u^*} \right]^{1/4} \text{ after Thackston-Krenkel (1967),}$$

$$K_c = 0.5u^* \frac{S^2}{R^3} \text{ after Liu (1978),}$$

$$K_c = 0.011 \frac{U^2 L^2}{hu^*} \text{ after Fischer (1979).}$$

This equation can be used for several classes of particles. In particular, it is sufficient to assess the longitudinal distribution of the wash load, since the term of exchange $\phi=0$. When this term is different from zero, it can be assessed with the spatial delay effect laws presented further.

Nevertheless, to solve this second order differential equation, we need to know two boundary conditions, for instance the concentrations at two different abscissae.

4.3.2 Exchange (or spatial delay effect) laws.

4.3.2.1 formula of Daubert-Lebreton (1967)

This formula writes as follows:

$$\frac{\partial q_s}{\partial x} = K.(q_s^e - q_s)$$

where K is a constant of erosion or deposition obtained by calibration, and $q_s^e - q_s$ the difference the equilibrium and actual solid discharges per unit width.

To obtain this formula, Daubert and Lebreton assume that the probability for a particle to be deposited is function of the distance dx made by the particle, namely $P(dx)$ and propose

$$P(dx) = 1 - \exp(-K \cdot dx).$$

They follow then a similar development as Einstein's one.

The authors also assume that the coefficient K is inversely proportional to the difference between the actual and the critical shear stress at the bed level.

This formula is appropriate to bed load and is not supposed to be valid for suspended load.

4.3.2.2 Han's formula

With a similar idea, Han (ref. [12], [13]) proposes the following loading law:

$$\frac{\partial C}{\partial x} = K(C^* - C)$$

$$\text{with } K = \frac{\alpha \cdot w}{u^*}$$

This formula seems to be more appropriate to suspended since the deposition dynamics of the sediments is taken into account through the fall velocity w and the shear velocity u^* .

4.3.2.3 Models of Krone and Partheniades

These empirical models give good results for cohesive sediments. They assume that the term of exchange is proportional to the gap between the total shear stress and a critical shear stress, which is not the same for erosion and deposition, and not the same as the critical shear stress given by Shields curve.

For erosion, Partheniades (1965) obtains $\phi_e = M \cdot \left[\frac{\tau}{\tau_{ce}} - 1 \right]$ for $\tau > \tau_{ce}$; M and τ_{ce} must be determined experimentally

For deposition, Krone (1962) introduces the terminal velocity as well as a reference concentration C_f in the vicinity of the bed. He proposes:

$$\phi_d = -w \cdot C_f \left[1 - \frac{\tau}{\tau_{cd}} \right] \text{ for } \tau < \tau_{cd}$$

Two other models are presented in appendix 3.

4.4 Euler-Lagrangian models

ref. [18]

These models simulate the trajectories of each particle. The global value are obtained after integration. The first one was developed by Bayazit (1972) We can also mention the one developed by Cemagref (Yvergniaux 1990) with an accurate modelling of turbulence and suspension. It could be applied for decantation basins (Frey 1995).

4.5 A few operational models

- IALLUVIAL (Karim and Kennedy, 1982, ref. [11]), replaced now by SEDICOU, developed at the Iowa Institute of Hydraulic Research;

- CARICAR, Firstly developed by the Laboratoire d'Hydraulique de France. In Ref. [20], Rahuel (1988) introduces sorting, armoring and modelling of the active layer.

- HEC6: American model developed to simulate the siltation in rivers and reservoirs, when the sediments are of same characteristics as in the irrigation canals but for which it has not been applied. In particular, it was applied to simulate the siltation in Tarbela reservoir (Pakistan) for 4 years.

These models try to represent the physics of the phenomena as well as possible (for instance with concepts of active layer, cohesivity of the sediments...)

- SEFLOW (ref. [15], [16]) has been developed at the hydraulic laboratory DELFT (the Netherlands) is more appropriate to the irrigation canals. It has already been applied to irrigation canals of Pakistan.